THE JOHNS HOPKINS UNIVERSITY

# BETA-ARRESTIN MEDIATED CELL CHEMOTAXIS

by
Hao Chang

A thesis submitted to the Johns Hopkins University in conformity with the requirements for the degree of Doctor of Philosophy

Baltimore, Maryland
Aug 6, 2014

# Abstract

Eukaryotic chemotactic signaling networks which regulate the cell's ability to sense the gradient of chemotactic cues frequently have the dual property of perfect adaptation to spatially homogeneous inputs, and persistent activation by inputs that are spatially graded. This property is also shared by bacterial chemotaxis networks, raising the question of whether these two types of chemotactic processes also have similar organizations of the underlying biomolecular processes. Interestingly, perfect adaptation can only be achieved robustly through a handful of mechanisms. Eukaryotic chemotactic networks appear to rely on one of these—the incoherent feed-forward loop, while bacterial chemotaxis depends on another—the negative feedback loop. In this dissertation, we will discuss how this conclusion can be reached even if the details of the molecular networks are incompletely understood. Furthermore, we argue that the use of distinct network architectures is not accidental and may be a consequence of the nature of the signaling inputs and the limitations of the sensory properties of different cell types.

Biological systems always appear as diverse and complicated. Not all the chemotaxis can be classified into the two categories we discussed above. For example, the beta-arrestin2, an important G-protein coupled receptor signaling mediator and scaffold, -mediated cell chemotaxis did not show perfect adaptation. We explored the mechanisms by both experimental and computational approaches and found that the beta-arrestin2 is the key component in the chemotaxis pathways in several aspects: 1) It

prompts receptor desensitization to achieve non-perfect adaptation; 2) It assembles signaling complex to response to the input gradients; 3) It amplifies the external gradient by its unique scaffold biphasic regulation; 4) It organizes the receptor recycling to achieve persistent gradient sensing capacity; 5) It reorganizes the cytoskeleton during cell chemotaxis. Due to the biphasic regulation, the scaffold level is important in signal transduction. By manipulating the expression and distribution of the beta-arrestin2, we can convert chemoattractance to chemorepulsion or co-existence of both.

**Advisor**: Andre Levchenko, PhD

**Thesis committee**: Pablo Iglesias, PhD

Jin Zhang, PhD

# Acknowledgements

A number of people and organizations deserve special recognition for their contributions to this thesis.

I would like to thank my thesis advisor, Dr. Andre Levchenko, not only for his enormous support during my PhD study, but also for being a good friend sharing his life experience with me. Dr. Levchenko is a great scientist. His enthusiasms in science, talents in research and motivation for success set him an example of a great scholar for me. Dr. Levchenko is an excellent advisor. I really appreciate his constant encouragement and invaluable advice on my scientific research, and also the time he spent with me on planning my future career. He has constantly taught me to be confident and persistent on what I have determined to do, which is actually the key for every success and will benefit me for my whole life time.

I am very grateful to Dr. Jin Zhang and Dr. Pablo Iglesias, who have served on my thesis committee. They gave me valuable advice on my research project from time to time, helping me move forward steadily. I really appreciate that. I also want to thank them for proof-reading and commenting on my thesis.

I benefit a lot from Dr. Robert Lefkowitz and Dr. Jonathan Violin for the fruitful and joyful collaboration and helpful insights on my projects. I would also thank Dr. Takanari Inoue for sharing the reagents.

I would like to thank all members of Levchenko lab, former or present, for making Levchenko lab such a lovely and friendly place to work in. I owe much gratitude

to Dr. David Noren and Adriel Bergman for assisting me during the completion of this thesis. Their guidance and patience was highly appreciated.

I would like to thank the IMMBI project and Department of Biomedical Engineering at Johns Hopkins for helping my transition from physics to biology and supporting my study and research. I would also thank Dr. Joel Bader and Dr. Mario Amzel for the fantastic experience during my rotation in their labs.

I would like to thank my mother and father for supporting me in the completion of this thesis research. I honestly could not have finished this thesis without their love. I would also like to thank my wife Yu Chen for her contributions to this project. She helped me to fine tune my paper so that it not only it made sense but was error-free. Without her encouragement and faith in my abilities to complete this thesis and this program, I might not have been able mentally able to continue. Thank you.

# Table of Contents

# Chapter 1

# Introductions

## *1.1 GPCRs and beta-arrestins*

G-Protein-Coupled Receptors (GPCRs) are the extremely important targets of therapeutically relevant drugs. They are encoded by more than 800 genes (about 4% of the human genome) and are targeted by 40% of all marketed drugs [1]. The large variety of stimuli ligands can range from small amines to hormones and chemokines [2], yet more and more synthetic ligands. Since their long track of success, GPCRs are sill the main targets for new drug research and development. Due to their highly conserved seven-transmembrane structure, they are also called 7TMRs [3].

More importantly, the structural conservation provide extra conveniences for studying their functions and mechanisms [4]. Most current ligands to GPCR are thought to act via the "orthosteric" bundle binding sites in Family A (containing 80% of the GPCRs) receptors [5]. The conservation in structure of these receptors have been assessed base on a subset of 44 residues that are thought to form the majority of the binding sites [6]. Upon activation, the conformational changes of GPCRs act as a guanine nucleotide exchange factor (GEF) [7]. The GPCRs then activate G-proteins' α subunit by

changing its bound GDP for a GTP and dissociating it from the β and γ subunit. The activated α subunit in turh actives downstream signaling proteins depending the specificities. The two principal downstream signaling pathways of GPCRs are: the cAMP pathway and the phosphatidylinositol pathway [8]. The ligands activate the receptors are categorized as "agonist", while the ligands block or dampen the agonist mediated responses are so called "antagonist".

After binding to agonist, the receptors not only trigger downstream signaling pathways, but also undergo modifications by other proteins. A significant family of kinase that modifies GPCRs is G protein-coupled receptor kinases (GRKs). GRKs phosphorylate serine and threonine residues to induce conformational changes and form binding sites for arrestins [9]. The arrestins' binding to the receptors prevents the re-association of the G-protein, and internalize the receptor from plasma membrane, thereby preventing the reactivation of downstream pathways.

Mammalian arrestin family has four members: arrestin-1 (also known as visual arrestin or S-antigen), beta-arrestin-1 (also known as arrestin-2), beta-arrestin-2 (also known as arrestin-3), and arrestin-4 (also known as the cone arrestin), and they are all cytosolic proteins [10]. The visual arrestin and cone arrestin are mostly found in visual system. They interact with upstream photoreceptors and downstream transducins to regulate the light sensitivity of eyes. In contrast, beta-arrestin1/2 are ubiquitously expressed. The word 'ubiquitously' means not only in all eukaryotic organisms, but also in virtually every eukaryotic cell. When initially discovered, beta-arrestins are thought to be similar to the arrestin1 and arrestin-4 and recognized as the negative regulator of

GPCRs which desensitize the GPCRs after being activated by ligands. After extensive studies, they are now known as crucial signaling mediators and molecular scaffolds [11].

Beta-arrestins have a hugelong list of interaction partners by proteomic analysis [12-14]. They bind Src family non-receptor tyrosine kinases to activate dynamin and other Src downstream pathways. They associate AP2 and clathrin to from coated pits, together with dynamin, they contribute to the GPCR endocytosis. They interact with E3 ubiquitin ligases, p53, and MDM2 to determine the endosome fate: whether it should go to lysosome or recycling. They bind cofilin, LIMK and filamin to change the cytoskeleton arrangement. They recognize NF-kB to regulate cell apoptosis and necrosis. They contribute to regulation of the calcium signaling through calmodulin. They also bind many multi-functional proteins like PI3K, small GTPase family (Ras, Rho, Rac, Rab, Ral-GDS and ARF6), PDE4D and DGK [15]. In summary, the beta-arrestins function as signal transduction hub.

Despite the fact that beta-arrestins play essential roles in GPCR signaling, it also involved in mass of other pathways like EGF receptor tyrosine kinases transactivation [16]. Even more, beta-arrestins are also work as molecular scaffolds. The molecular scaffold in signaling network is a protein that can assemble other signaling protein together to facilitate the signaling transduction. Beta-arrestin2 is a multi-pathway scaffold. It can assemble MAPK cascades like Raf-MEK-ERK, ASK1-MKK3-p38 and ASK1-MKK4-JNK3 for activation [17]. It can also coordinate PP2A-Akt-GSK3, however, for inhibition [18]. Scaffold molecules not only provide a highway for signal

transduction but also raise complex dynamic patterns which provide more ways for cells to control the spatial and temporal behaviors [19].

Interestingly, beta-arrestins binding partners include themselves by forming either homo- or hetero- oligomers. The self-association feature of beta-arrestins are highly conserved in mammalian evolution [20]. The function of the oligomerization is still not very clear. But a few hypotheses are being tested: 1) It provides a mechanism to maintain physiological concentration of beta-arrestins monomers; 2) Hetero-mers help beta-arrestins to regulate each other.

Beta-arrestins also undergo complicated post-translational modifications. Phosphorylations of beta-arrestins at different sites can result in its inactivation or activation. Ubiquitination can decide the degradation or recycling of beta-arrestins. S-Nitrosylation can strength the binding capacity of beta-arrestins. Recently, people even found that the GRKs can phosphorylate the different sites of receptors to alter the ligand-dependent recruiting patterns of beta-arrestins. This novel finding is named as ‘barcode’.

Beta-arrestins-mediated endosome is long lasting signaling platform. Taking Angiotensin II-actived ERK phosphorylation as an example: When activated, the G-protein-mediated signaling is rapid and transient. It leads to nuclear translocation of activated ERK which can initiate the function of many transcription factors. On the other side, beta-arrestins-mediated ERK activation is slow but much greater persistent. In contrast, the activated ERK stably stays with the endosomes without going into the nuclear (Figure 1.1). The endosomes are involved in many other cytosolic protein activations. But finally, the endosome has two destinations: lysosome or exocytosis.

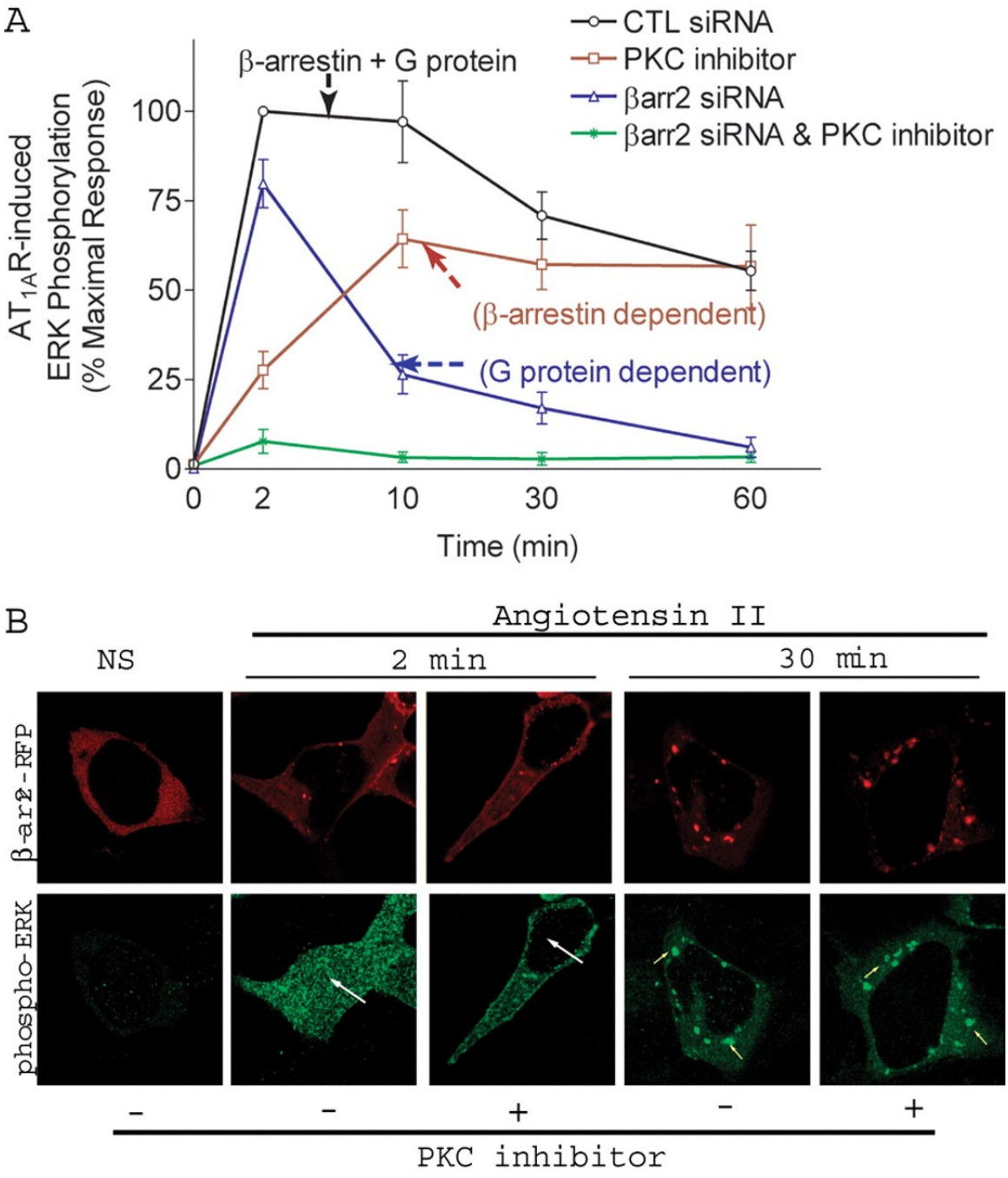


**Figure 1. 1 A) Beta-arrestin2 in charge of the long-term signaling of pERK, while G-protein mediated signaling is very transient. B) beta-arrestin2 mediated ERK activation are mainly on the arrestin-contain vesicles [11].**

It is surprising that the GPCR signaling can be so clearly separated into two branches (Figure 1.1 A): the G-protein dependent and beta-arrestin2 dependent. Such a distinct cut makes beta-arrestins the popular therapeutic targets for drug developments. A new era come into our sight: beta-arrestins-biased ligands shed light on the new idea of drug design. Conventional studies of GPCRs therapeutics discovered unavoidable side effects of targeting ligands, as distinct ligands are all cut through the same mechanism for a particular receptor [21]. Now, the researchers believe that, if we can find some drugs that only affect beta-arrestins side without disturbing the G-protein, we can provide much better treatment. Indeed, a number of drugs based on this mechanism are on the way [22, 23].

## *1.2 Chemotaxis*

Chemotaxis is cells' or organisms' sensing and migrating to the gradient of a chemical stimulus gradient in the environment. This phenomenon happens at both single cell level and multicellular organism level, in eukaryotes as well as in prokaryotes, by spatial detection or temporal measurement. Bacteria approach food source or avoid poisons by chemotaxis. Immune systems chase infectious foreign organisms through chemotaxis. Cancer cells metastasizes by chemotaxis. Amoeba stands together to defend starvation using chemotaxis. In addition, chemotaxis is critical for the development in the multicellular organisms.

Cell chemotaxis research is very important and hot for the several aspects: 1) It helps us to understand the biochemical process happened inside cell better. With non-uniform environment, the cell displays imbalanced signal and molecule distribution in small scale. These polarizations lead us to explore the signaling transduction mechanisms that can not be observed under uniform treatment. 2) Almost all the information we gained from chemotaxis can be applied to other polarization behavior, including yeast shmooing, epithelial polarity or epithelial-mesenchymal transition, non-uniform development of organisms and even animal migration. 3) Clinically, chemotaxis study provides promising targets for preventing bacterial infections expanding, increasing immune system's sensitivity, stopping cancer metastasis, and guiding correct development.

Cell chemotaxis mechanisms have evolved to enable cell navigation in chemically and mechanically complex microenvironments, along with guidance by a range of signaling inputs reflecting spatially complicated extra- and intra-cellular conditions. Responsiveness to diverse cues permits individual cells to integrate diverse pieces of information and convert this information into the directionality of cell polarity and migration. This decision-making process is frequently complex, presenting interesting challenges to the experimentalists and modelers alike. Indeed, it is frequently hard to unravel complex intracellular signaling networks distributed in space and differentially activated in time, and it can be even harder to understand how activation of these networks can control both qualitative and quantitative characteristics of something still poorly understood, i.e. how cells define where their front and rear parts should be localized. The experimental approaches require sophisticated and still largely immature

tools allowing simultaneous imposition of multiple extra-cellular cues, precisely controlled both in space and in time. The modelling approaches need to rely on the appropriate level of description of biological complexity, so that the model and experiment can inform each other, a notion that is still not quite rooted in the modelling community.

Two model organisms are well built for studying chemotaxis: bacteria and *Dictyostelium discoideum.* The molecular mechanisms of chemotaxis of the two remarkably differ from each other. Bacteria sense gradient using so called "temporal sensing": sensing the chemical gradient over time. Binding the chemoarrractants causes chemoreceptor clustering at cell poles. Chemoreceptors clusters link Che-W and Che-A , and form signaling complex. The complexes phosphorylate Che-B to Che-Bp and dephosphorylate Che-Yp to Che-Y. Che-Bp gives negatively feedback to disassemble the signaling complex. Che-Y is released to regulate flagellar motor rotation from clockwise rotation (stop and tumble) to counter-clockwise (move forward) (Figure 1.2 A).

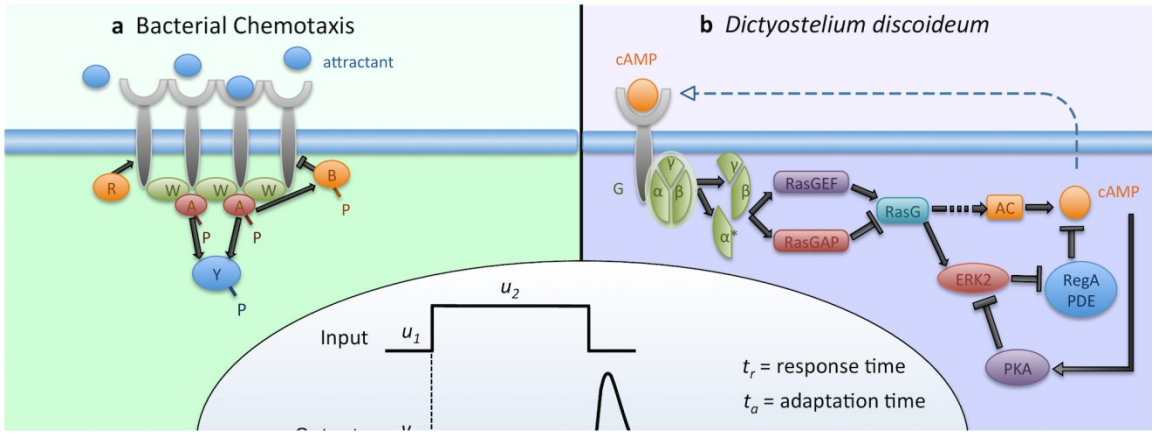


**Figure 1.2 Bacteria and *Dictyostelium discoideum* using different mechanisms to achieve chemotaxis: A) Bacteria using feedback and B) *Dictyostelium* using incoherent feed-forward loop. Figure is adapted from [24].**

But the *Dictyostelium discoideum* senses gradient using "spatial sensing". They can feel the concentration change along their body length. Their chemoreceptors are usually GPCRs. When activated, the G-protein signaling diverges into two branches: one through RasGEF and the other one through RasGAP. The two branches share the same downstream target Ras: RasGEF actives Ras while RasGAP inhibits Ras. This signaling motif is called incoherent feed-forward loop (Figure 1.2 B).

Why different cells adapt different signaling motifs (feedback V.S. feed-forward)? We will answer this question at Chapter 2 by comparing them in detail by mathematical modeling.

## *1.3 Cell chemotaxis and beta-arrestin2*

Both bacterial and *Dictyostelium discoideum* chemotaxis pathway can achieve full adaptation (Stimulated pathways can drop to base-line after a period). Presumably they can re-sense the updated concentration after moving to a new location of the gradients, so the signaling motifs that can achieve full adaptation are well studied and thought to be the basics of cell chemotaxis. However, as shown in Figure 1.1, the beta-arrestin2 signaling pathway does not fully adapt to the stimuli. Previous studies showed that beta-arrestin2 is involved in cell chemotaxis [25-27]. Moreover, they are critical in many GPCR mediated cell chemotaxis.

Chemokines are the most well-known cell chemotaxis induction factors and all the chemokine receptors identified so far are GPCRs. Several lipids, hormones, and peptides also trigger the cell chemotactic behavior by binding to the GPCRs. Beta-arrestins are required by a long list of chemokine receptor-mediated chemotaxis including: CXCR1 and 2, CXCR5, CCR2, CCR5 and CCR7. CXCR4 and 7 are general chemical cues used by many cells for chemotaxis: macrophages, T/B cells, neutrophils tumor cells, and germ cells. It is reported that the absence of beta-arrestin2 will impair the CXCR4-mediated chemotaxis.

In addition to the chemokine receptors, beta-arrestins scaffolded MAPK activation is required by protease-activated receptor- [26, 27] and angiotensin receptor- [25] mediated cell chemotaxis. Regarding the beta-arrestins' role in chemotaxis, a couple

of studies suggested that the MAPK activation assisted by beta-arrestin2 are crucial, while some other papers inferred that the beta-arrestins can regulate a bunch of cytoskeleton proteins like LIMK, filamin, and cofilin to reorganize the actin or microtubule. Despite of many pieces of information strongly supporting beta-arrestins' importance in chemotaxis, yet, at cell biology level, the big picture that how beta-arrestin2 help cell to detect and amplify the external gradient remains unclear.

## *1.4 Organization of my thesis*

My thesis will aim to investigate two major aspects in chemotaxis. First, we will discuss how perfect adaptation is achieved via different mechanisms, i.e. why some cells use negative feedback as chemotaxis motif but other cells use incoherent feed-forward loop. In chapter3, we will suggest how these important and pressing challenges can be addressed in the context of eukaryotic cell polarity and migration, highlighting insights that begin to emerge as a result of promising developments in this area.

Second, we will address the mechanism issues about beta-arrestin2-mediated imperfect adaptation in chemotaxis. How does beta-arrestin2 prompt chemotaxis without perfect adaptation? With this question in mind, we carried extensive survey of beta-arrestin2's function in chemotaxis. We will present our results and answer the question in chapter 4.

Before stating the result in Chapter 3 and Chapter 4, we are going to describe out experimental and simulation setups in Chapter 2.

# Chapter 2

# Materials, Experimental and Computational Setups

## *2.1 The microfluidic chip design and fabrication*

In order to study cell chemotaxis *in situ*, we have to build an environment of uniform, repeatable and stable chemical gradients which can be applied to the cell. In the meanwhile, we should be able to observe the signaling events and cell behaviors with gradients applied. Traditional gradient generating devices like Boyden chamber, Zigmond Chamber, Dunn chamber, agarose assay, and micro-pipet either lack the ability to do live-cell imaging or can not generate stable and consistent chemical gradient. Microfluidic chips became the only choice [28-30]. Beyond the essential needs stated above, this novel technology offers several extra advantages: high through-put, small reagents consumption, dynamical controllability, customizability and extremely long stability (days).

Basically, two types of microfluidic chips are well designed to generate chemical gradients: Christmas tree and H-chip. The Christmas tree chip is popular for fast gradient generation (minutes) and flexibility in gradient shape, but has the cons that cells in the chip usually suffer from the shear stress of flow and the gradient goes unstable after hours of running. On the other side, the H-chip is slower in gradient generation (take about half hour to build up the gradient) and mostly restricted to linear gradient, but has the pros like no flow shear stress and gradients stable for days. The comparison of all these features made us to use the H-chip for our studies.

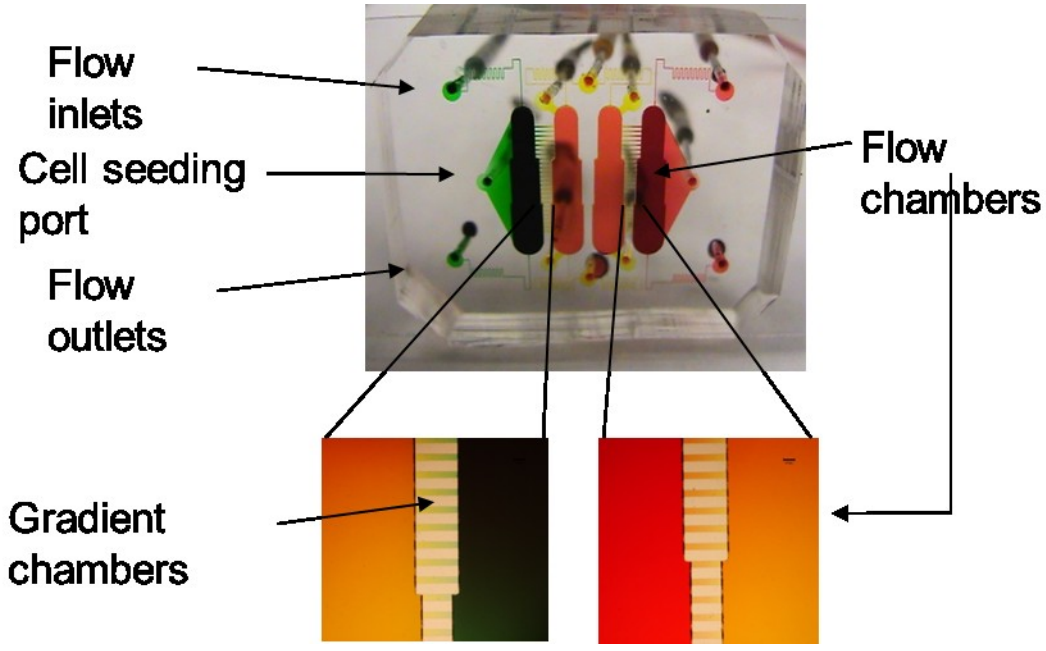


**Figure 2. 1 The Microfluidic chip we used for cell chemotaxis experiments. Food colors are used to show the flow of each channel. The real flows come from the inlets on the top, flow out through the outlets at the bottom. This chip has two experimental units in parallel: left two channels form one, the right two form the other one. In each unit, the vertical small gradient chambers between two channels are cell**

**migration chamber. The flows in two channels will diffuse cross the gradient chamber and be applied to the cells seeded there [31].**

The design of our chip showed in fig above. We used the food color to show the generated gradients. Four major design features are highlighted: 1. we designed three different cross channel lengths so that we can have 3 different steepness of gradients at the same time; 2. we fabricated the gradient chambers as 11~13 microns to simplify the cell-seeding process; 3. The ratio of heights between the flow chamber and gradient chambers are set to >10 to maintain the gradient stability; 4. In each chip, we introduced two parallel experiments side-by-side as showed in Figure 2.1. This scheme allows us to have control or compare two conditiosn in the same experiment which increase the reliability of data.

## *2.2 Plasmids and Cell lines*

The Rat Type 1A Angiotensin II receptor (AT1aR) with monomeric-CFP cloned in pcDNA3.1 and Rat beta-Arrestin2 with monomeric-YFP cloned in pcDNA3.1zeo were gifts from Dr. Lefkowitz. Beta-Tubulin with mCherry was a gift from Dr. Zhang. Beta-Actin with mCherry was shared by Dr. Kim. The following are obtained from Addgene: cytoplasmic EKAR-Cerulean-Venus (No. 18679), Rab11-WT-dsRed (No. 12678), and Rab11-DN-dsRed (No. 12678). We scissor the monomeric-CFP out and put the mCherry

fluorescence protein to make the AT1aR-mCherry construct in order to be compatible with other fluorescence markers.

Fugene 6 and Fugene HD are used to transfect the cells. The rat vascular smooth muscle cell line is purchased from ATCC. The HEK293 cell line is obtained from Dr. Yarema.

In our experiments, the results are very sensitive to the protein expression level of exogenous genes. In order to reduce the cell-to-cell variation, we decided to pick clonal cell lines after plasmid transfection. We created the following cell lines for our study:

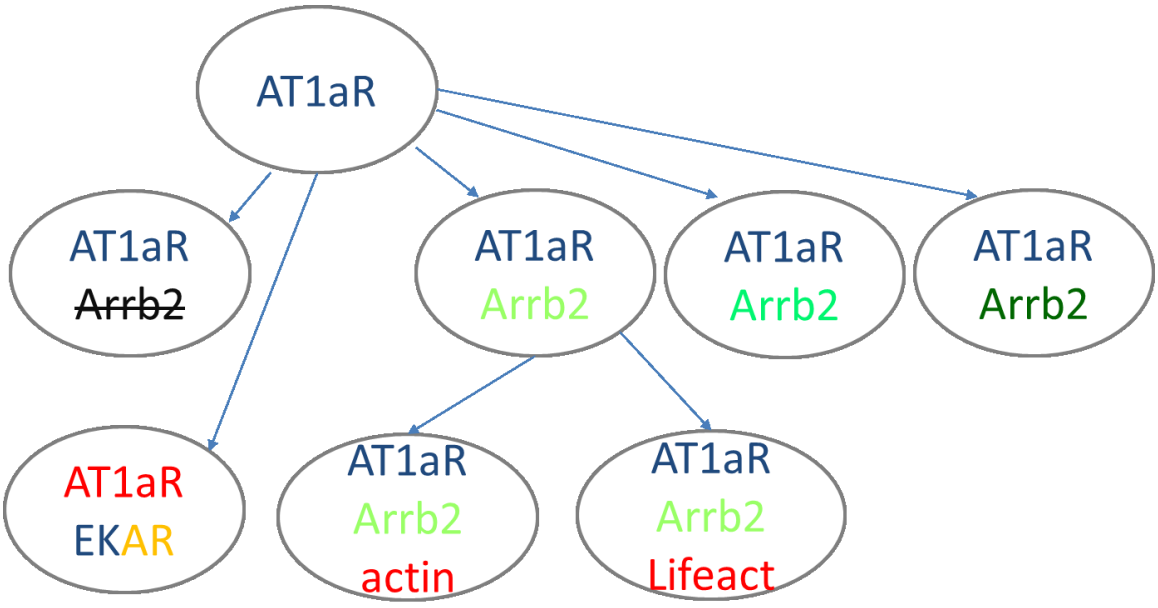


**Figure 2. 2 Cell lines created for our study. The colors indicated the fluorescence protein fused to the gene of interest. The arrow indicates the derivation relationship. The strikethrough sign denote knockdown by shRNA.**

The HEK cell do not express AT1aR endogenously. We transfected the cells with AT1aR-mCFP to create the cell line with the receptor only. After picking a clonal cell line, we started to manipulate the beta-arrestin2 level. Since beta-arrestin2 is ubiquitous expressed, we used shRNA (Sigma) to knockdown endogenous the beta-arrestin2 level. To increase the expression level of beta-arrestin2, we transfected the receptor-only cell line with beta-arrestin2-mYFP, then picked 3 different YFP fluorescence intensity visually. The total expression level of beta-arrestin2 for 5 cell lines (knockdown, native, and 3 overexpressed) are confirmed by western blots.

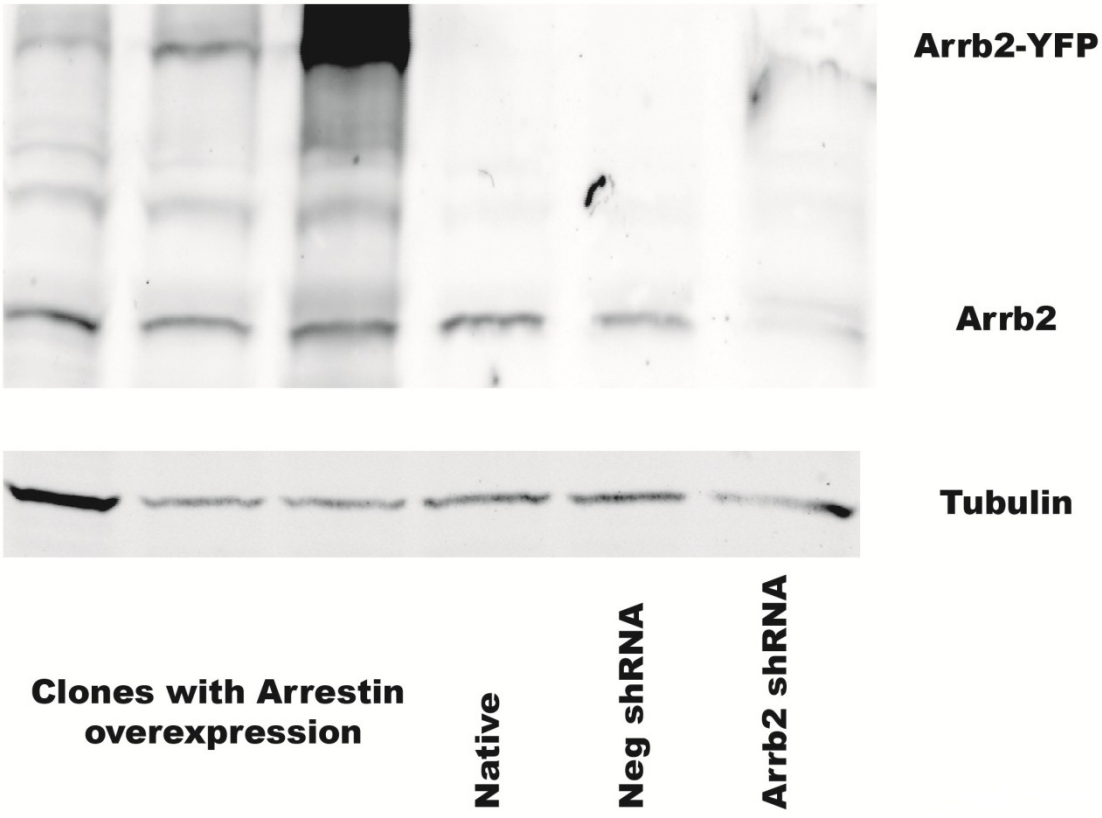


**Figure 2. 3 Cell lines with various beta-arrestin2 expression levels are quantified by westernblot. Overexpressed beta-arrestin2 is fused with mYFP.**

## *2.3 Antibodies and Reagents*

The anti- phos-ERK, beta-Arrestin2, and phos-p90RSK antibodies were purchased from Cell Signaling. The anti-alpha-Tubulin is from Abcam. Alexa Fluor 488-conjugated goat anti-rabbit and Alexa Fluor 595-conjugated goat anti-mouse antibodies are from Life Technology.

AngiotensinII (Ang) ligand was obtained from Sigma, AngiotensinII analog – [Sar1, Ile4, Ile8]-Angiotensin II (SII-Ang) was custom-synthesized at Cleveland Clinic Protein Core Facility (Cleveland, OH).

## *2.4 Image acquisition and Data processing*

Images ware acquired on a Zeiss Aviovert 200M microscope with moving stage, isothermal incubator and CCD camera controlled by Slickbook 4.2. The cell migrations were observed under 10x air objective. The fluorescence and FRET images were taken at 40x oil objective with numerical aperture of 1.4. CFP was detected through a 436/20 excitation filter, a 455 dichroic longpass mirror and 480/30 emission filter. YFP was detected through a 500/20 excitation filter, a 515ichroic longpass mirror and 525/30 emission filter. FRET is detected through a 436/20 excitation filter, a 455 dichroic longpass mirror and 525/30 emission filter. To quantify the FRET signal, we used the ratio of corrected FRET to square root of product of CFP and YFP:

$$FRET\ ratio = \frac{FRET - 0.63 \times CFP - 0.18 \times YFP}{\sqrt{CFP \times YFP}}$$

as proposed by Tadross [32] and Berney [33]. And the mCherry and RFP were detected through a 545/30 excitation filter, a 570dichroic longpass mirror and 610/75 emission filter.

Images processing and data analysis were performed using Matlab R2010a (MathWorks). Field illumination correction, background subtraction, image segmentation, FRET ratio calculation and fluorescence quantification were performed according to the lab generalized protocol [34].

## *2.5 Cell Culture and Chemotaxis*

Cells were cultured at high-glucose DMEM (Life Technology) with 10% heat-inactived FBS (Life Technology) added. To maintain the exogenous gene expression, 400ug/ml G418 (Sigma), 100ug/ml Zeocin (Life Technology), 50ug/ml Hygromycin (Sigma), or 8ug/ml puromycin (Sigma) was added to the medium for certain cell lines.

Microfluidic chips were coated with 10ug/ml human Fibronectin (Sigma) overnight at 4 ºC, washed with DPBS (Life Technology), filled with cell culture medium as above without antibiotics. Cells were seeded 6-8 hours before imaging. Right before the experiment, the ligands (or drugs) were perfused by being diluted in imaging medium: F12K without phenol red (Crystalgen) + 1% heat-inactived FBS + 20mM

HEPES (Sigma) +5mM MOPS (Sigma) + 0.2% BSA (Sigma), and replaced the cell culture medium.

## *2.6 Western Blot*

Cell were pelleted and lysed by RIPA buffer (Thermo Scientific) with Halt protease and phosphatase inhibitor added (Thermo Scientific). Equal micrograms of cellular extracts were separated on 10% TGX mini-precast gels and then transferred to 0.22um nitrocellulose membranes. Washed membranes were blocked by 5% non-fat dry milk (non-phospho-protein detection) or BSA (phospho-protein detection) for 2 hours at room temperature (RT), and then incubated in primary antibodies with recommended dilution overnight at 4 ºC. Infrared-labeled secondary antibodies were applied for 2 hour incubation at RT after. LICOR scanner was used for imaging the western blot.

## *2.7 Immunocytochemisty*

Cells were seeded at 30% confluence onto 20mm diameter circular coverslips (Fisher Scientific) coated with mixture of 0.1% poly_l_lysine (Sigma) and 0.1% gelatin (Sigma) and placed in a well of a 6-well tissue culture plate, then serum starved in medium with reduced serum medium (0.1 % FBS + 0.1% BSA) overnight before experiment.

After exposure to Ang for desired concentration and duration, the cells were washed three times with ice-cold DPBS (Life Technology). 4% paraformaldehyde (Electron Microscopy Sciences) was applied to fix the cells for 30 minutes. The cells were then permeabilized and blocked in blocking buffer contains 0.1% Triton X-100 (Sigma) and 10% goat serum (Life Technology) in DPBS for 1 hour. Primary antibody incubation was done by incubating the cell with mouse anti-phospho-ERK1/2 (1:200 dilution) or rabbit anti-phospho-p90RSK (1:200 dilution) in blocking buffer for 2 hours. Next, the cells were incubated in secondary antibody solution consisting of Alexa Fluor 488-conjugated goat anti-rabbit (1:200 dilution) and/or Alexa Fluor 594-conjugated goat anti-mouse antibodies (1:200 dilution), 2ug/ml Hoechst-33258 (Sigma) for 2 hours. Finally, the stained coverslips were mounted on microscope glass slides and imaged. Cells were thoroughly washed with DBPS between each step.

## *2.8 Computation and simulations*

The ordinary differential equations were setup in Matlab or Mathmatica (Wolfram). The time-lapse results were solved by ode45 or ode15a solvers in Matlab. The steady-state results were obtained in Mathematica. Parameter spaces were explored by Latin hypercube sampling method [35].

# Chapter 3

# Adaptive molecular networks controlling chemotactic migration: dynamic inputs and selection of the network architecture

## *3.1 Adaptation to spatially homogeneous stimuli: why and how?*

Perfect adaptation to step-like increases in the chemoattractant concentration has been observed both in bacterial and eukaryotic chemotactic signaling networks [36-38]. It has been argued that the ability to perfectly adapt to persistent ligand stimulation can provide a signaling system with many important advantages, including but not limited to the ability to extend the range of chemoattractant concentrations over which the gradient sensing would be sufficiently precise [39-41]. This property can, in turn, enlarge the

overall spatial extent of guided navigation, increasing the probability that a cell can successfully locate the source of the signal.

Perfect adaptation of a signaling response turns out to be quite restrictive in terms of the number of possible ways it can achieved. A recent analysis suggested that the 'architecture' or topology, of the underlying signaling networks would be expected to fall into two classes: those containing a negative (integral) feedback (NFB) and those that contain two parallel initially diverging and ultimately converging pathways, affecting the output in opposite ways. The latter network type has been termed an 'incoherent feed-forward' loop (iFFL) [42]. The basic topologies of the two types of networks are showed as in Figure 3.1:

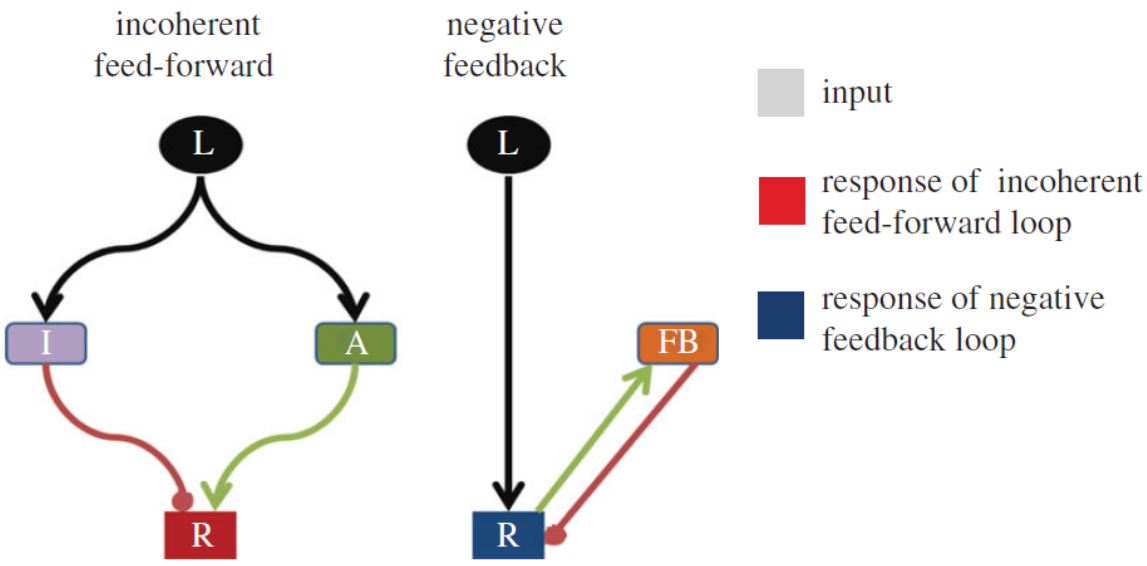


**Figure 3. 1 Structural comparison of the incoherent feed-forward loop and the negative feedback networks. The two types of networks that can achieve perfect adaptations. Upon ligand (L) stimulation, signal is transduced through an activating (A) and a delayed inhibitory (I) pathway to the response (R) node for the iFFL network; by contrast, the signal directly affects the response node (which has a feedback node attached) for NFB;**

We built the mathematical model based on the above structure. The ordinary differential equations (ODE) for the iFFL model are:

$$\frac{dA}{dt} = \rho_A(k_l \times L - k_d * A(t) + k_c)$$

$$\frac{dI}{dt} = \rho_I(k_l \times L - k_d * I(t) + k_c)$$

$$\frac{dR}{dt} = \rho_R(A(t) \times (R_{tot} - R(t) - I(t) \times R(t))$$

The ODEs of NFB model are:

$$\frac{dFB}{dt} = \frac{k_{cb} \times R(t) \times (1 - FB(t))}{1 - FB(t) + K_{cb}} - \frac{k_{Fbb} \times FB(t)}{FB(t) + K_{Fbb}}$$

$$\frac{dR}{dt} = \frac{k_{ac} \times L \times (1 - R(t))}{1 - R(t) + K_{ac}} - \frac{k_{bc} \times R(t)}{R(t) + K_{bc}}$$

The parameters and initial conditions are listed as in Table 3.1:

| | |
|---|---|
| A(0) | 0.05nM |
| I(0) | 0.05nM |
| R(0) | 0.5nM |
| L | input |
| $k_l$ | 0.3 |
| $k_d$ | 2.0 |
| $k_c$ | 0.1nM |
| $\rho_A$ | 0.1/sec |
| $\rho_I$ | 0.01/sec |
| $\rho_R$ | 0.01/sec |

| | |
|---|---|
| $R_{tot}$ | 1.0 nM |
| $K_{cb}$ | 0.007 |
| $K_{Fbb}$ | 0.1473 |
| $k_{cb}$ | 0.0769 |
| $F_b$ | 1 |
| $k_{Fbb}$ | 0.0041 |
| $k_{ac}$ | 0.4695 |
| $K_{ac}$ | 4.7339 |
| $k_{bc}$ | 0.079 |
| $K_{bc}$ | 0.0069 |

**Table 3. 1 Parameters and conditions for simulation**

For the purpose of direct comparison, we modified the parameter of NFB model to fit its curve peak and time to the iFFL curve as showed in Figure 3.2. This helped us to recognize the discrepancy of the two models.

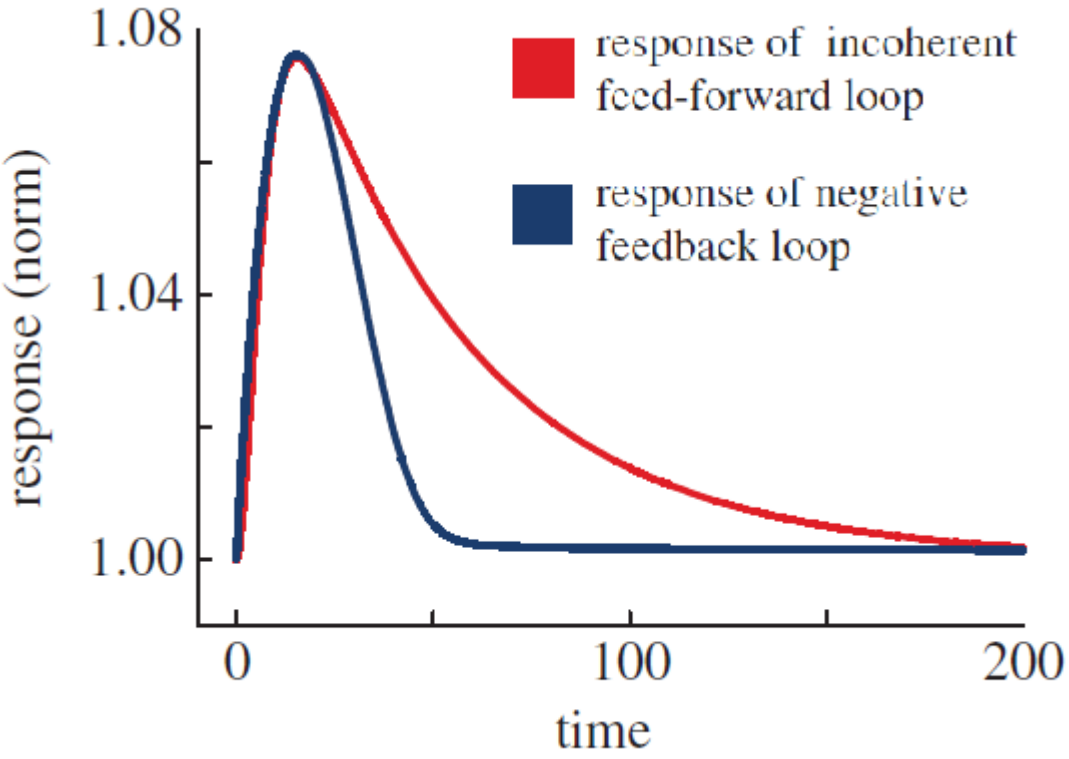


**Figure 3. 2 We modified the parameter to fit the time courses of NFB and iFFL curve: when the time to peak and the peak amplitude are matched in the models of iFFL and NFB, both models display perfect adaptation to a step input, with longer adaptation for iFFL**

It is of interest, and as suggested below, of possible importance, that the current biochemically informed models of bacterial chemotaxis postulate a type of negative feedback that carries information about a time integral of the input [6]. On the other hand, the prevailing model of an adaptive chemotactic signaling network, particularly in the archetypal examples of eukaryotic chemotactic motility of the amoebae cells of Dictyostelium discoideum and mammalian neutrophils, postulates an underlying iFFL [43-47]. Whereas the NFB model of bacterial chemotaxis has rarely been questioned, the

iFFL model in eukaryotic cells has been under continuous debate, in part because the molecular components constituting the feed-forward loop are still not established with certainty [48]. However, recent analysis has argued particularly convincingly that iFFL is indeed the main driving molecular network type underlying both the perfectly adaptive response to spatially homogeneous changes in chemotactic stimuli and persistent non-adaptive signaling in the presence of spatially graded distributions of the same stimuli [49, 50]. The experiments used to provide this evidence relied on exposing cells to dynamic stimuli more complex than a simple step-like increase in the stimulant concentration, with the temporal complexity of the inputs used in particular not only to argue in favor of iFFL model, but also against NFB models.

## *3.2 Deciding between two mechanisms of perfect adaptation*

What signaling inputs can help to distinguish between two possible different network architectures, both of which can account for adaptive behavior, particularly if the molecular components of these networks are not precisely established? A popular test of network connectivity widely used in engineering and, more recently, in biology is to expose cells to oscillatory inputs [51-57].

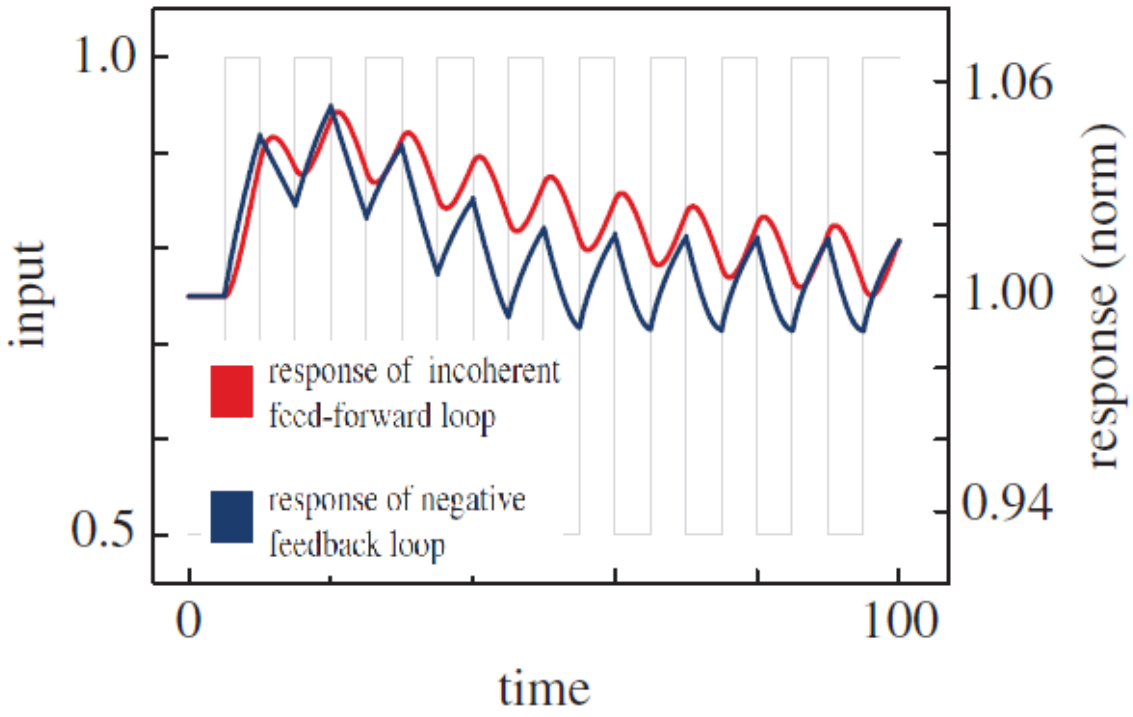


**Figure 3. 3 We applied oscillatory input to both models. Both of them showed periodic response.**

Measurement of the signaling outputs when the frequency of the input is varied can reveal inherent filtering capabilities of the molecular circuit, so that the response is maximized at high ('high-pass filter'), low ('low-pass filter') or intermediate ('band-pass filter') input frequency. In the case of yeast osmoregulation, the signaling pathway mediation of cell adaptation to high osmolarity has been shown to have band-pass filtering properties, the property that was used to infer the existence behind a negative feedback network structure. Unfortunately, although band-pass filtering requires considerable network complexity, both negative feedback and iFFL circuits can be powerful band-pass filtering devices (Figure 3.4).

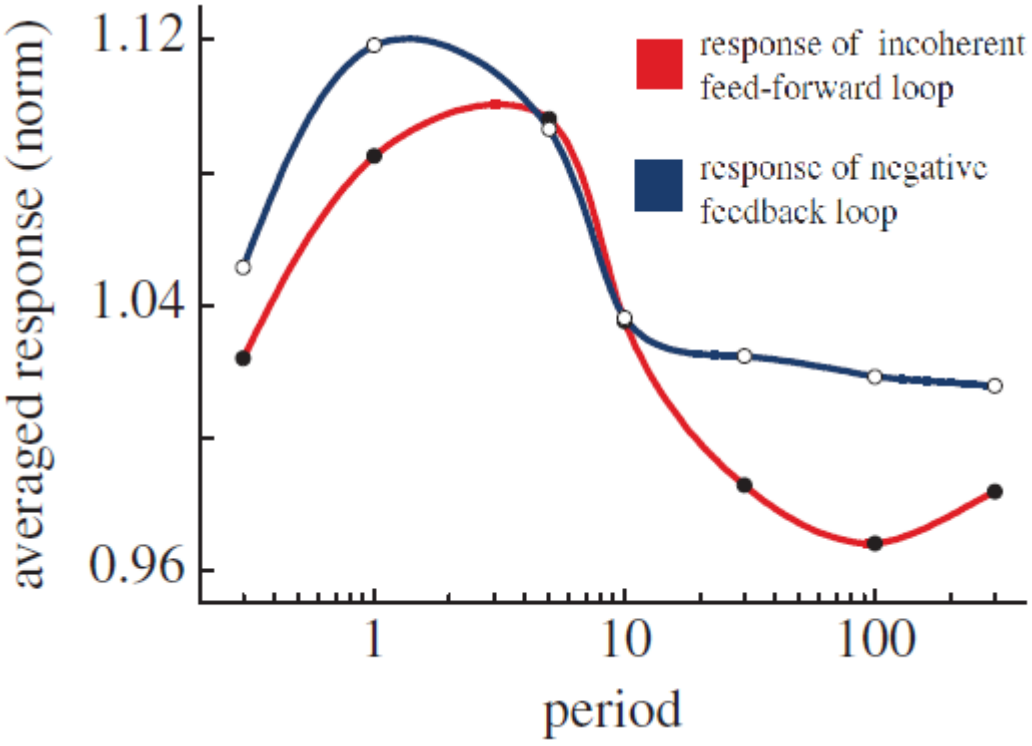


**Figure 3. 4 Both models showed band-pass filter behavior**

Indeed, if simple NFB and iFFL models are matched in such a way that the adaptation to a step input yields identical timing and amplitude of the transient response ('matched iFFL and NFB models'), their responses to various dynamic stimuli [58] can be meaningfully contrasted (figures 3.4, 3.5 and 3.6). If such matched iFFL and NFB models are subjected to oscillatory stimuli, both show essentially indistinguishable dynamic response characteristics and qualitatively similar band-pass responses (figure 3.4). Thus, even though a recent analysis has demonstrated that the network underlying adaptation in *D. discoideum* chemotaxis has band-pass filtering characteristics [49], this fact could not be used to determine whether the adaptive response relied on iFFL or on NFB signaling circuits.

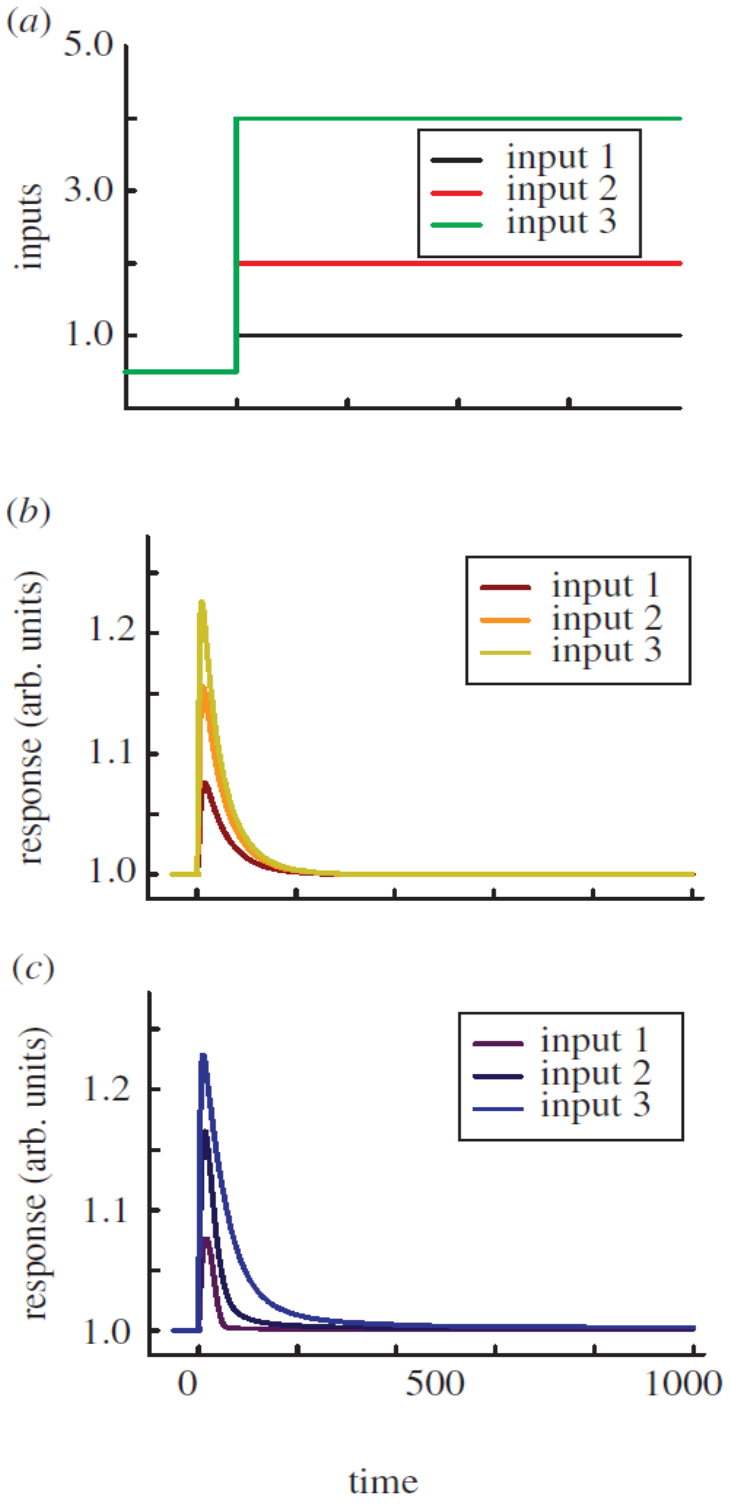


**Figure 3. 5 The two networks behave similar at stepped stimuli input in a), both b) iFFL and c) NFB showed perfect adaptation.**

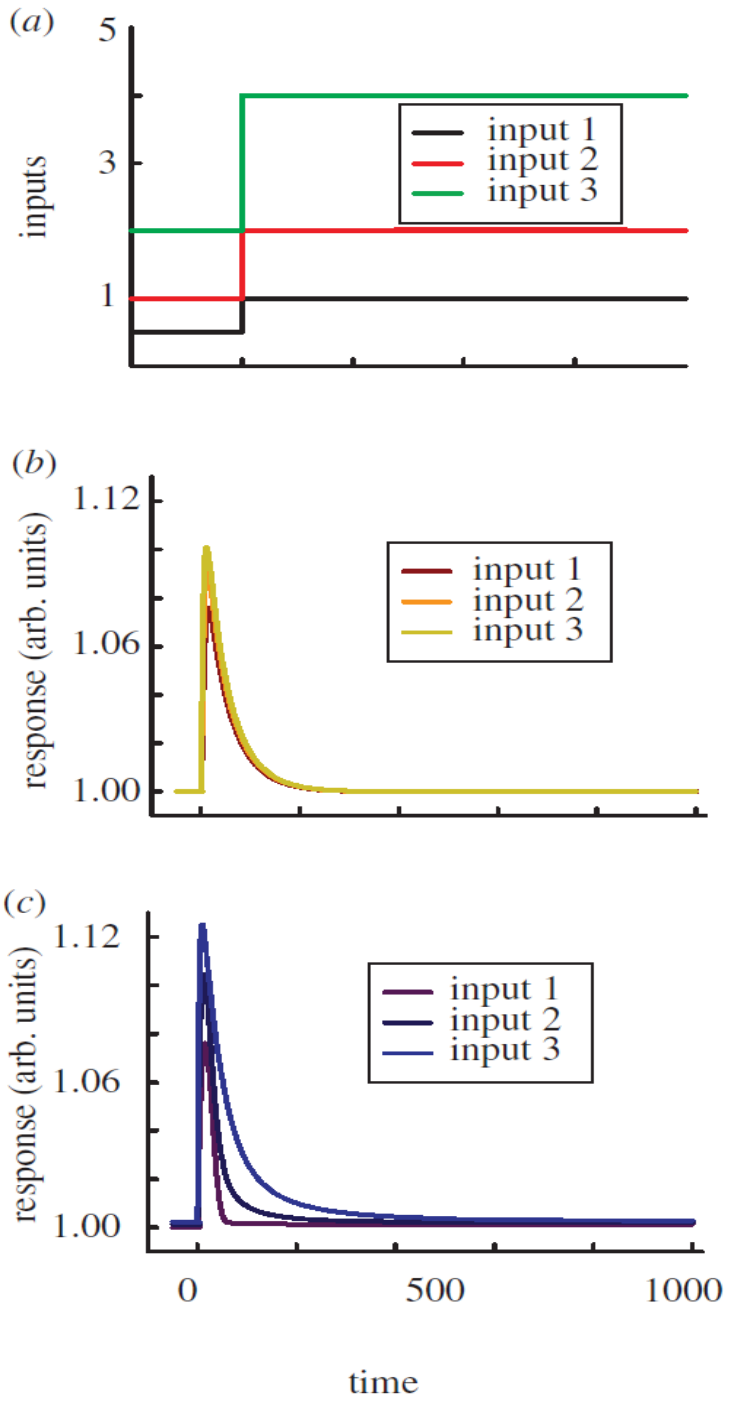


**Figure 3. 6 The two networks behave similar at fold-change stimuli input in a), both b) iFFL and c) NFB showed perfect adaptation. And iFFL keep its shape to all fold-change inputs**

What might be the input that discriminates between the underlying iFFL and NFB architectures? It turns out that 'ramp' inputs, i.e. the inputs that persistently increase with constant rates, can be such discriminating dynamical test inputs. Indeed, as can be easily seen from stimulation of the matched iFFL and NFB networks (Figure 3.7), and shown on more theoretical grounds, the NFB does not adapt perfectly to ramp stimulation, instead, coming to a steady-state activity proportional to the slope of the ramp [49]. In this sense, its output is proportional to the time derivative of the input, with the NFB serving as the 'differentiator'. On the other hand, the iFFL can perfectly adapt to the ramp stimuli, with the transient response but not the steady-state behavior affected by the slope of the ramp. This test, when applied to the *D. discoideum* chemotactic signaling network, strongly suggested that it indeed has the embedded iFFL but not NFB structure. However, when applied to the high osmolarity response pathway in yeast or in bacterial chemotaxis, the lack of adaptation to ramp stimulation strongly supported NFB architecture [59].

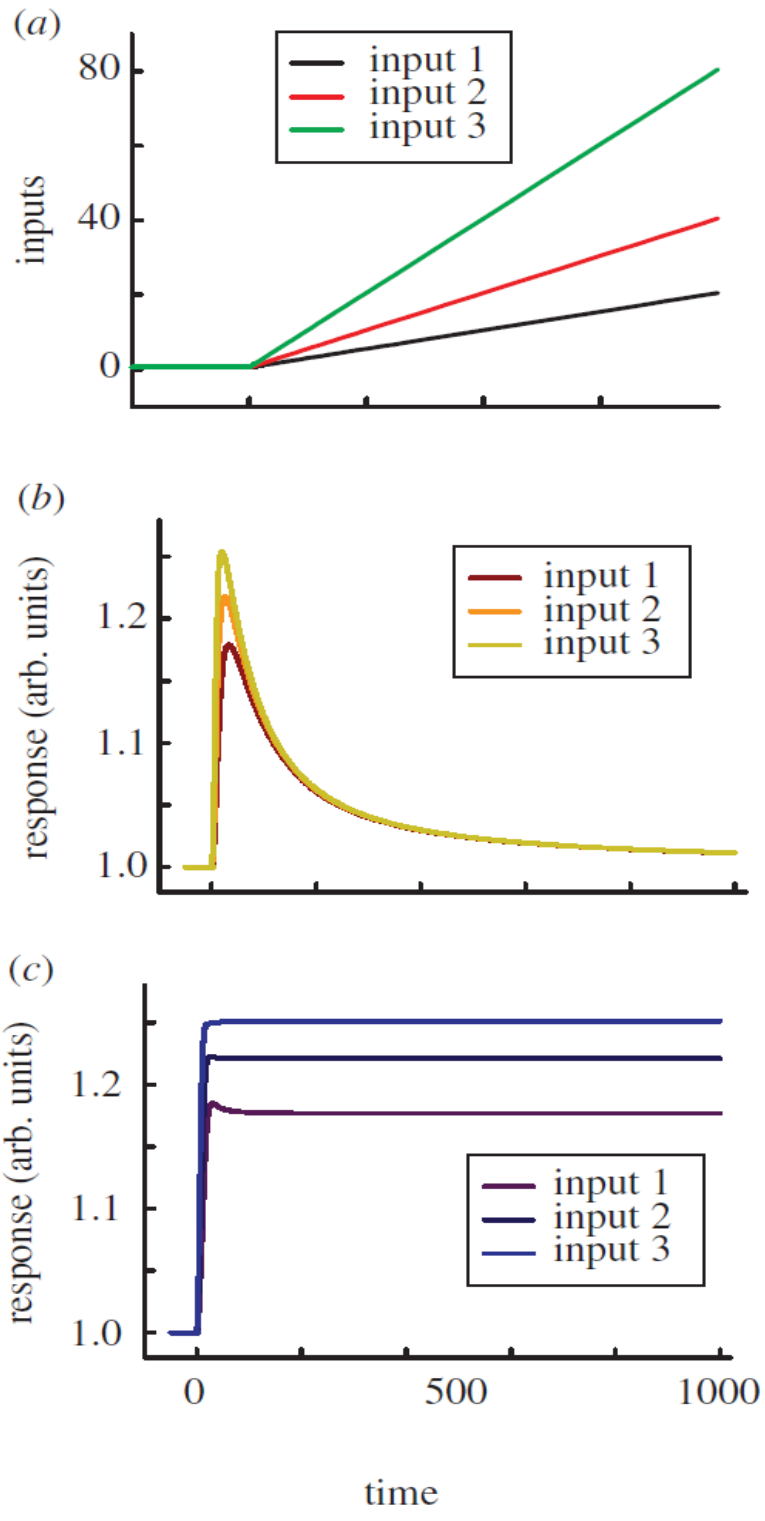


**Figure 3. 7 The ramp inputs in a) can distinguish the two network architectures: b) iFFL and c) NFB. NFB can not adapt to ramp inputs, but is a good choice for measuring the slop of ramp.**

## *3.3 Can there be different selective pressure for evolution of different adaptation mechanisms?*

Mounting evidence suggesting that adaptive molecular networks responsible for chemotactic responses can rely on both iFFL and NFB architectures begs the question of whether this evolutionary choice is biased by the demands of the chemotactic response itself for different organisms or whether it is more random. Where can the selective pressure stem from? As shown above, the key difference in dynamic responses between these network types can lie in their response to the dynamically complex stimuli, in particular, ramp inputs. Can this difference also suggest why these networks can present unique advantages in the real-world chemotactic behavior? This is an important consideration, in part because laboratory analysis is frequently designed to present cells with simplified inputs versus those faced by the cells in more natural situations. Fortunately, for both bacterial chemotaxis and the chemotaxis of the amoebae *D. discoideum*, much is known about their natural environmental inputs, thus permitting the analysis of what the relevant input distribution is and what the cells might in fact respond to incoherent feed-forward loop or negative feedback.

The key difference between bacterial chemotaxis and chemotactic responses by eukaryotic cells, including *D. discoideum*, is that bacterial cells, given their small size, have to actively explore the chemotactic fields by actively moving within them, whereas the eukaryotic cells are large enough to reliably measure the difference between the concentrations of the chemoattractant across the cell length. Therefore,

bacterial cells effectively measure the spatial gradients of chemoattractant by exploring them in time, sampling concentrations as they actively navigate through them during their own locomotion. Thus, the measurement that the cells rely on is the measurement of the rate of change of the chemotactic input, corresponding to the ramp stimulation discussed above. As the rate of the change increases, the cells would tend to maximize their response, recognizing that they move in the direction leading them more precisely towards the source of the chemoattractant. As suggested above, NFB circuits are perfectly suited for this type of computation, with the steady-state response proportional to the slope of the ramp stimulus (a complication here can arise from the properties of the receptors involved in bacterial chemotaxis, so that in fact exponential rather than linear ligand ramps need to be delivered to ensure linear ramp input into the NFB signaling network downstream of the receptor [60-62]). The situation in the natural *D. discoideum* responses is more complex. During the developmental response, individual cells assemble into a multicellular organism by virtue of both secreting and responding to a chemoattractant, presenting in the form of self-sustained waves propagating through the cell community. Therefore, individual cells are exposed to a complex input presenting them with crests and troughs of chemoattractant concentration, and gradients that can change their sign (direction) as the crest (trough) of the wave passes over a cell. Although a cell can measure the gradient without moving or while moving relatively slowly, the conflicting cues have the potential to force its movement both towards and against the direction towards the source of the chemoattractant. Therefore, it can be hard to make progress; yet individual cells appear to solve this problem well. This fact strongly suggests that the cells can be sensitive to the spatial gradient on only one side (trough to

crest) but not the other (crest to trough) of each incoming wave. Furthermore, the cells can maximize the response if the fact that the average concentration changes during the passage of each wave does not interfere with their spatial gradient measurement. Hence, adaptation to temporally changing input can be a key in this response, necessitating the iFFL but not the NFB architecture.

These considerations, although still largely speculative, strongly suggest that the complexity of the environmental inputs faced by individual chemotactic organisms as well as the internal limitations inherent in these organisms (e.g. the size of a cell undergoing chemotaxis) can impose important constraints in selection of one of the available adaptive network architectures. This observation is linked to a more general question often ignored in the analysis of signaling networks which aspect of the input do cells really 'care about'? More precisely put, which aspect of the input contains the most information relevant to the cell decision- making? [63, 64] The information about spatial gradients can be contained both in space and in time, and individual networks may evolve to respond to one of this information sources while ignoring the other.

Another important aspect of functioning of different molecular networks is their noisy nature. Indeed, chemical reactions can be subject to considerable fluctuation in concentration and thus rates of various reactions. Again it may be instructive to determine whether the ability of iFFL and NFB circuits to withstand such fluctuations may be similar. Simulation results for the matched models (Figure 3.8 and 3.9) suggest that the NFB can robustly ensure constant duration of the output to the step increase in the chemoattractant input (the duration of the transient peak) but not the amplitude of the output (the height of the peak).

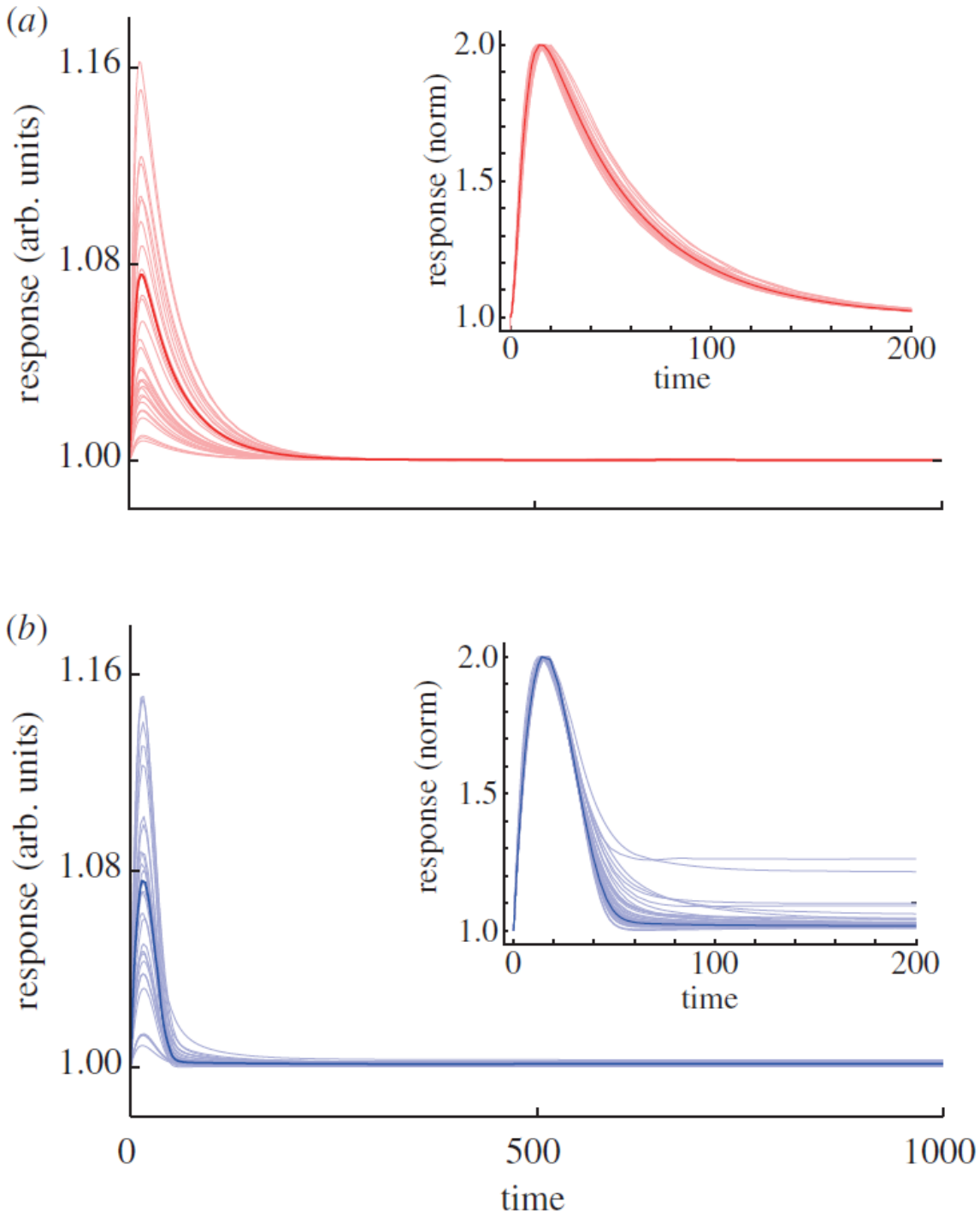


**Figure 3. 8 Comparison of iFFL and NFB model outputs under noisy parameter sets. Variation of parameter values by 10% introduces variability of responses to step inputs for the matched iFFL (red, a) and NFB (blue, b). The inserts are normalized response by overlapping their peaks. Normalization to the value**

**of the amplitude of the peak responses suggests the possibility for a substantial reduction of variability in all responses, but in particular in the response of the iFFL model to the step input.**

On the other hand, the response of the iFFL model is much more variable in terms of the peak duration, since, in this response, the amplitude is linked more tightly to the duration of the peak. This result may suggest lower robustness of the iFFL circuit to the 'noise' or small variations in the activity of the signaling pathways. However, the tight coordination between the amplitude of the peak and its duration also implies that correcting for variability in either amplitude or duration can also decrease the overall variability of the response (Figure 3.8 and 3.9), making iFFL more robust to noise than NFB. This property of the iFFL circuit can be connected to the so-called 'fold- response' capacity, i.e. the ability of the sensory system to robustly measure fold-changes in response, while being less sensitive to either average value of the input or the less substantial input changes. This property may in turn relate to inherent ability of iFFL to adapt to linear ramp inputs, as discussed earlier, suggesting that nonlinear inputs characterizing fold responses can be more effective in eliciting sustained responses. The consequences of this property for gradient sensing capabilities of *D. discoideum* and other chemotactic cells and organisms remain to be explored.

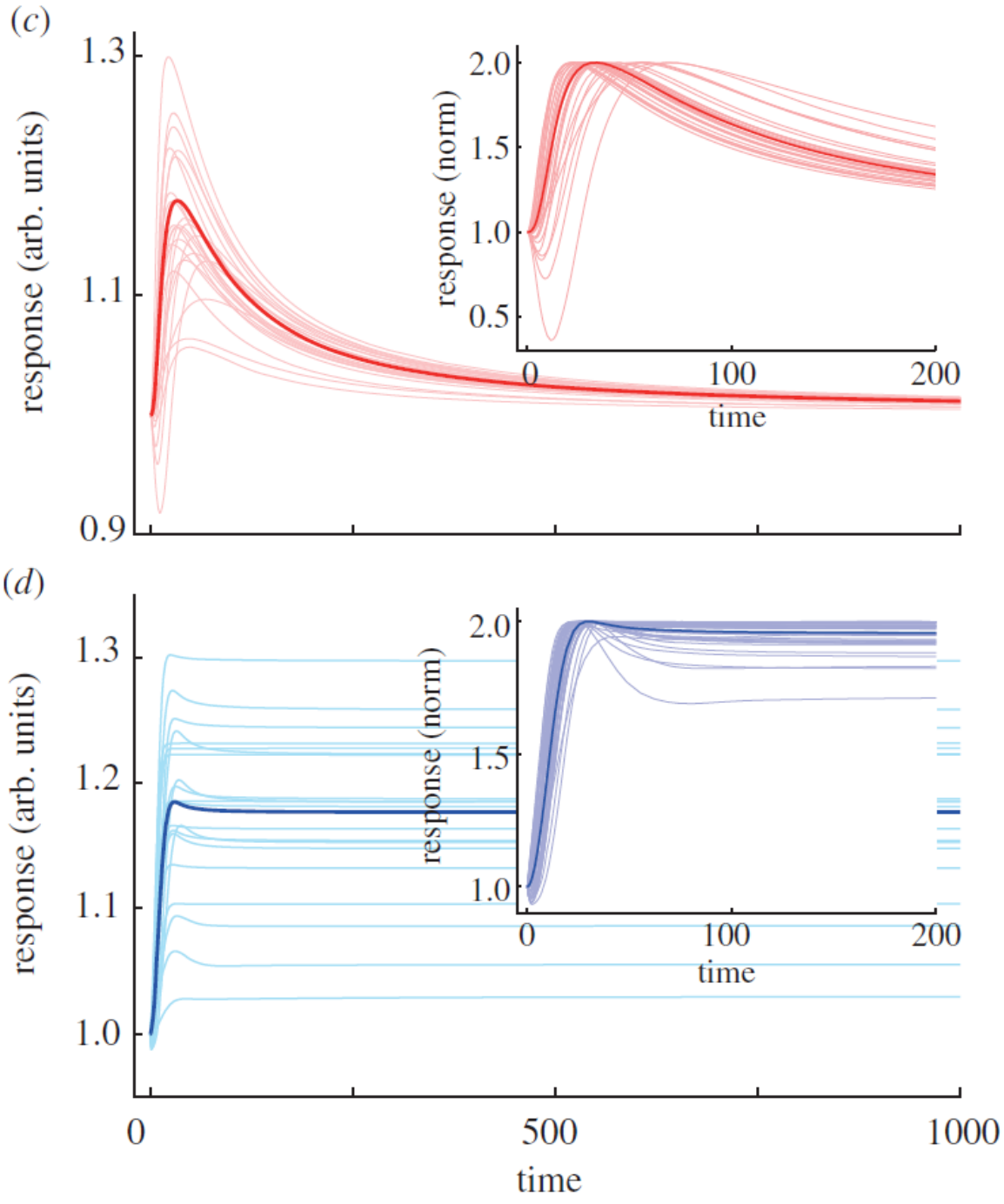


**Figure 3. 9 Comparison of iFFL and NFB model outputs under noisy parameter sets. Variation of parameter values by 10% introduces variability of responses to ramp inputs for the matched iFFL (red, a) and NFB (blue, b). The inserts are normalized response by overlapping their peaks' heights.**

## *3.4 Analysis of other signaling networks with incompletely known chemical composition and organization*

Understanding the structure of signaling networks is paramount for investigation of their dynamical behavior and function. However, frequently, the molecular components of these networks and their inter-molecular interactions may not be completely known or easily assayed using classical tools of genetics and molecular biology. As illustrated earlier, the ability to expose live cells to tightly controlled dynamically complex stimuli can help distinguish between alternative models that can account for observed signaling responses. This analysis involves a combination of mathematical analysis and matched quantitative experimentation, which together can help unravel the functional characteristics of the signaling apparatus. Importantly, this analysis can also be suggestive of the nature of the environmental inputs processed by the networks. The fact that the natural, *in vivo* signaling fields are known for at least some chemotactic responses, along with the knowledge of limitations on the sensory capabilities of chemotactic cells, has been used above to justify the use of alternative sensing strategies. However, for many other signaling networks, the dynamics and spatial distribution of signaling inputs are frequently unknown. Controlled presentation of large sets of distinct, dynamically complex stimuli can allow one to determine which aspects of the input can be sensed best and which stimuli can trigger qualitatively distinct outputs. This analysis should inform both the hypotheses about the wiring and composition of

signaling networks, and the analysis of how evolutionary selection of a particular network type might have taken place. Signaling networks underlying cell polarization and chemotactic migration can thus serve as important and influential archetypes for the new era of quantitative analysis of noisy and dynamical cellular information processing.

# Chapter 4

# Beta-arrestin2-mediated Chemotaxis

## *4.1 Background*

Scaffold proteins can both facilitate or inhibit signaling processes in a concentration-dependent manner [65]. This dual function can be achieved since scaffolds expressed at low or optimal levels can enforce juxtaposition of interacting molecular species, whereas scaffold over-expression can titrate these molecular species away from each other. This dose dependence suggests that uneven spatial distribution of scaffold molecules within a cell can result in a spatially inhomogeneous signaling outcome, which in turn might lead to polarization of cellular functions regulated by the signaling. If these functions are associated with re-organization of cellular cytoskeleton, oriented cell growth or migration may ensue. Indeed, within the context of the yeast mating response, inhomogeneous distribution of a scaffold protein within a cell responding to a pheromone gradient can result in a spatially graded distribution of the associated MAPK signaling [66]. Furthermore, global variation of the scaffold levels within the same signaling system has the predicted biphasic effect on the downstream gene regulation [67]. However, it is not clear whether the scaffold-mediated gradient of MAPK activity in the yeast mating response is causally related to the associated directed cell growth [31].

Furthermore, in spite of these suggestive findings in budding yeast, the existence of similar cell polarization mechanisms and their possible relationship to directed migration response in other cell types, e.g., in mammalian migratory cells, remains unclear.

beta-arrestin2 is a ubiquitous mammalian scaffold molecule implicated in the control of chemotactic responses. Subsequent research also implicated these proteins in classical scaffolding functions, by demonstrating their association with and regulation of multiple signaling pathways [68]. Furthermore, a recent study demonstrated that beta-arrestin-2 function is essential for directed migration of HEK293 cells expressing Angiotensin II (AngII) receptor (AT1aR) in sharp gradients of AngII [25]. This result however, left open multiple questions about the putative beta-arresin2 role in control of chemotaxis. Does it enforce chemotaxis, by promoting polarization of signaling and cytoskeletal components as proposed above, or is its role in regulation of chemotaxis purely permissive? Is the signaling pathway scaffolding or receptor internalization function of beta-arrestin2 primary in this response? Moreover, it is unclear if the distribution of beta-arrestin2 within the cells exposed to AngII gradients is spatially inhomogeneous, and if so, whether the polarization of the signaling can be compromised in very shallow AngII concentration gradients. Answering these questions may reveal a previously unappreciated, new mechanism of cell polarization and chemotactic response.

In this study, using a combination of diverse experimental techniques and computational modeling, we set out to ascertain the importance of beta-arrestin2 in chemotactic regulation and to investigate the underlying mechanisms. We found that the control of chemotactic behavior by beta-arrestin2 depends on its ability to serve as a classical scaffold protein in the ERK1/2 MAPK (ERK) signaling pathway, but also,

surprisingly, that both receptor internalization and signal scaffolding functions of beta-arrestin2 are critically important for effective chemotaxis. Trafficking of internalized receptor complexes is essential for amplification of shallow input gradients, whose direction was decoded by signaling through the ERK pathway. Overexpression of beta-arrestin-2 leads to dramatic changes in cell migration behavior, including conversion from chemo-attraction to chemo-repulsion. Overall, the interplay between the scaffold expression, input dose, and intracellular trafficking is found to be critical in defining this new mechanism of cellular polarization and chemotactic migration.

## *4.2 Results*

### *Beta-arrestin is necessary in chemotaxis*

The initial evidence for the importance of beta-arrestin2 in chemotactic response to AngII gradients was obtained from trans-well experiments [25]. However, these assays did not always have unambiguous interpretation, as the results may depend on both migratory and invasive cell behavior. We therefore first validated AngII-mediated chemotactic behavior by direct monitoring of live cell migration within a microfluidic device, which design allowed the analysis of cell responses to diffusion-based gradients [31]. We indeed found that HEK293 cells with exogenously expressed AT1aR displayed a pronounced chemotactic behavior within shallow AngII gradients (Figure 4.1).

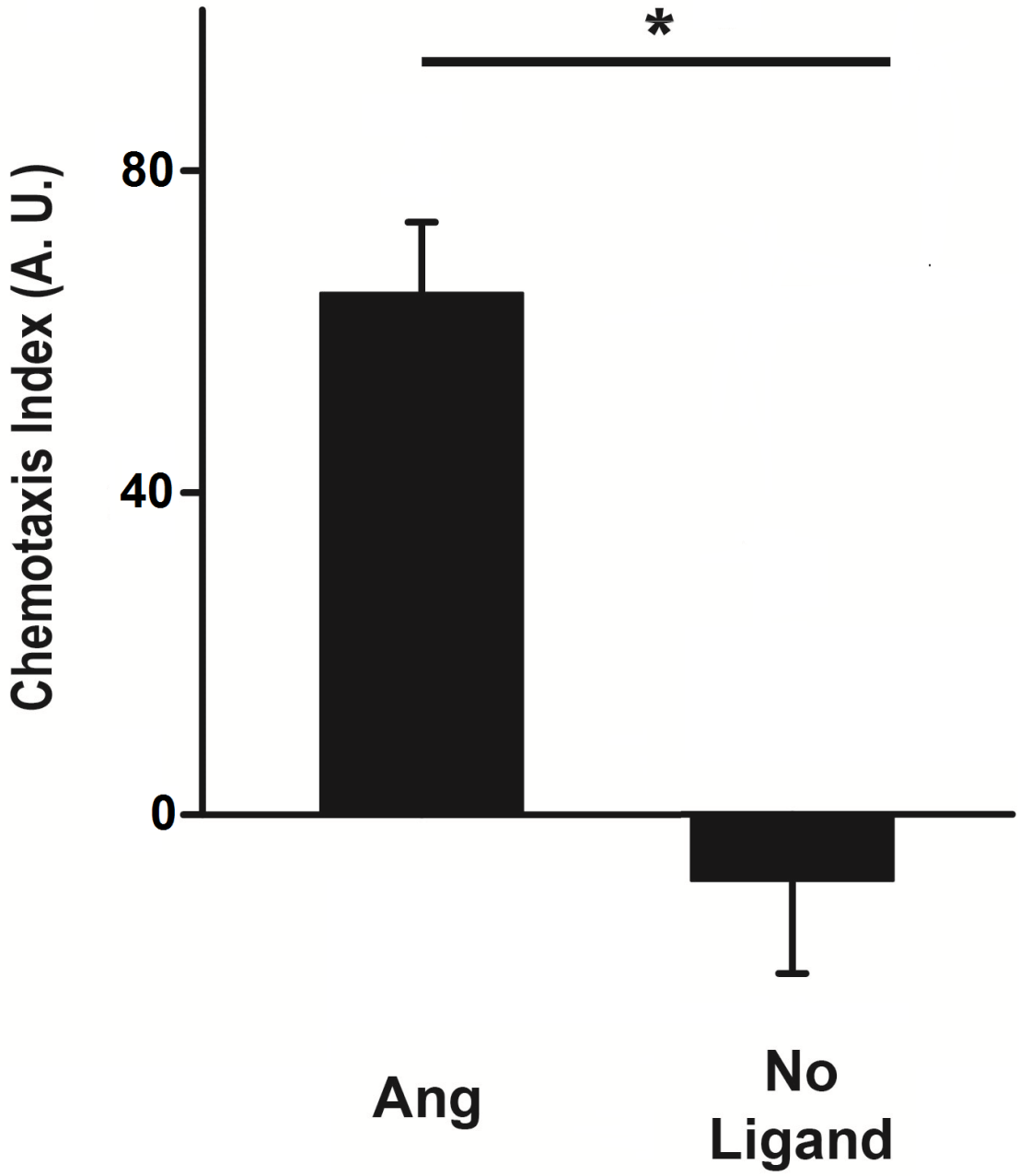


**Figure 4. 1 HEK cells expressing Angiotensin receptor are chemotactic to angiotensin II gradients. * denote p<0.01. Error bars denote the standard error of the mean.**

We also observed that A7r5 rat vascular smooth muscle cells endogenously expressing AT1aR displayed a strong chemotactic response to AngII, supporting its function as an effective natural chemoattractant, and consistent with prior results [69] (Figure 4.2).

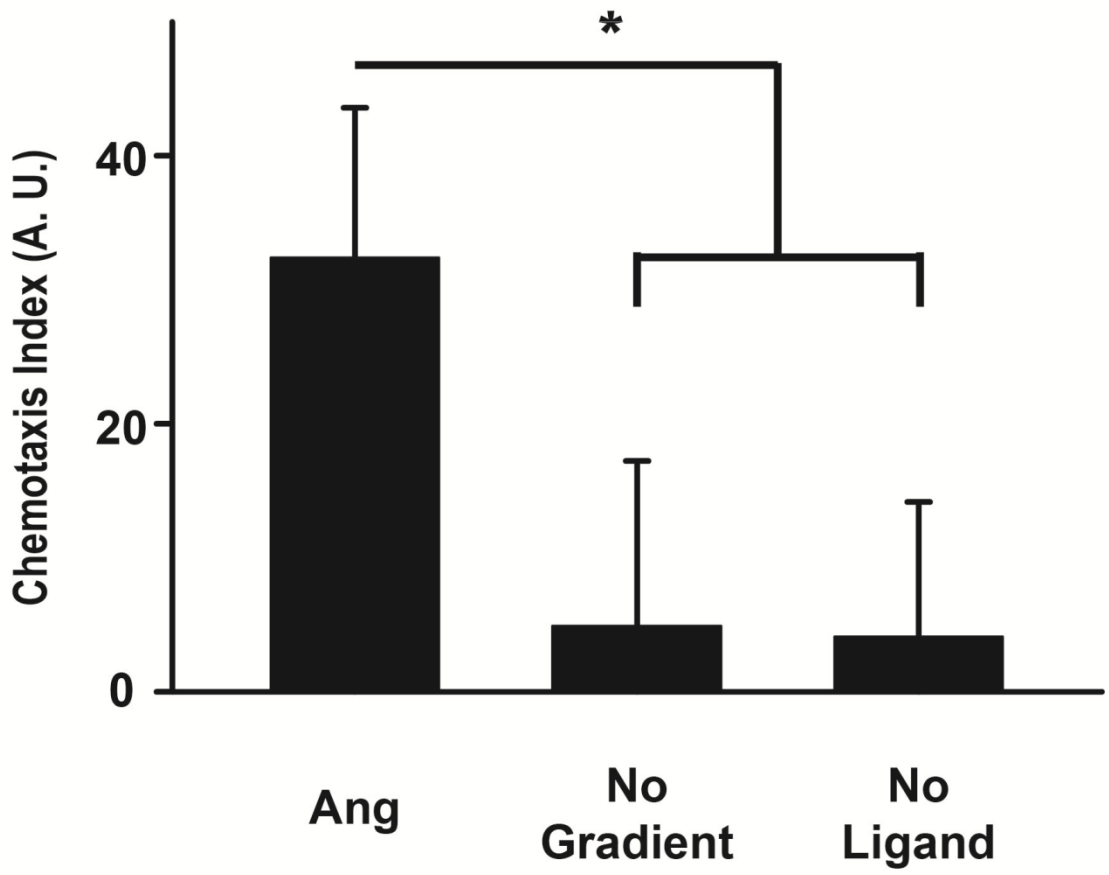


**Figure 4. 2 Vascular smooth muscle cell shows chemotaxis behavior in our microfluidic devices. * denote p<0.01. Error bars denote the standard error of mean.**

Increasing the value of the AngII gradient led to stronger chemotactic attraction of HEK293 cells, the response that was further amplified when the levels of beta-arresin2 were moderately over-expressed (Figure 4.3).

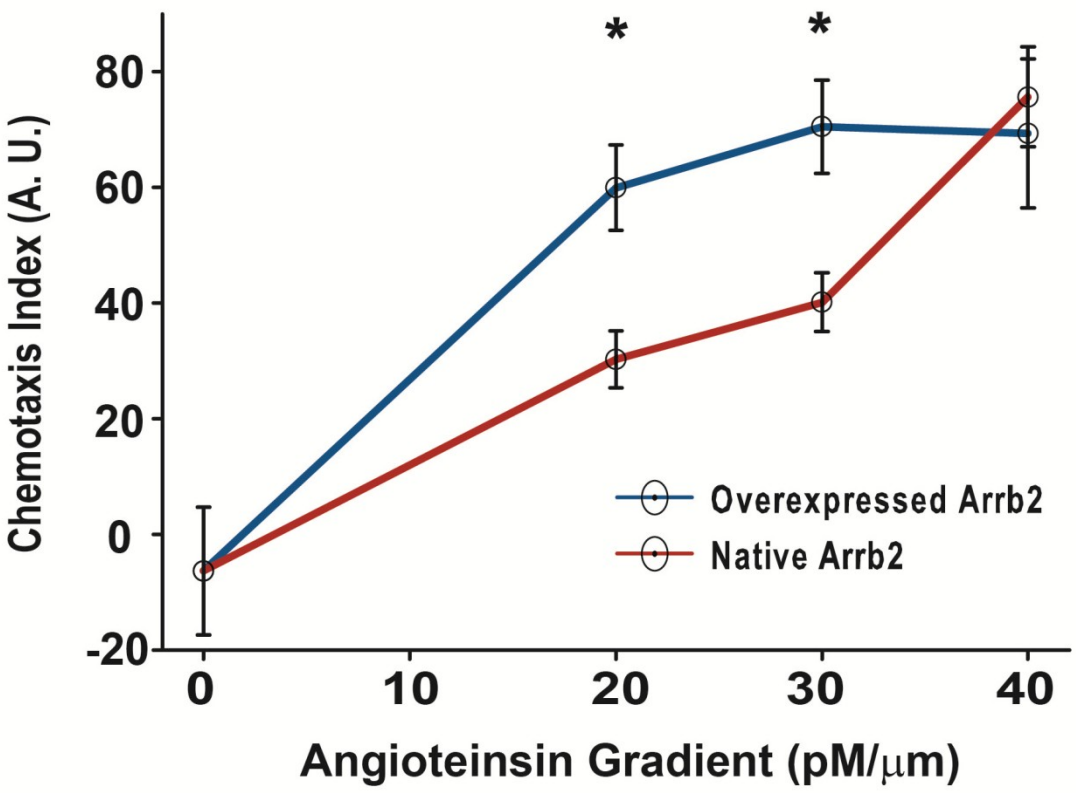


**Figure 4. 3 Cells response to different gradients. Moderately expressed beta-arrestin2 increases the cell sensitivity to external gradient. * denote $p<0.01$. Error bars denote the standard error of mean.**

We also confirmed that shRNA mediated silencing of beta-arrestin2 expression severely suppressed chemotaxis (Figure 4.4), and that chemotaxis could occur in the gradients of a biased AT1aR agonist, SII (Figure 4.5).

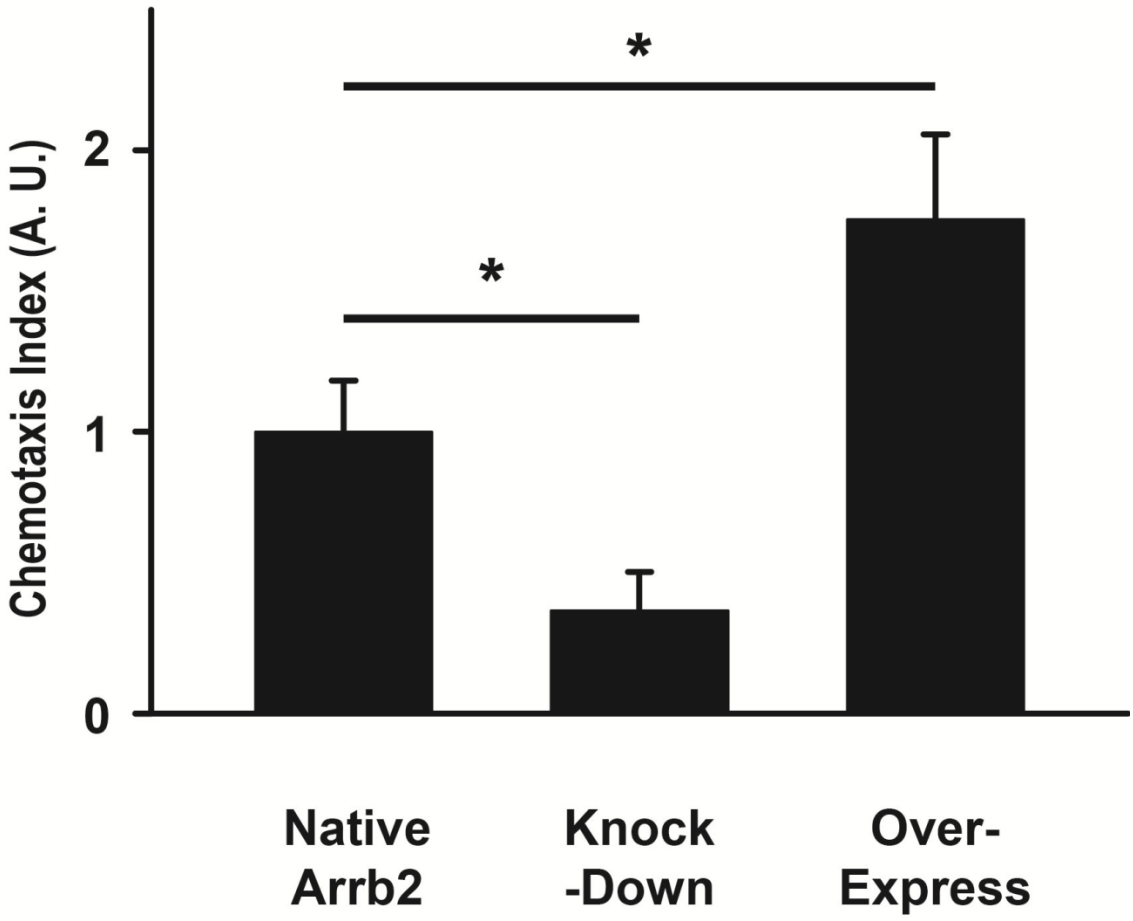


**Figure 4. 4 Knockdown of beta-arrestin2 will reduces the cell chemotactic response. * denote p<0.01. Error bars denote the standard error of mean.**

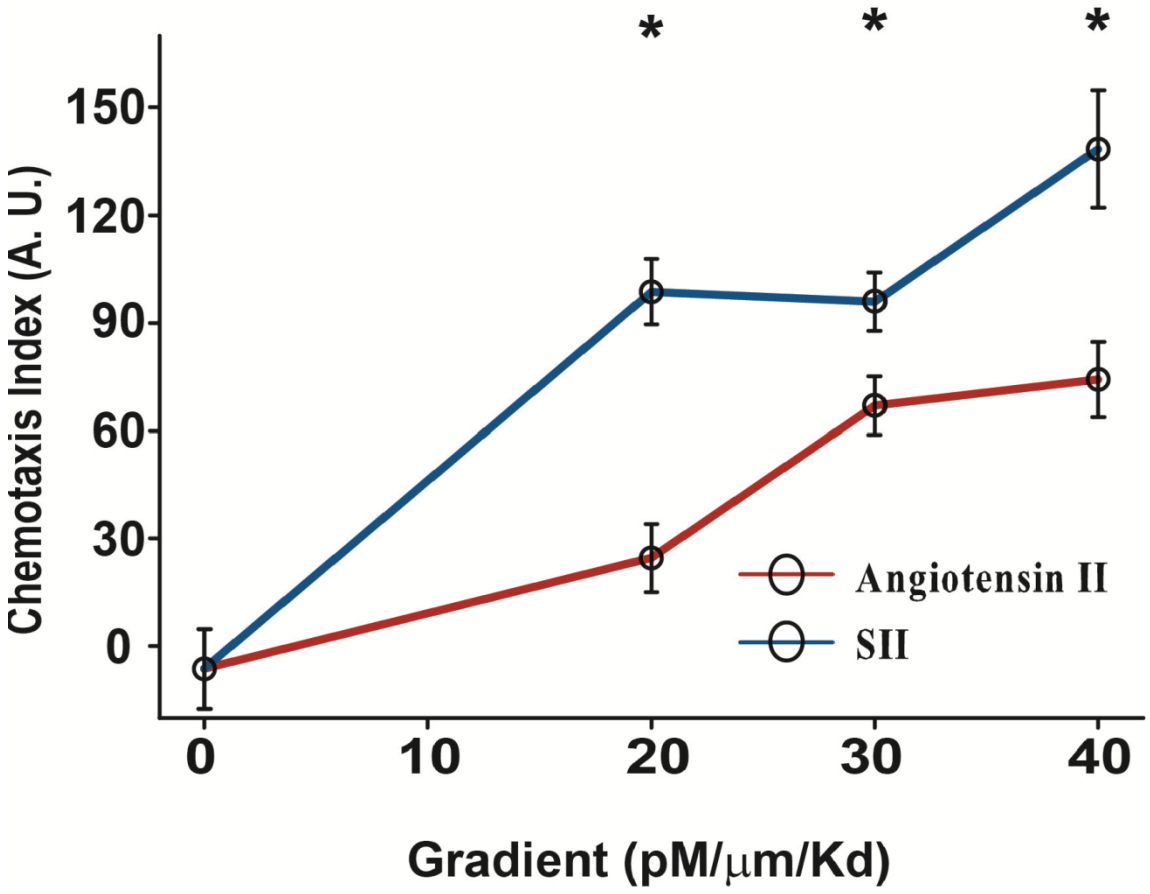


**Figure 4. 5 Angiotensin analog, SII, which only activates the beta-arrestin2-dependent pathway without triggering the G-protein depend pathway, enhances the cell chemotactic behavior. * denote $p<0.01$. Error bars denote the standard error of mean.**

Furthermore, we observed that chemotactic response to SII was surprisingly stronger than chemotaxis to AngII, as evidenced by the normalization of the results to account for different receptor affinity of these two compounds. These findings suggested that the bone fide chemotactic response to AngII was indeed beta-arrestin2 and ERK dependent.

## *What other molecules are involved in beta-arrestin2 mediated chemotaxis*

How does beta-arrestin2-mediated signaling control the chemotactic response? To analyze the underlying molecular mechanisms in greater details, we first exposed the cells to spatially homogenous step-wise elevations of AngII concentration. We used several live cell probes to follow different stages of the AngII triggered signal propagation. We found that, at different AngII doses, beta-arrestin2 displayed transient translocation to the membrane, followed by persistent cytosolic localization (Figure 4.6) in complex with AT1aR within internalized vesicles (Figure 4.7).

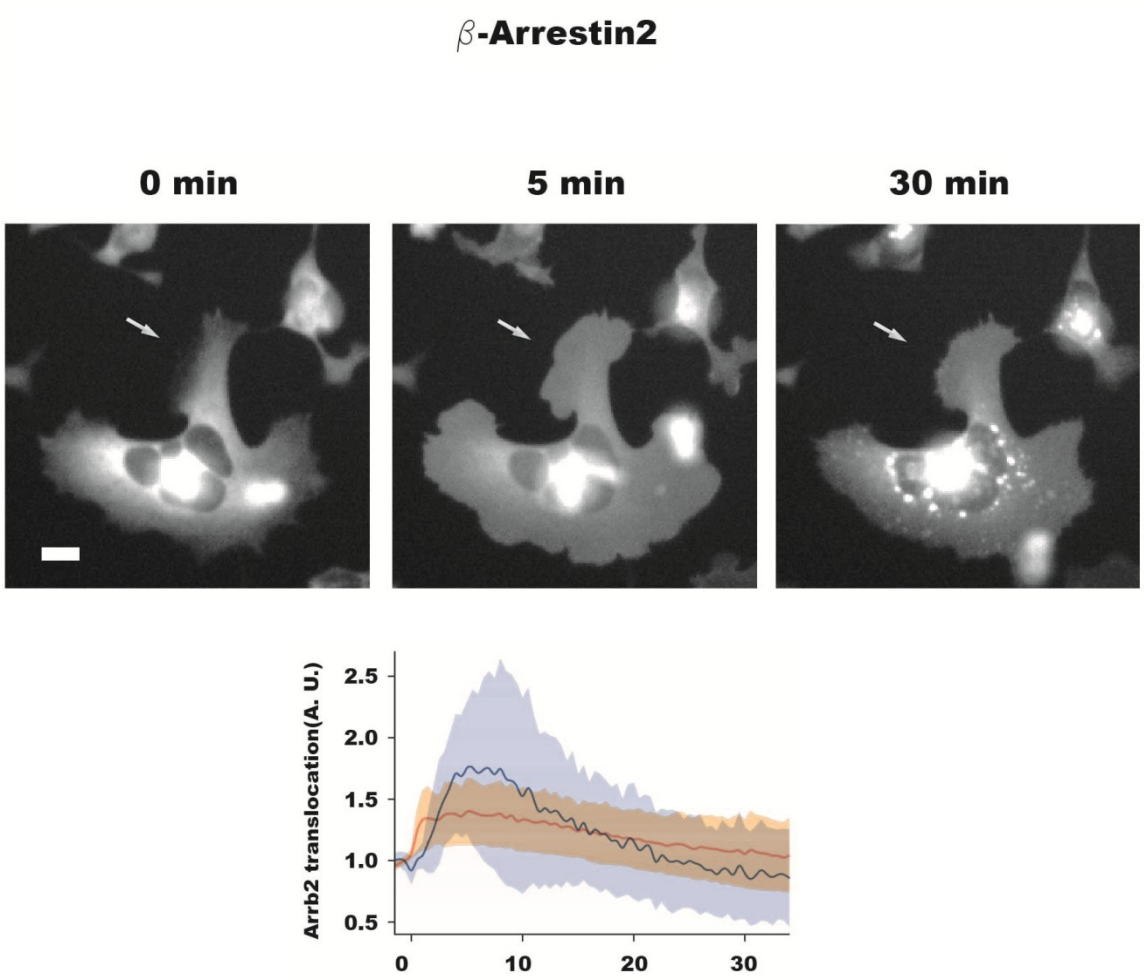


**Figure 4. 6 Beta-arrestin2 is recruited to the membrane upon AngII stimulation (5 minute), then binds to receptor and forms internalized vesicle (30 minute). The plot showed the time course of beta-arrestin2 translocation to membrane. Shades denote the standard error of the mean while solid lines are the mean values. Blue is for high dose of AngII (30ng/ml) and orange is for low dose (1.6ng/ml). Scale bar size: 5um.**

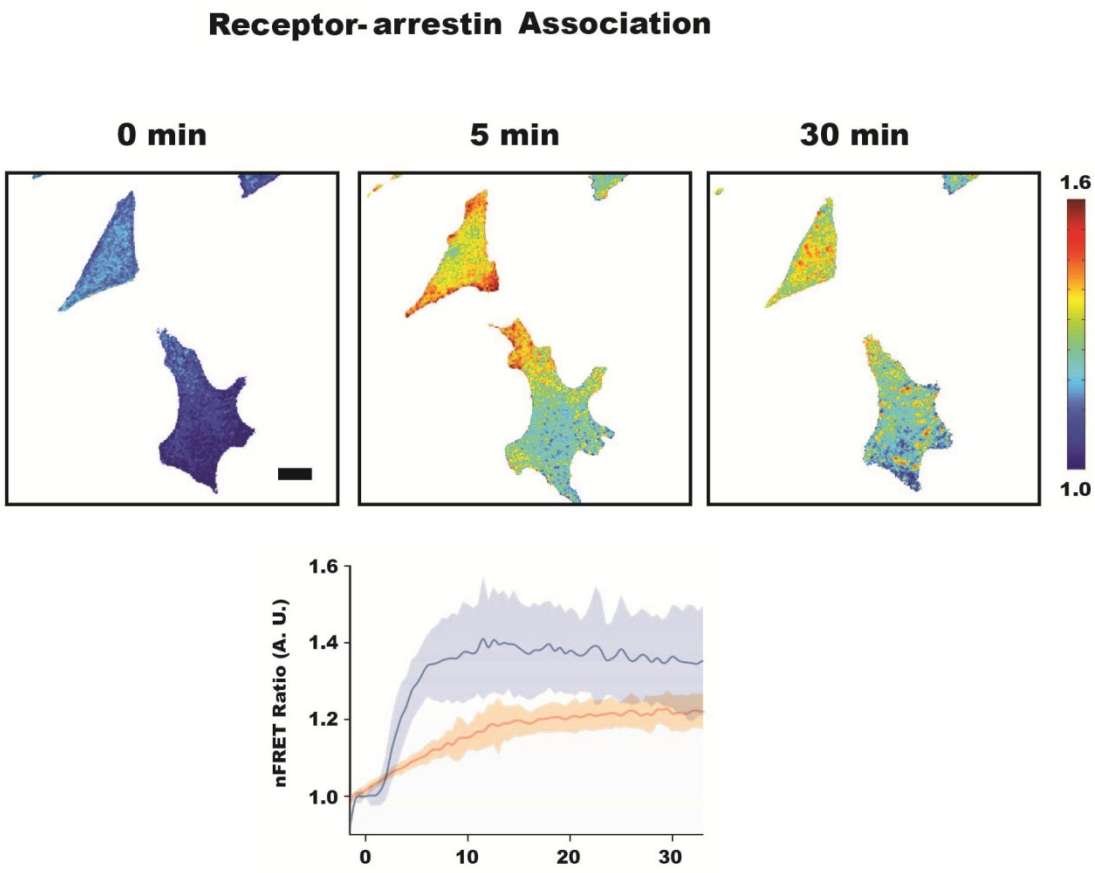


**Figure 4. 7 Beta-arrestin2-receptor complex is displayed by FRET technology. The receptor is fused with CFP and beta-arresitn2 is fused with mYFP. When they approach each other (<10nm), the FRET happens. When cells just gets stimulated by AngII, the FRET is stronger at membrane which means the beta-arrestin2 is attached to the receptor. After vesicle formation, the vesicles are exhibiting higher FRET signal. Color bar shows the FRET strength. Shades denote the standard error of the mean which solid lines are the mean values. Blue is for high dose of AngII (30ng/ml) and orange is for low dose (1.6ng/ml). Scale bar size: 5um.**

The complex formation was reported by the FRET signal between AT1aR and beta-arrestin2 [70]. Furthermore, prevention of endocytosis and resulting vesicle formation led to the inhibition of the chemotactic response, suggesting that internalized

AT1aR-beta-arrestin2 complex was the functionally important form of beta-arrestin2 in chemotactic signaling (Figure 4.8). This result further suggested that the signaling species activated by this complex would be associated with internalized vesicles.

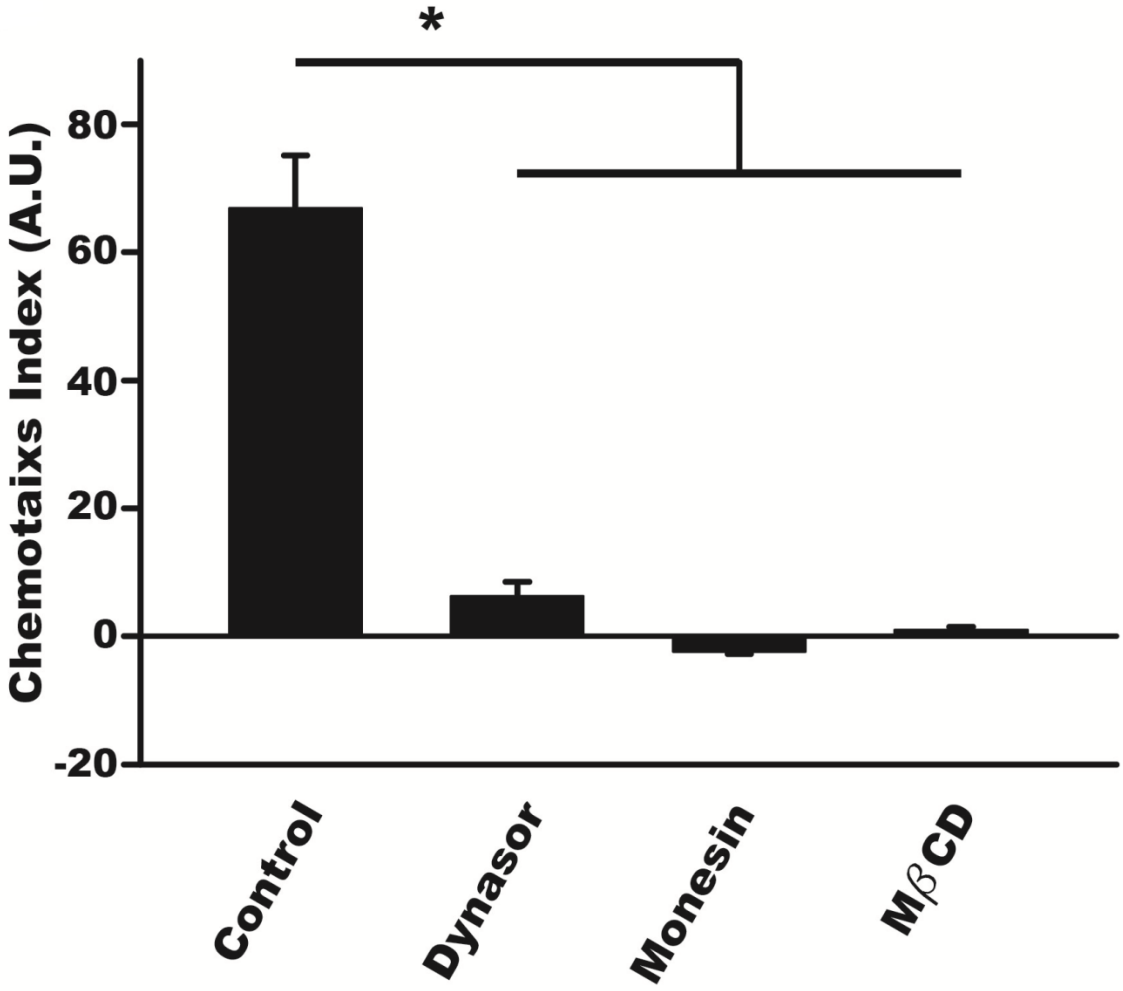


**Figure 4. 8 Endocytosis inhibitors inhibit the cell chemotaxis. Three different inhibitors were chosen and they block the receptor endocytosis by different mechanisms: Dynasor blocks the dynamin activity to stop the vesicle scissoring at membrane; Monesin blocks intracellular protein transport; MβCD disrupts lipid rafts by removing cholesterol from membranes. * denote $p<0.01$. Error bars denote the standard error of the mean.**

We found that ERK activity was upregulated contemporaneously with AT1aR-beta-arrestin2 complex formation (Figure 4.9). The kinase activity underwent strong, dose-dependent activation followed by incomplete adaptation to the steady levels dependent on the AngII dose.

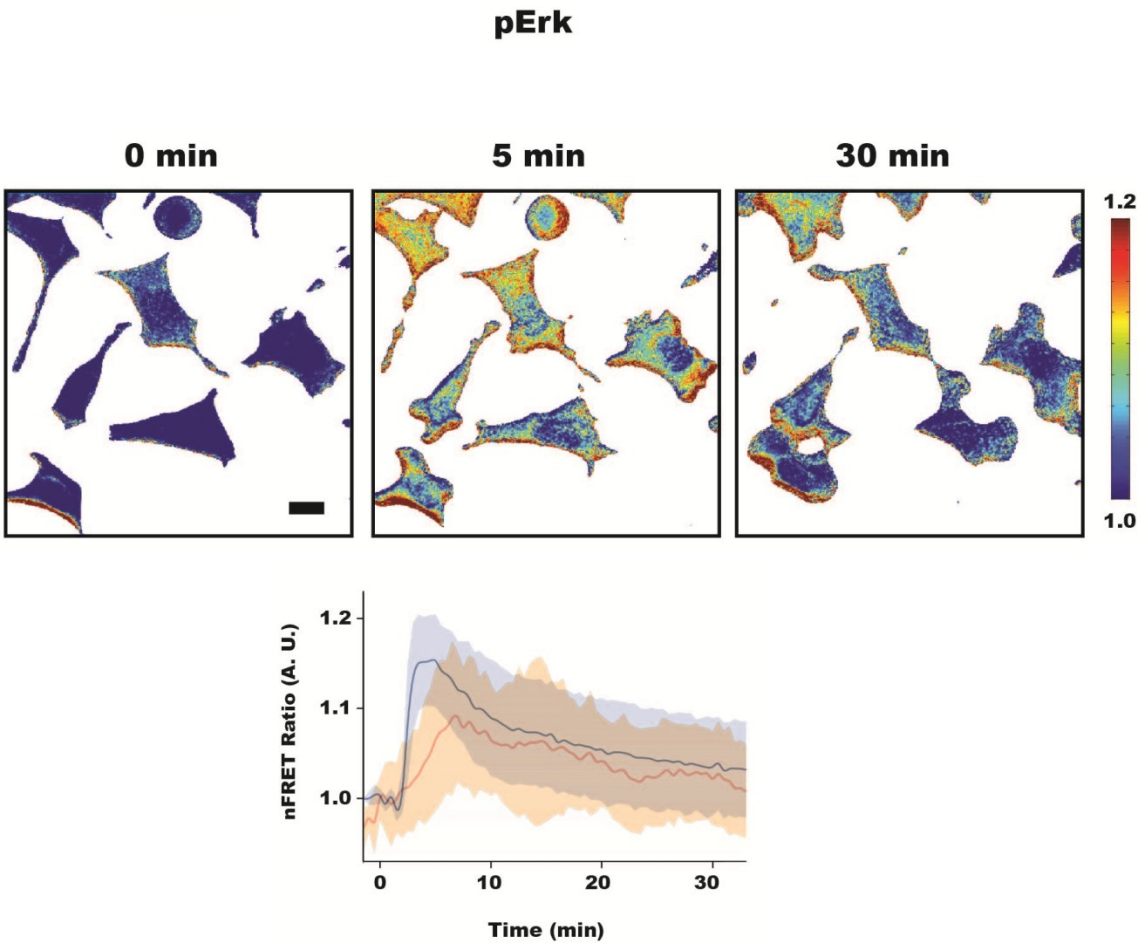


**Figure 4. 9 The ERK phosphorylation activities are displayed by FRET probe EKAR. The ERK phosphorylation starts right after cell stimulation by AngII, reaches its peak at after 5~10 minutes then decreases. But after a long term, it still does not achieve full adaptation. Color bar is showing the FRET strength. Shades denote the standard error of the mean while solid lines are the mean values. Blue is for high dose of AngII (30ng/ml) and orange is for low dose (1.6ng/ml). Scale bar size: 5um.**

ERK is a direct and important downstream signaling molecule. Whether it is involved in beta-arrestin2 mediated chemotaxis is still controversial [71]. But our device can easily test this ambiguity in our system. Indeed, we found ERK signaling is crucial to the AngII stimulated cell chemotaxis, since upon the inhibition of ERK pathway by U0126, the cell chemotaxis will be dramatically suppressed (Figure 4.10).

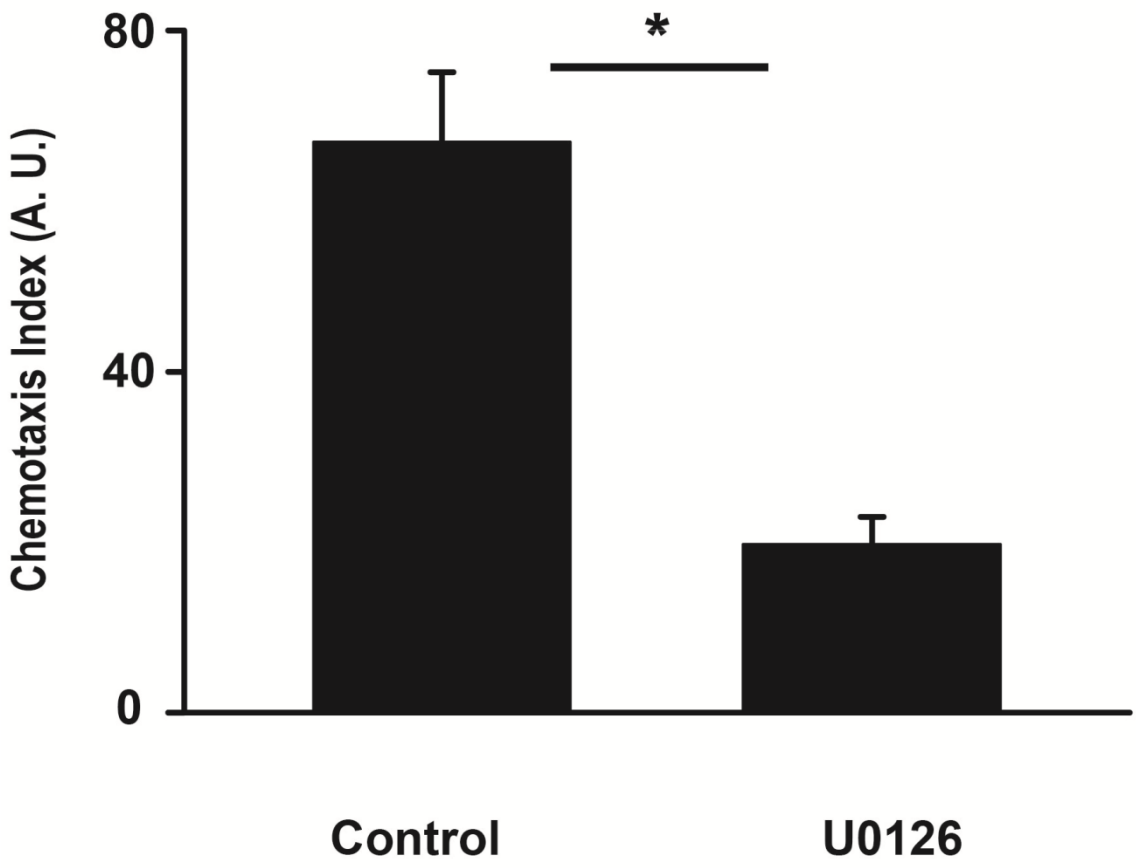


**Figure 4. 10 U0126, a specific ERK pathway inhibitor, can reduce the cell AngII induced chemotaxis .* denote p<0.01. Error bars denote the standard error of the mean.**

When averaged time-dependent responses of the distinct signaling species analyzed above were normalized to the time of AngII addition and overlaid on the same graph, it became clear that ERK activation closely follows the kinetics of AT1aR-beta-arrestin complex formation, prior to its partial adaptation (Figure 4.11).

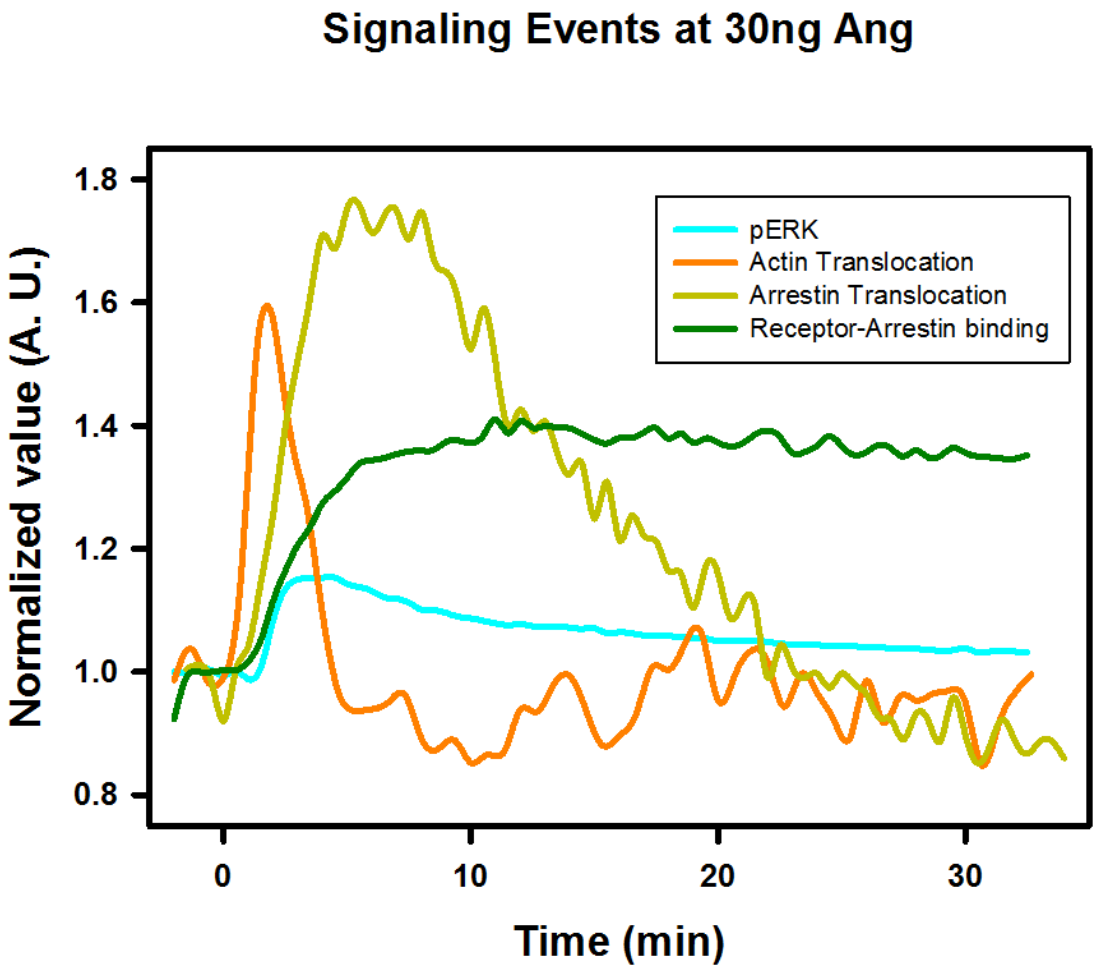


**Figure 4. 11 Overlay of the signaling events.**

## *Regulation of beta-arrestin2 by actin*

Addition of AngII also triggered strong and transient translocation of actin to the plasma membrane (Figure 4.12) and associated expansion of the membrane, in an AngII dose-dependent manner.

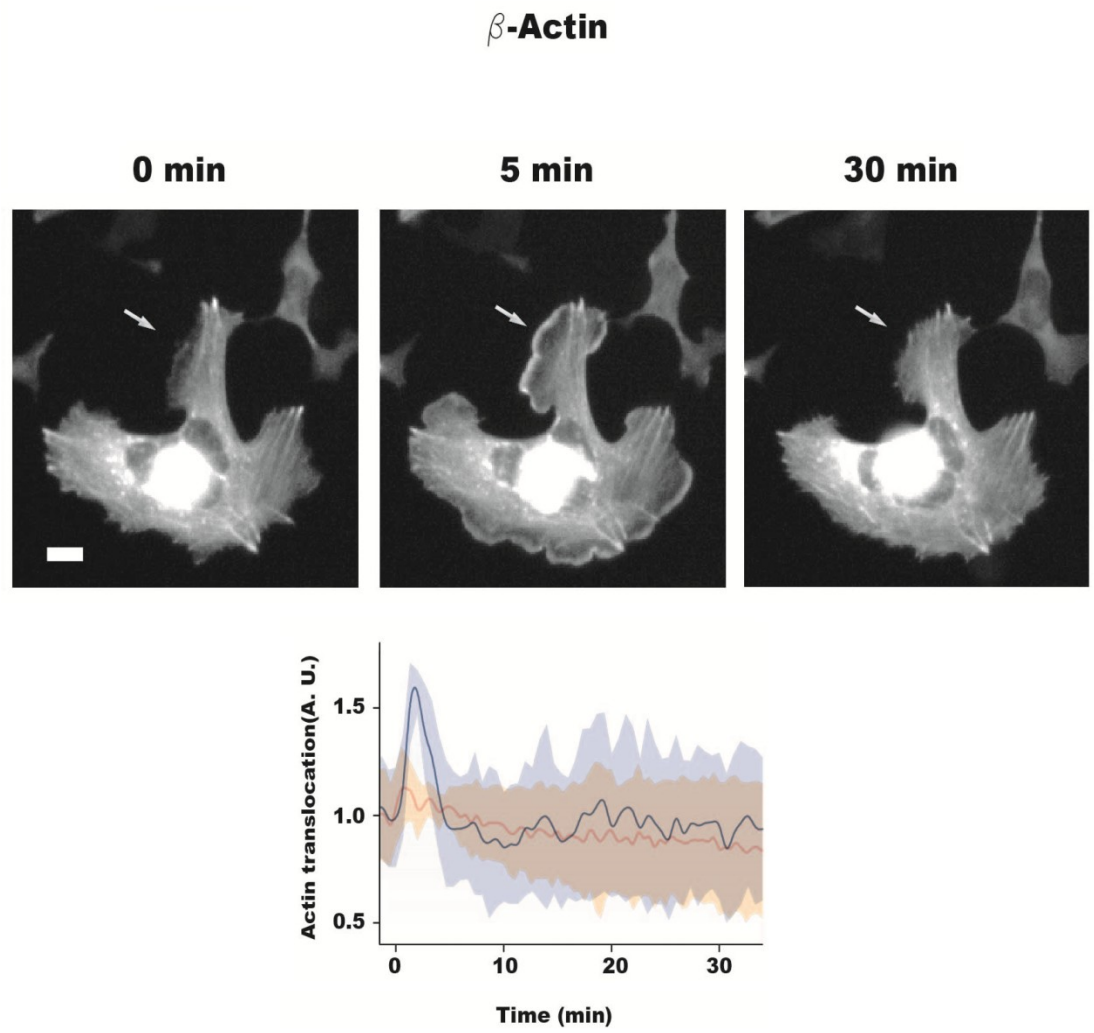


**Figure 4. 12 Actin translocation to the plasma membrane starts when AngII is applied to the cells. Actin facilitates vesicle forming and receptor internalization, moves away after vesicle forming. Shades denote the standard error of the mean which solid lines are the mean values. Blue is for high dose of AngII (30ng/ml) and orange is for low dose (1.6ng/ml). Scale bar size: 5um.**

The kinetics of actin response was hypersensitive to the AngII addition, exhibiting both rapid activation and rapid adaptation. Overexpression of actin within the cells led to an increased stress fiber formation and cell spreading. In such cells, the higher surface to volume ratio results in, on average, a shorter distance required for translocation of beta-arrestin2 to the plasma membrane, thus suggesting more rapid translocation kinetics, which was indeed experimentally confirmed (Figure 4.13). Faster scaffold recruitment dynamics was associated closely with a faster translocation of actin to the plasma membrane, further supporting the causative link between beta-arrestin2 activation and actin-based morphology change. In summary, these results suggested that AngII triggers a sequence of signaling events ultimately leading to both dose dependent Erk1/2 activation and actin-dependent morphological change, with both outcomes potentially relevant to promoting cell migration.

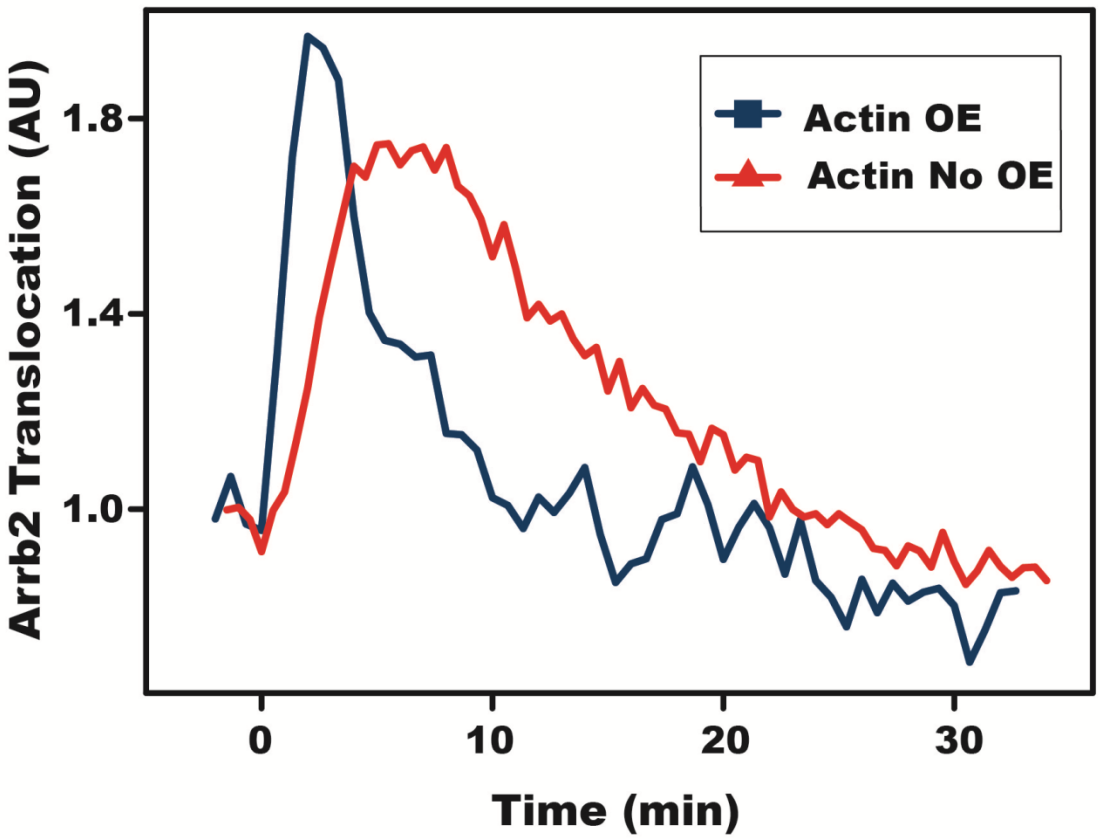


**Figure 4. 13 Actin overexpression induces faster beta-arrestin2 dynamics, both the translocation to membrane and endocytosis.**

## *Scaffold effect of beta-arrestin2 in chemotaxis*

Since beta-arrestin can regulate signaling events by both controlling receptor internalization and directly scaffolding signaling pathways, beta-arrestin2 overexpression can potentially affect signaling outcome through either or both of these processes. We thus explored, at several distinct doses of AngII, whether beta-arrestin-2 expression in amounts leading to strong impairment of cell migration directionality would negatively affect receptor internalization and/or ERK signaling. Indeed, we found that, for all doses

of AngII, high scaffold levels dramatically decreased beta-arrestin2-enriched vesicle formation (Figure 4.14). Conversely, the intermediate levels of beta-arrestin2 expression led to an increase in vesicle formation, in an AngII-dose dependent fashion (Figure 4.14).

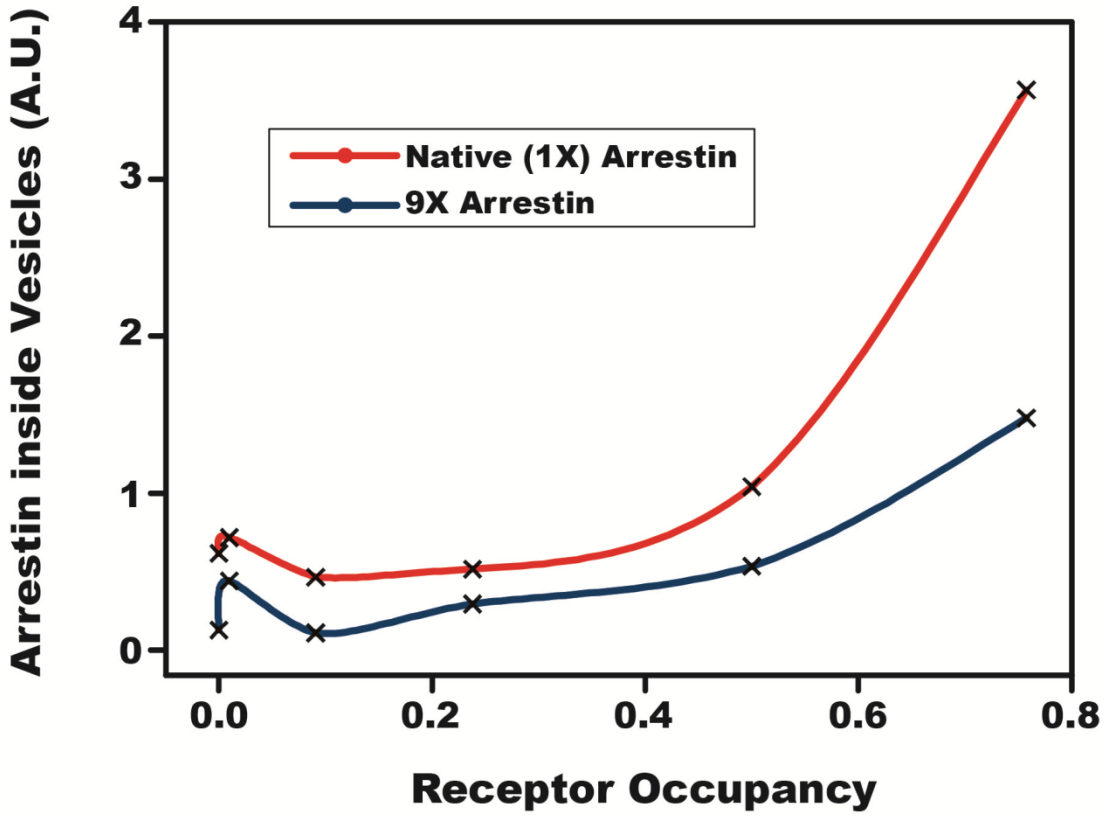


**Figure 4. 14 Beta-arrestin2 in vesicle is a non-linear function of receptor occupancy. When the beta-arrestin2 level is too high, the endocytosis mediated by beta-arrestin2 is actually decreased.**

ERK signaling was also negatively affected by high levels of beta-arrestin2 expression. However, it displayed a more complex dependence on the AngII dose (Figure 4.15). For both beta-arrestin2 levels analyzed, the ERK dose dependencies were biphasic, with the maximum levels reached at different AngII concentration values. These complex

cellular responses called for development of a computational model capable of interpretating for the experimental results obtained so far, and of predicting cell behaviors under different circumstances, particularly under the AngII gradient stimulation.

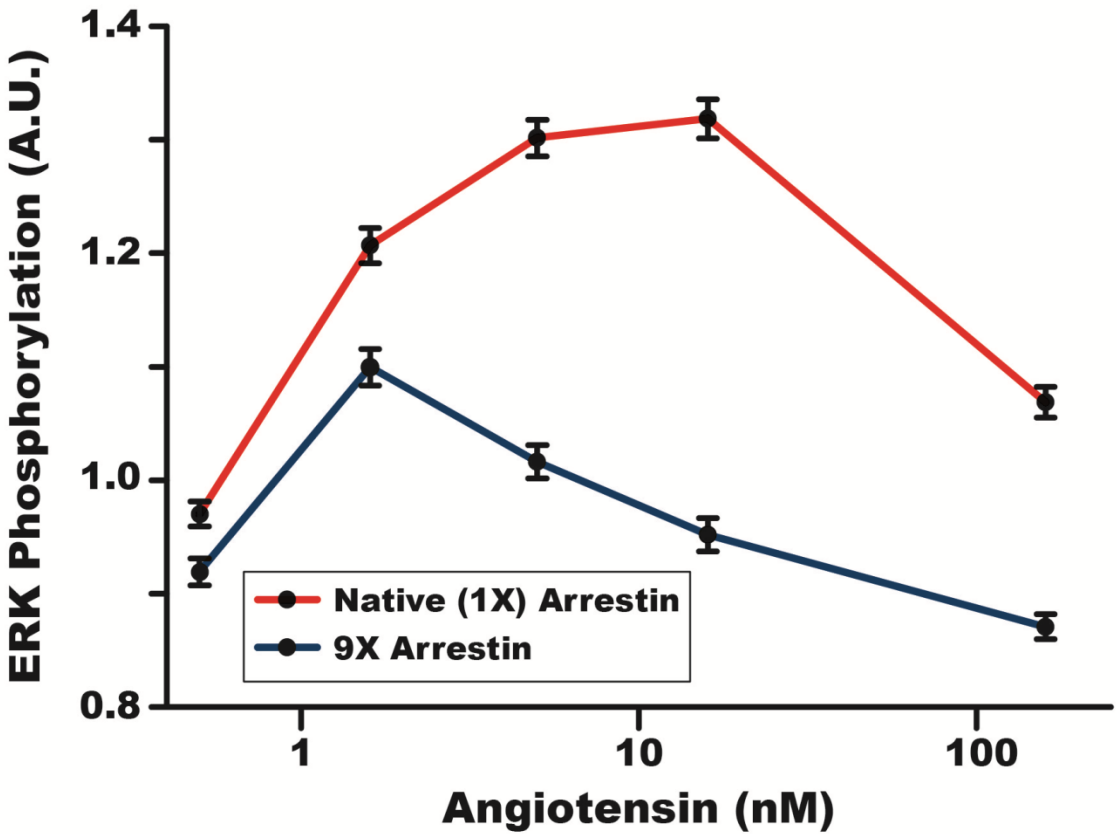


**Figure 4. 15 The ERK phosphorylation detected by immunocytochemistry. They showed standard scaffold-dependent biophasical curve. High level of the beta-arrestin2 scaffold decreased ERK activation. Error bars denote the standard error of the mean.**

## *Gradients amplification through endosome recycling*

The model illustrated in the schematic (Figure 4.16) was based on the assumption that beta-arrestin-2 can control the signaling outputs by biphasically affecting both receptor internalization at the plasma membrane and ERK activation in the vesicles. This type of biphasic dependence on molecular concentration is expected of any cross-linker molecule, including adapter and scaffold proteins [72]. Furthermore, it was assumed that ERK activity could display a degree of scaffold-independent activity in the cytosol. The resulting model was partially based on our prior model of the scaffold-mediated MAPK signaling, with the important modification to account for several cellular compartments: plasma membrane, cytosol, and vesicles. The model, after parameter adjustment, could successfully account for several experimental datasets described above. We next extended the model by introducing spatial dimensionality into simulations and attempting to predict cell responses to gradients of AngII. Although the model could account for some degree of cell polarization, the differences between the signaling activities in the rear and front portions of the cell tended to be very weak in shallow AngII gradients (data not shown). This suggested that an amplification mechanism may be present in the signaling network such that shallow ligand gradients are transduced into stronger polarized intracellular signaling responses. We next examined this prediction and modified the model to account for a possible amplification mechanism.

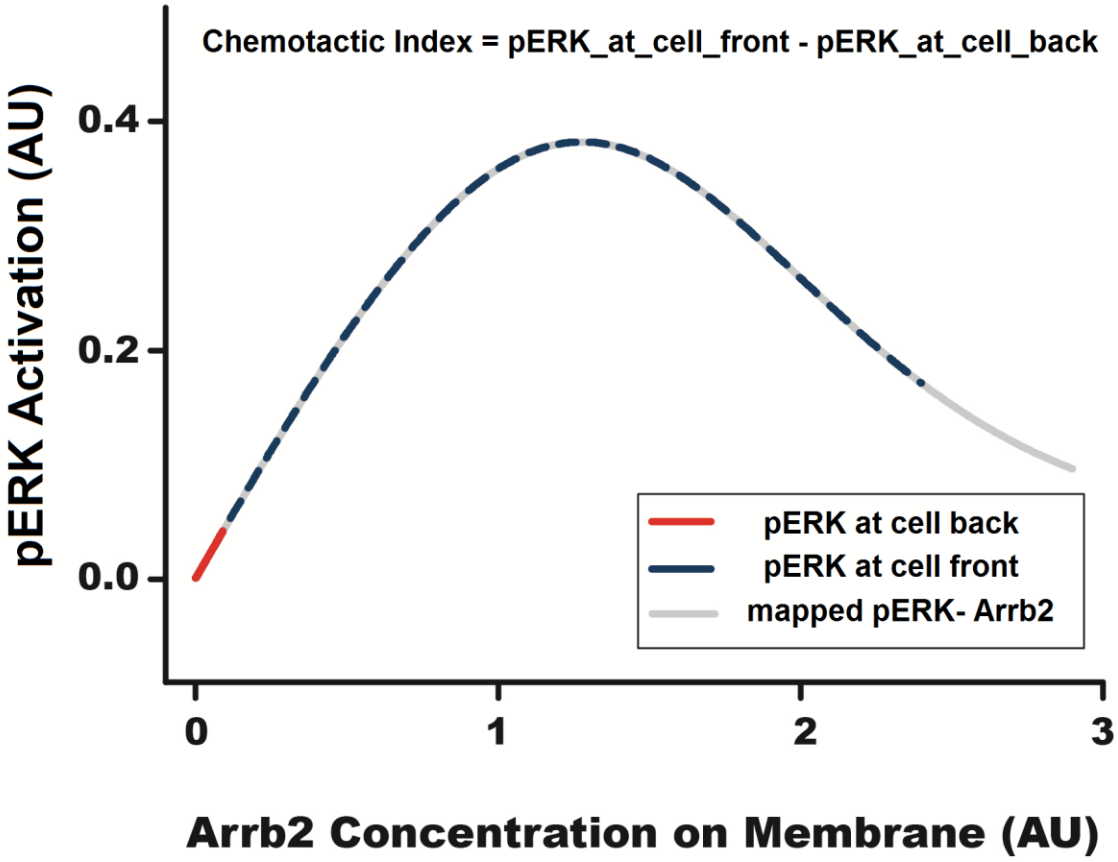


**Figure 4. 16 The basic model for calculating cell chemotactic index. ERK activity is biphasicly mapped on the beta-arrestin2 concentration. The cell chemotaxis index is the difference of ERK activity at cell front and back.**

When examined in AngII gradients, the intracellular distributions of internalized receptor, beta-arrestin2 and ERK activities displayed strong asymmetry, which exceeded the asymmetry expected based on the AngII input gradient alone (Figure 4.17).

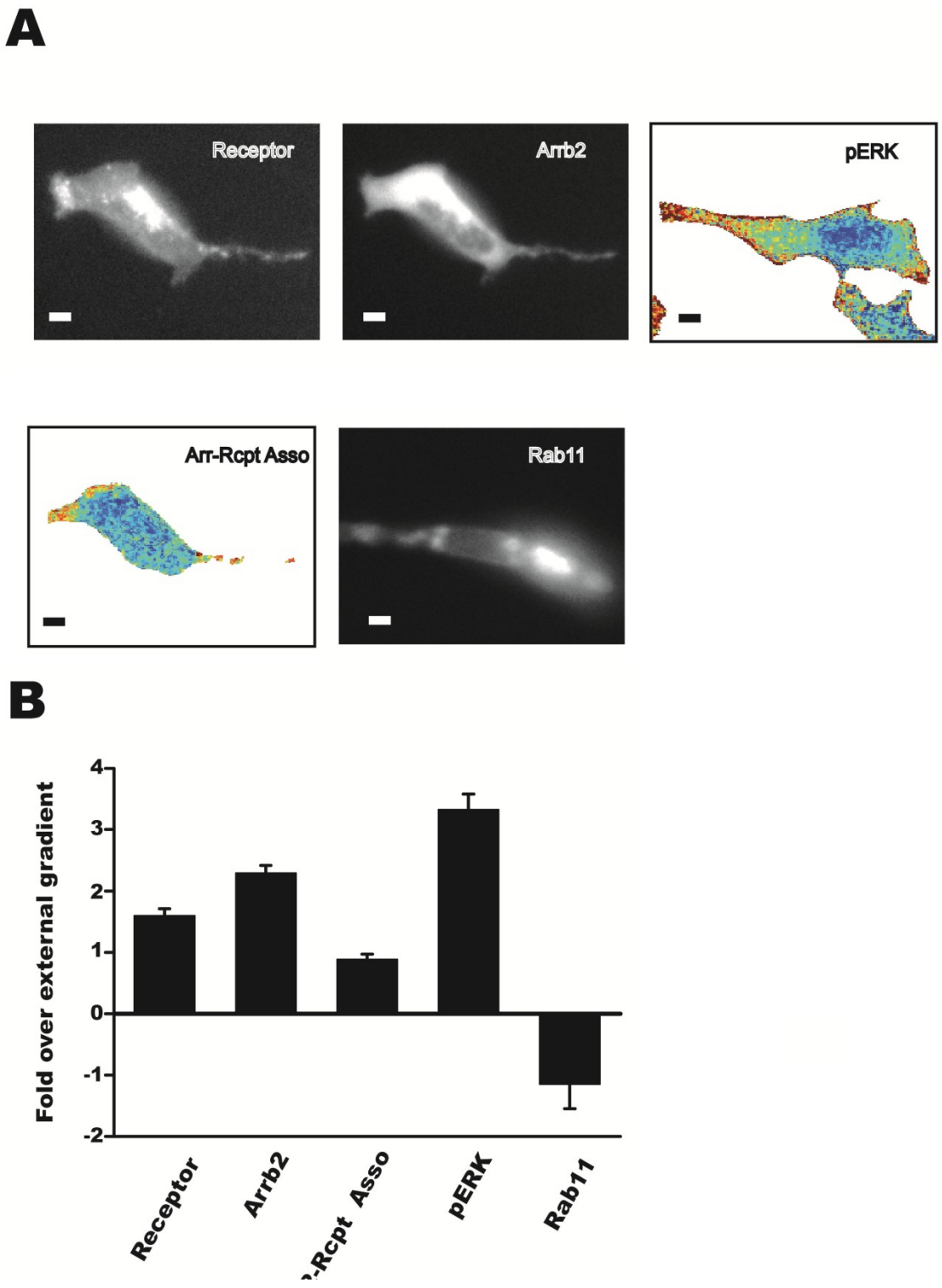


**Figure 4. 17 A) The receptor, beta-arrestin2, receptor-arrestin2 association in vesicles and pERK distributions are prominently polarized toward the upstream of gradient. But Rab11 accumulated at the back of cell. B) The quantification of molecular**

**polarization inside cells. The values are all normalized to the external gradient. Error bars denote standard error of the mean. Scale bars represent 10um.**

This result suggested the existence of a mechanism to amplify the difference between the signaling activities in the front and the rear of the cells. Since beta-arrestin2 localization and ERK activity were confined to the vesicles, one immediate possibility for an amplification mechanism was that not only vesicle formation (through internalization) was affected by the asymmetry of the input, but also vesicle recycling, with the gradient of recycling being opposite to that of the gradient of internalization. To test this idea we first noted that vesicle trafficking, but not vesicle formation, was microtubule-dependent (Figure 4.18).

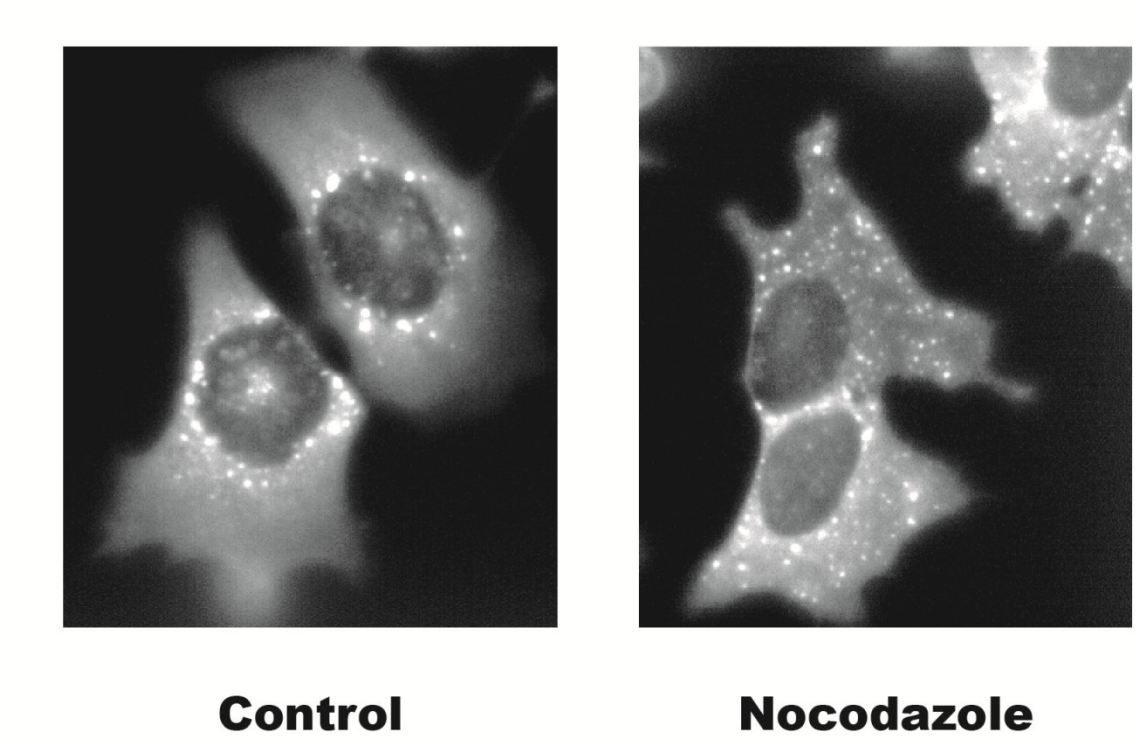


**Figure 4. 18 Inhibition of the microtubule polymerization prevented vesicle merge and formed many dangling small vesicles.**

Inhibition of microtubules with Nocodazole, a microtubule disrupting agent, also progressively reduced amplification of beta-arrestin2 polarization in the AngII gradients (Figure 4.19). This result not only confirmed potential role of microtubule-based vesicle trafficking in gradient amplification, but raised the question of whether this process could be linked to vesicle recycling.

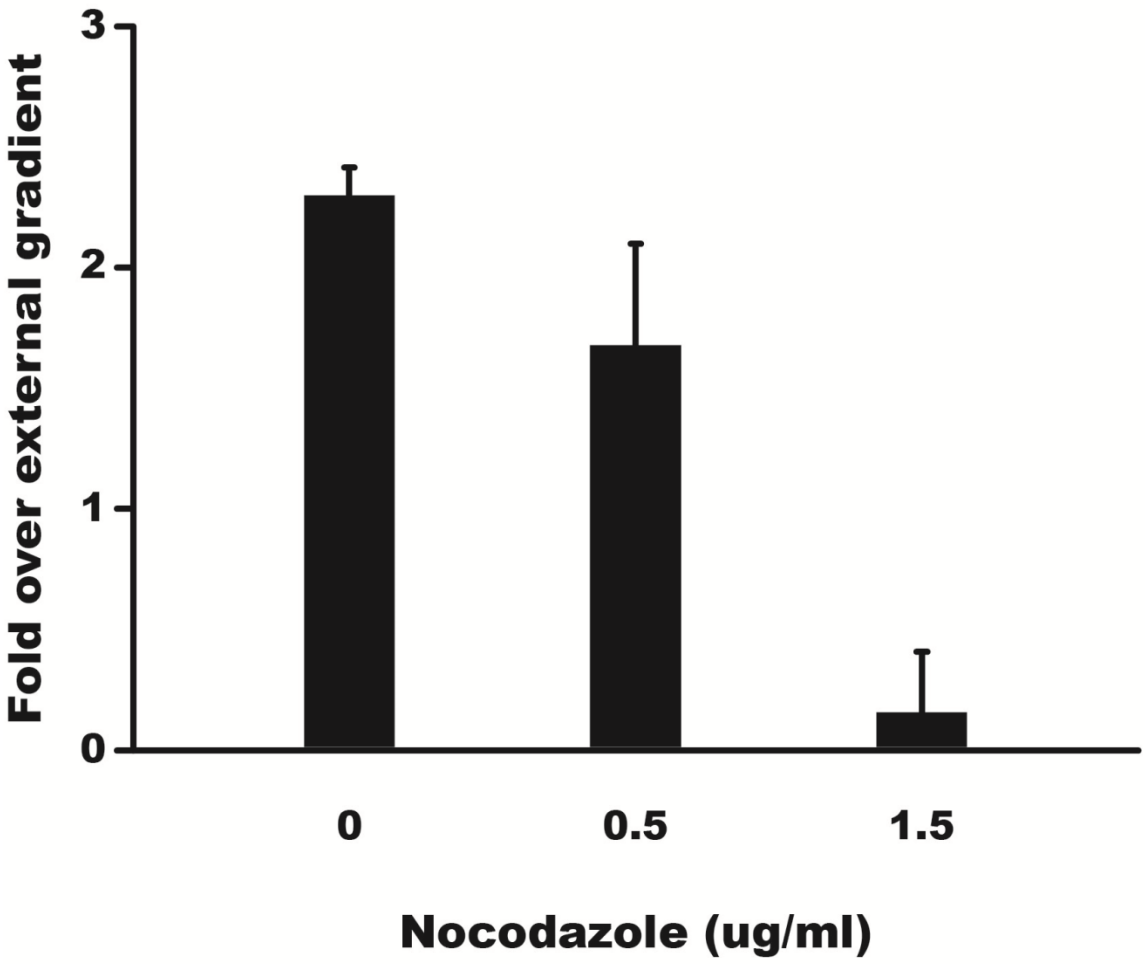


**Figure 4. 19 Inhibiting microtubule polymerization induced the suppression on the beta-arrestin2 polarization in cells under gradient. Error bars denote the standard error of the mean.**

Previously, it has been determined that a small GTP-ase Rab11 could control endosome recycling in a microtubule dependent fashion [73]. Furthermore, Rab11 has been associated with various forms of in vivo cell migration [73-75]. We found that, in cells exposed to AngII gradients, Rab11 translocated to the back of the cell, consistent with possible AngII gradient induced polarization of vesicle recycling (Figure 4.17). Inhibition of Rab11 by overexpression of its dominant negative form indeed resulted in a

loss of signal amplification and biased cell migration, further supporting its functionality in gradient sensing (Figure 4.20). We thus modified the model to account for asymmetric vesicle formation and recycling occurring in the beta-arrestin-2 and Rab11 manner (Figure 4.21), respectively.

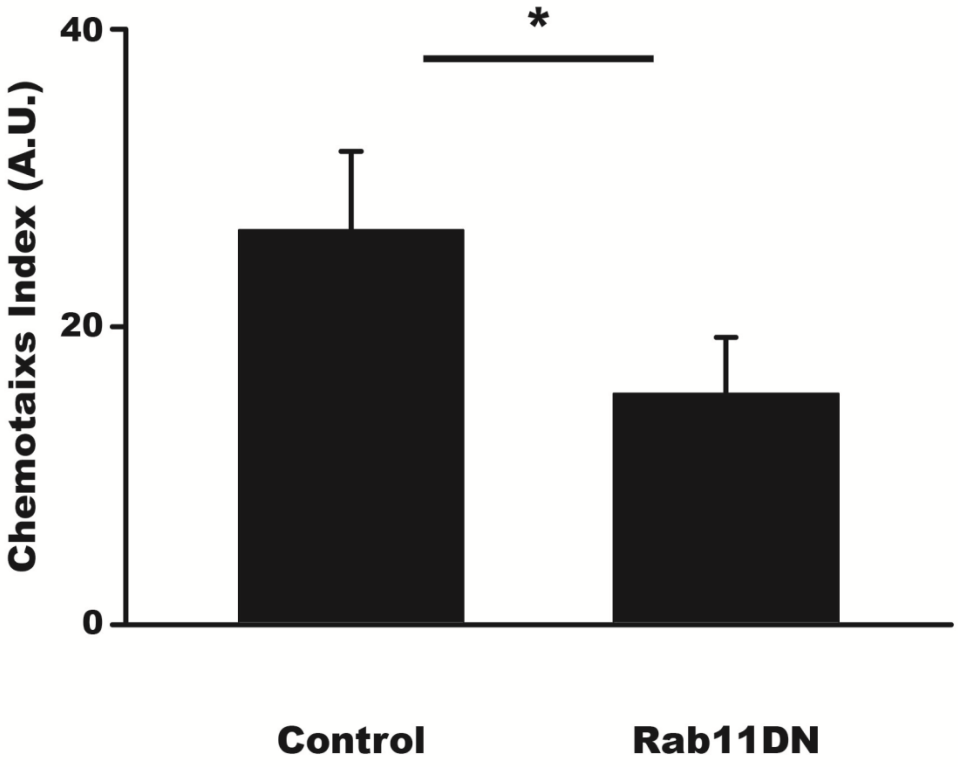


**Figure 4. 20 Inhibion of Rab11 activity by overexpressing its dominant negative mutation drastically annihilated the cell chemotaxis. * denote p<0.01. Error bars denote the standard error of the mean.**

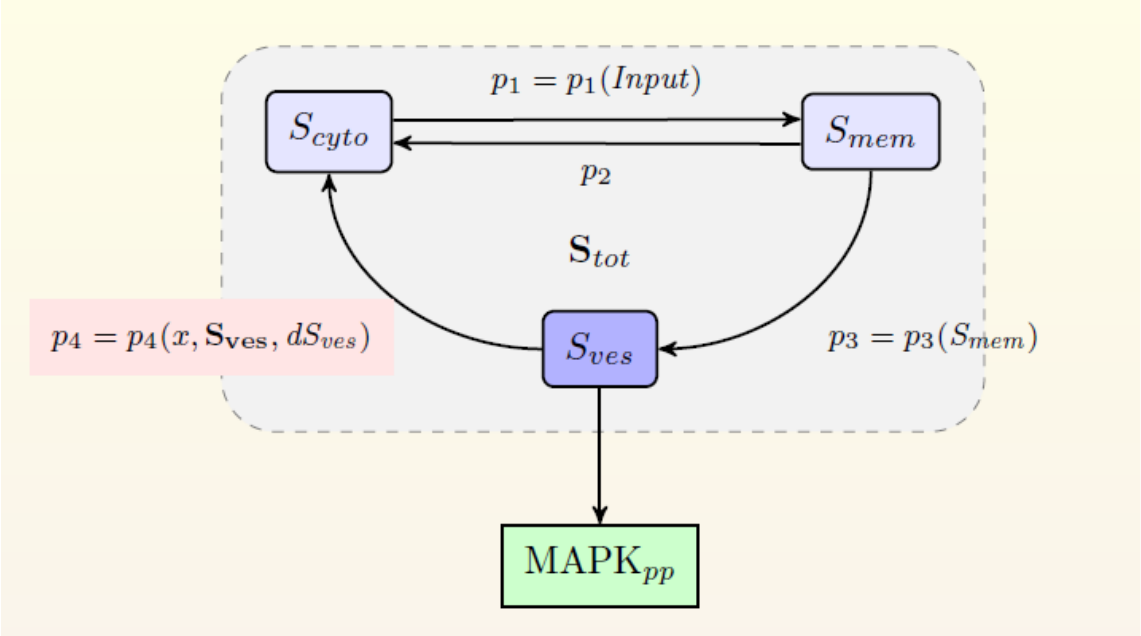


**Figure 4. 21 A more sophisticated model account that vesicle endocytosis and recycling are also biphasicly dependent on the beta-arrestin2 scaffold level.**

## *Models can predict the co-existence of chemoattractance and chemorepulsion.*

The model made several important predictions that we sought to validate experimentally. First, it predicted that, in line with beta-arrestin2 playing a role of a classical scaffold molecule, different levels of scaffold expression are expected to result in biphasic changes in both ERK activity and the corresponding bias in chemotactic response (Figure 4.22).

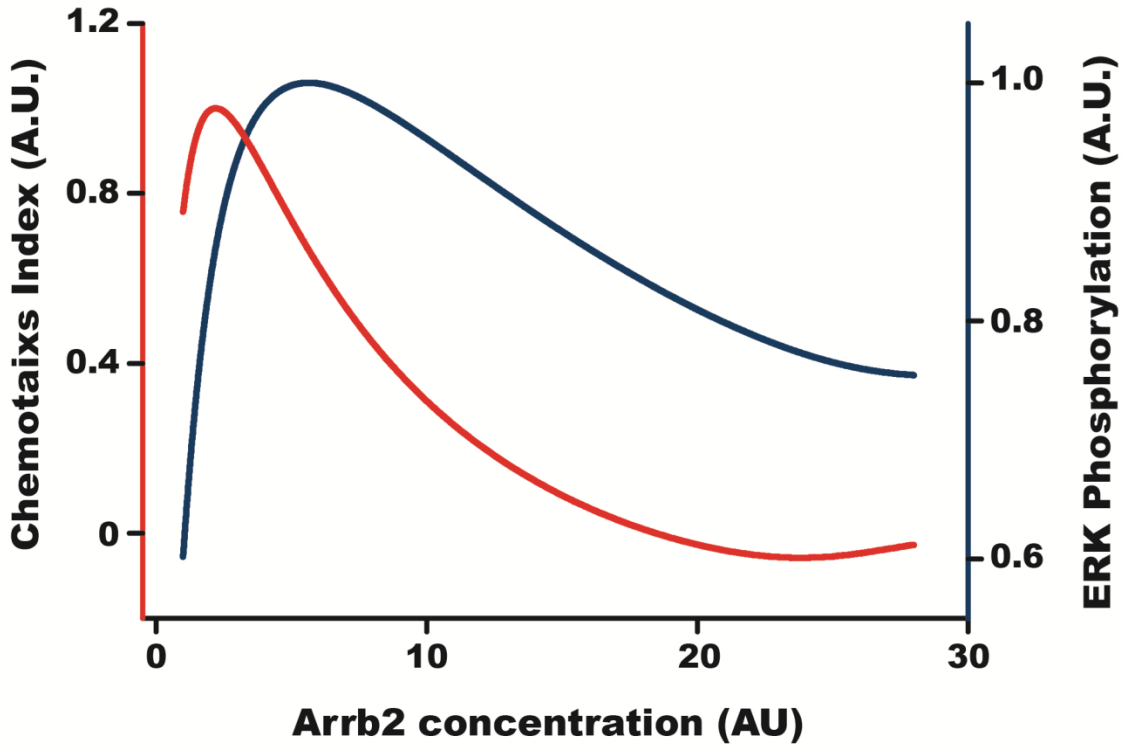


**Figure 4. 22 Model predicted that both the ERK phosphorylation and cell chemotaxis behavior will be biphasic as the function of beta-arrestin2 scaffold, and a lag phase is also expected.**

Furthermore, the optimal levels of the scaffold for these two responses were predicted to be shifted with respect to each other, so that chemotactic bias would peak at a lower scaffold level relative to the level of the scaffold optimizing ERK activation (Figure 4.22). This was indeed observed in the experiments, when clones expressing different levels of beta-arrestin were analyzed (Figure 4.23).

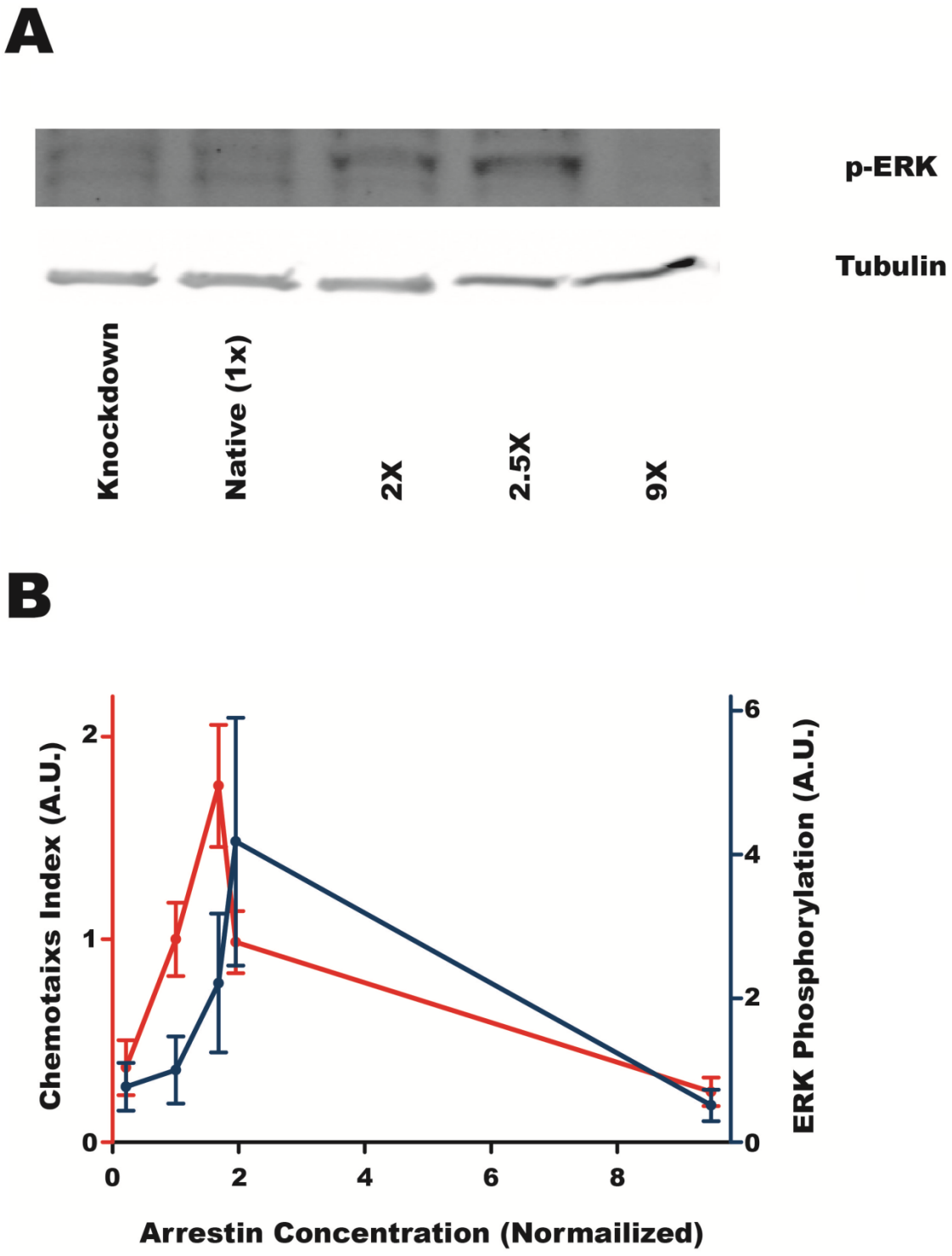


**Figure 4. 23 A) Westernblot showed that ERK activation is biphasic when increasing the beta-arrestin2 scaffold expression level. B) Both the ERK phosphorylation and cell chemotaxis are biphasic function of beta-arrestin2 scaffold concentration.**

**And The lag phase is appeared to be same as predicted in the mode. Error bars denote the standard error of the mean.**

The model also predicted (Figure 4.24) and experiments confirmed (Figure 4.25) that microtubule disruption by nocodazole can lead to a relative increase in the Erk1/2 activity, due to accumulation of intracellular vesicles, which is also experimentally confirmed (Figure 4.25).

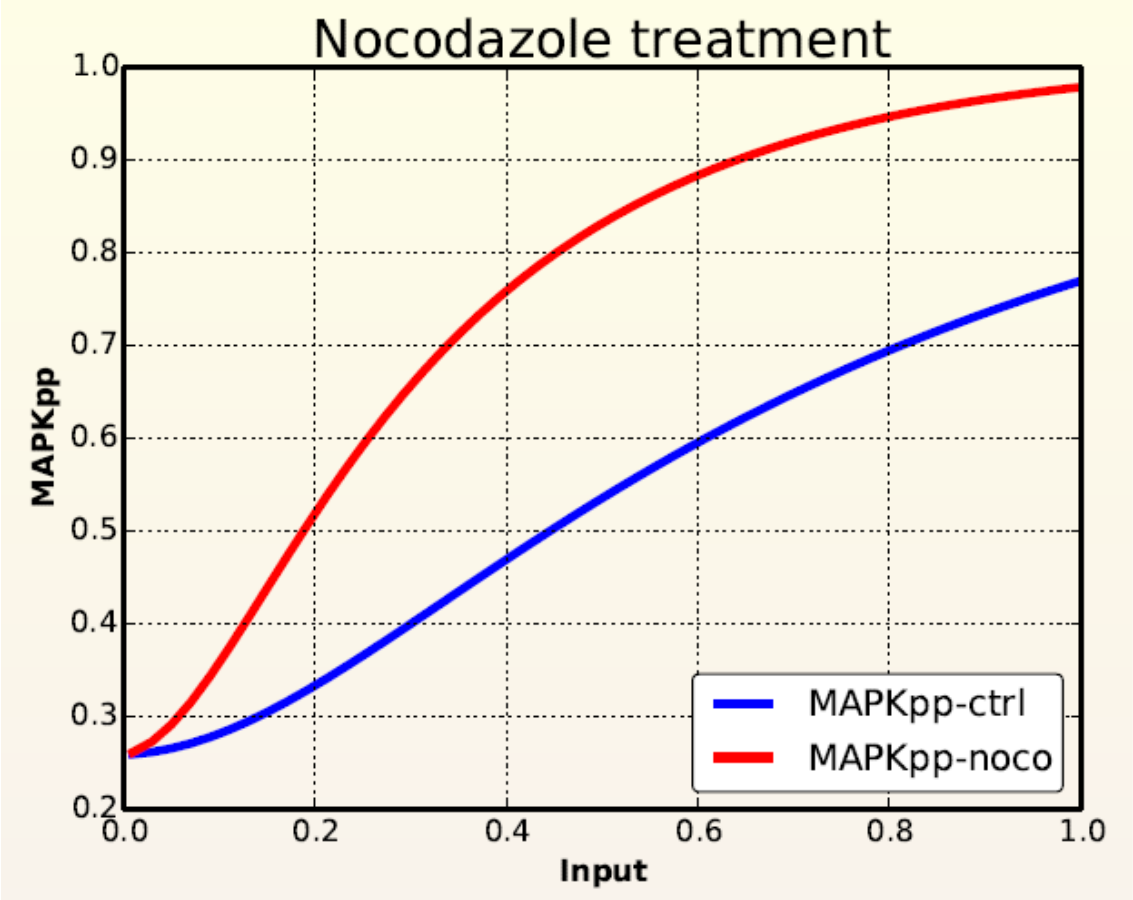


**Figure 4. 24 Model predicted that when the microtubule polymerization is inhibited, the accumulated vesicle will induce more ERK phosphorylation since the ERK phosphorylation mostly happened at endosomes.**

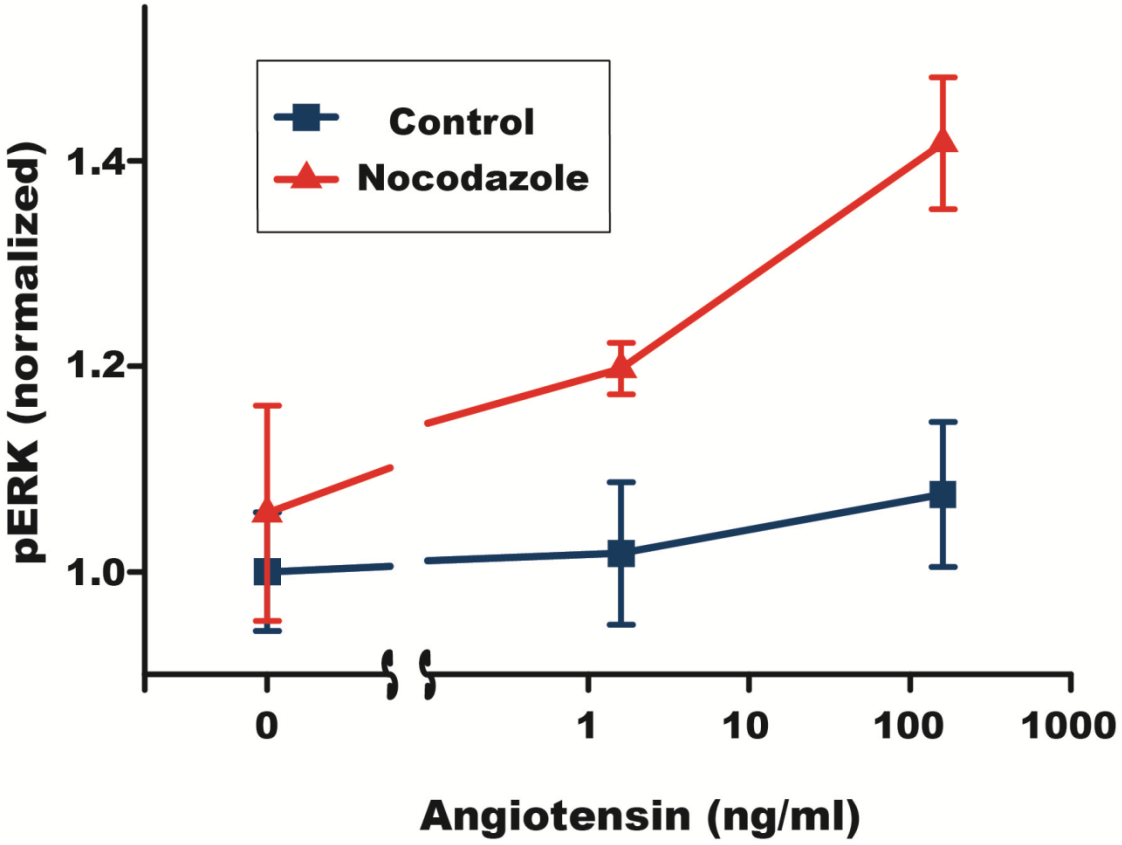


**Figure 4. 25 Experiments confirm that when microtubule polymerization is inhibited by Nocodazole, ERK activity is elevated. Error bars denote the standard error of mean.**

Variations of the scaffold levels and of the average local concentrations of AngII were predicted to lead to complex chemotactic responses. An important assumption here, stemming from the earlier experimental results, was that the vesicle formation was positively regulated by AngII levels, promoting beta-arrestin2 recruitment. For the level of the scaffold, optimal for chemotaxis, the model predicted (Figure 4.26), and

experiments confirmed (Figure 4.27), that the AngII gradient would be interpreted by the cells to be chemo-attractive at all levels of local AngII, with a weak or no dependence on the AngII dose. On the other hand, for the highly overexpressed beta-arrestin2 levels, the model and experiment showed that cells can switch from chemo-attraction to chemo-repulsion at the low AngII concentrations, and switch back to chemo-attraction at higher AngII levels.

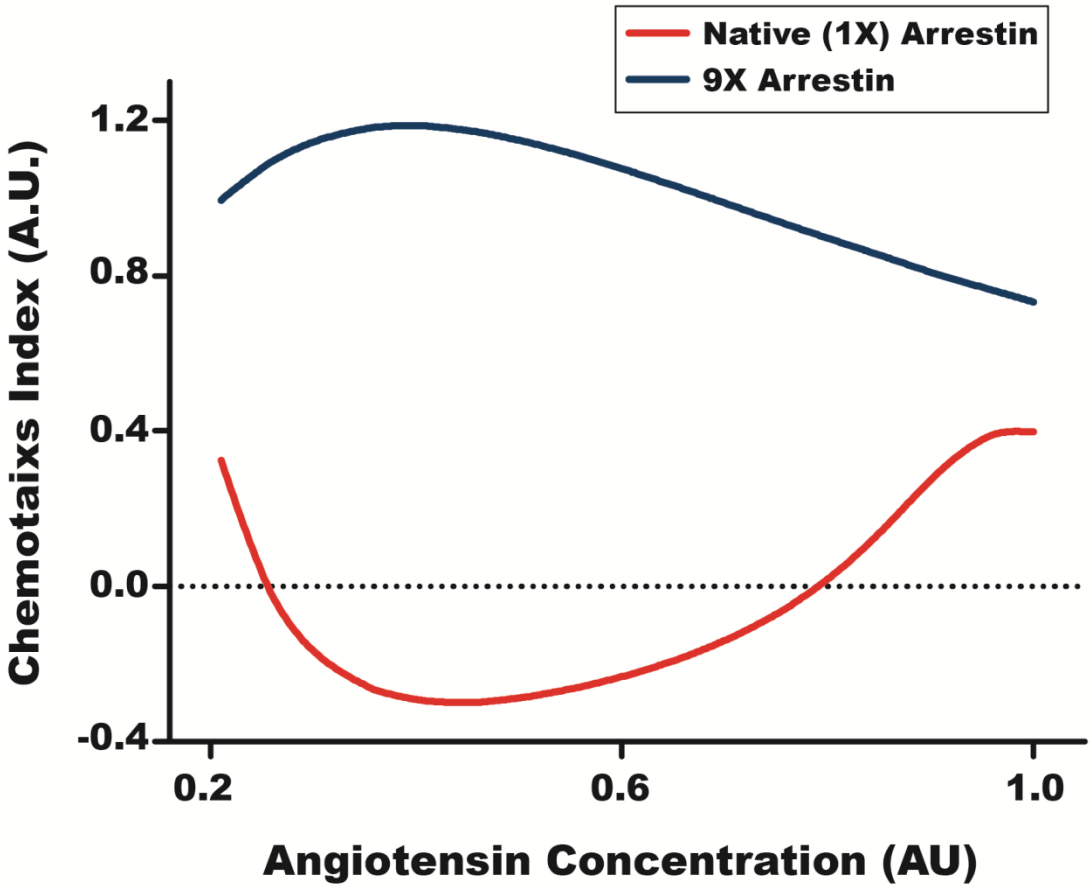


**Figure 4. 26 Model predicts the co-existence of chemoattraction and chemorepulsion when the beta-arrestin2 scaffold is too high. The chemoattraction happened at high local AngII concentration and chemorepulsion is at low local AngII concentration. While the scaffold level is moderate, the cell only showed**

chemoattraction phase which is only weakly depend on the local AngII concentration

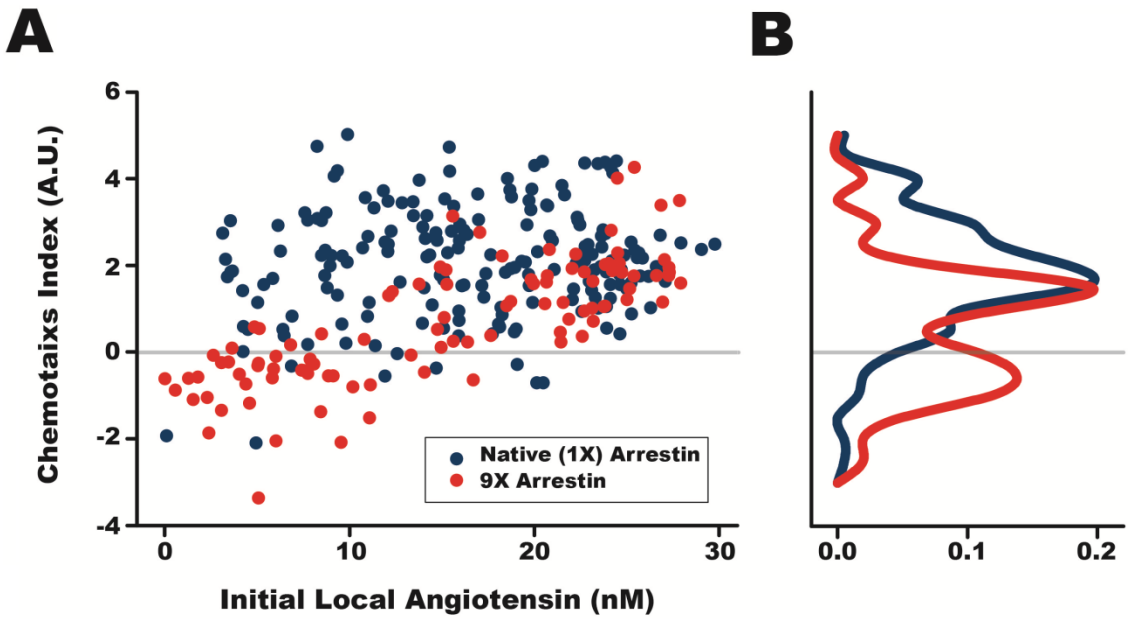


**Figure 4. 27 Experiments confirmed the the co-existence of chemoattraction and chemorepulsion when the expression level of beta-arrestin2 scaffold is too high. However, when the scaffold level is moderate, the cell only showed chemoattraction phase which is only weakly depend on the local AngII concentration**

The explanation suggested by the model was that the repulsive response was due to the inhibition of ERK signaling at high scaffold levels in the vesicles, thus maximizing ERK signaling on the side of the cell exposed to lower rather than higher AngII inputs. On the other hand, the switch back to attraction was associated with an additional effect of decreased vesicle formation when scaffold and AngII input levels were both high, thus negating the effect of the scaffold-based suppression of ERK signaling from the vesicles (Figure 4.28).

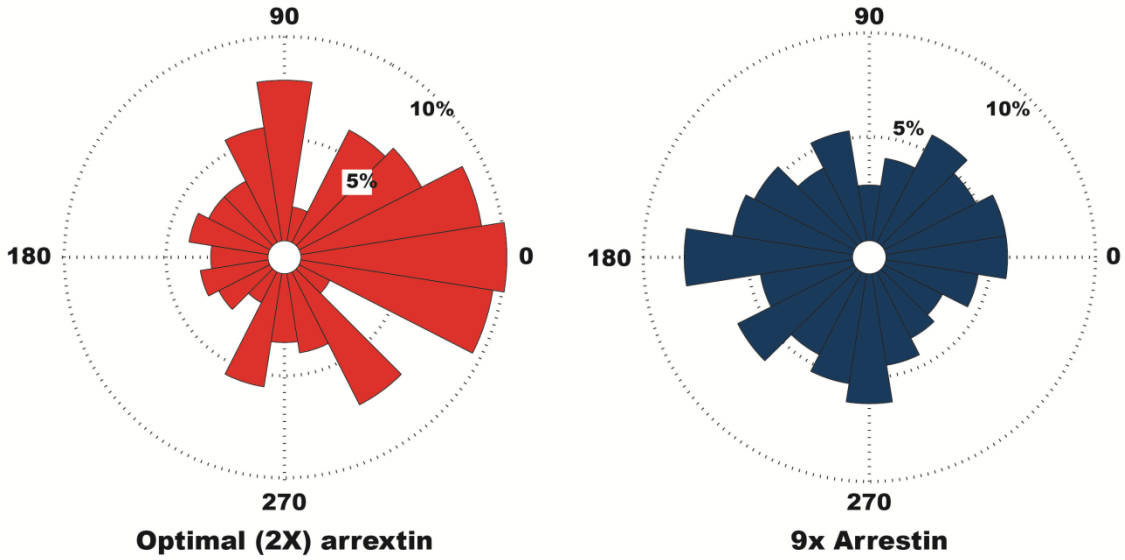


**Figure 4. 28 At optimal beta-arrestin2 scaffold level, the scaffold vesicle are more polarized towards the higher concentration of AngII. In contrast, the scaffold vesicle are more polarized towards the lower concentration of AngII at high beta-arrestin2 scaffold level.**

The model therefore predicted that this 'double negative' effect of the scaffold over-expression at high AngII levels should be compensated by a greater vesicle retention, e.g., by inhibiting microtubule-mediated vesicle trafficking and recycling. Indeed, treatment of cells containing over-expressed beta-arrestin-2 with Nocodazole led to repulsive response at all AngII concentration levels (Figure 4.29).

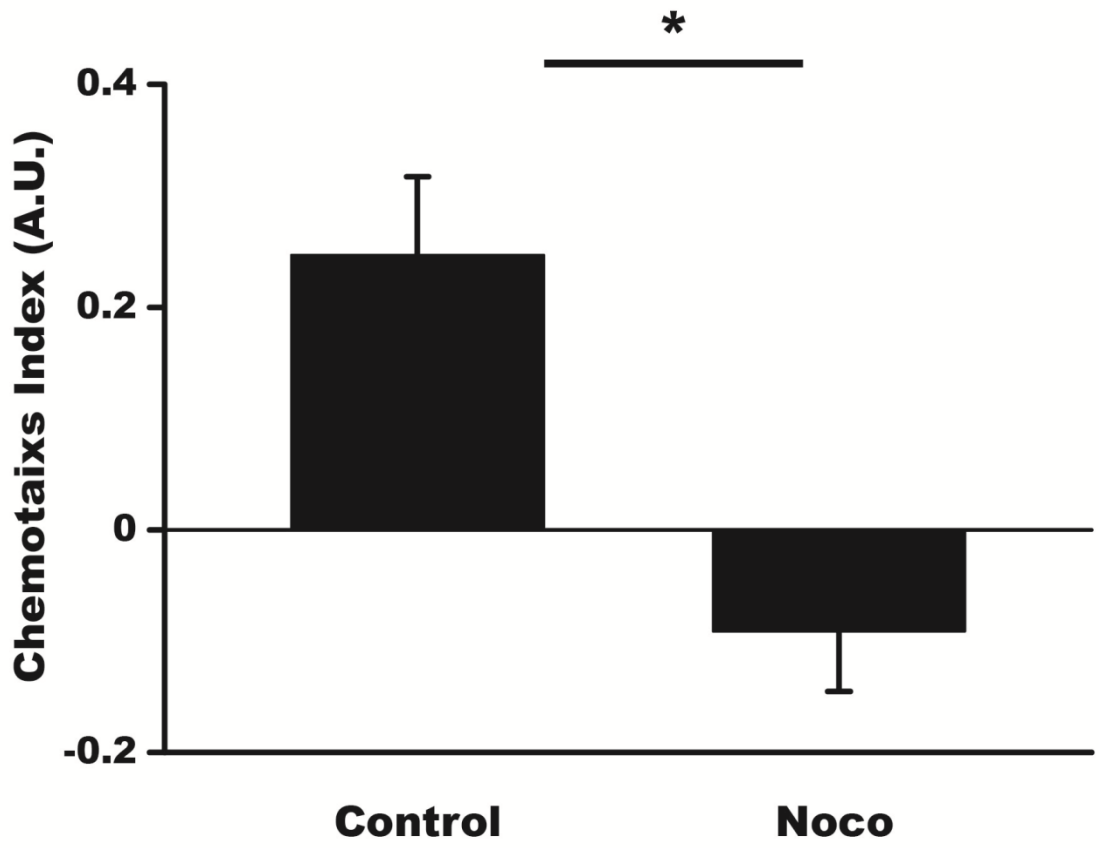


**Figure 4. 29 When the Nocodazole is applied to the high beta-arrestin2 scaffold expression cells, they showed chemorepulsion instead of chemoattraction in control experiments. .* denote p<0.01. Error bars denote the standard error of the mean.**

The model was also successful in predicting other properties of the cell migration response, including the dependence of the chemotactic bias on the gradient value (Figure 4.30). Overall, the consistency between the model and experiment strongly suggested that the model correctly captures the mechanism of the chemotactic response controlled by beta-arrestin2. Surprisingly, both the role of beta-arrestin2 in the scaffolding signaling species within the vesicles and its role in vesicles trafficking (along with the reciprocal role of Rab11), were critically important for effective chemotaxis in shallow ligand

gradients. The vesicle trafficking resulted in amplification of extracellular ligand asymmetry, which was then interpreted by the cells according to the combination of the input strength and scaffold expression, resulting in strongly asymmetric Erk activity, cell polarization, and directional migration.

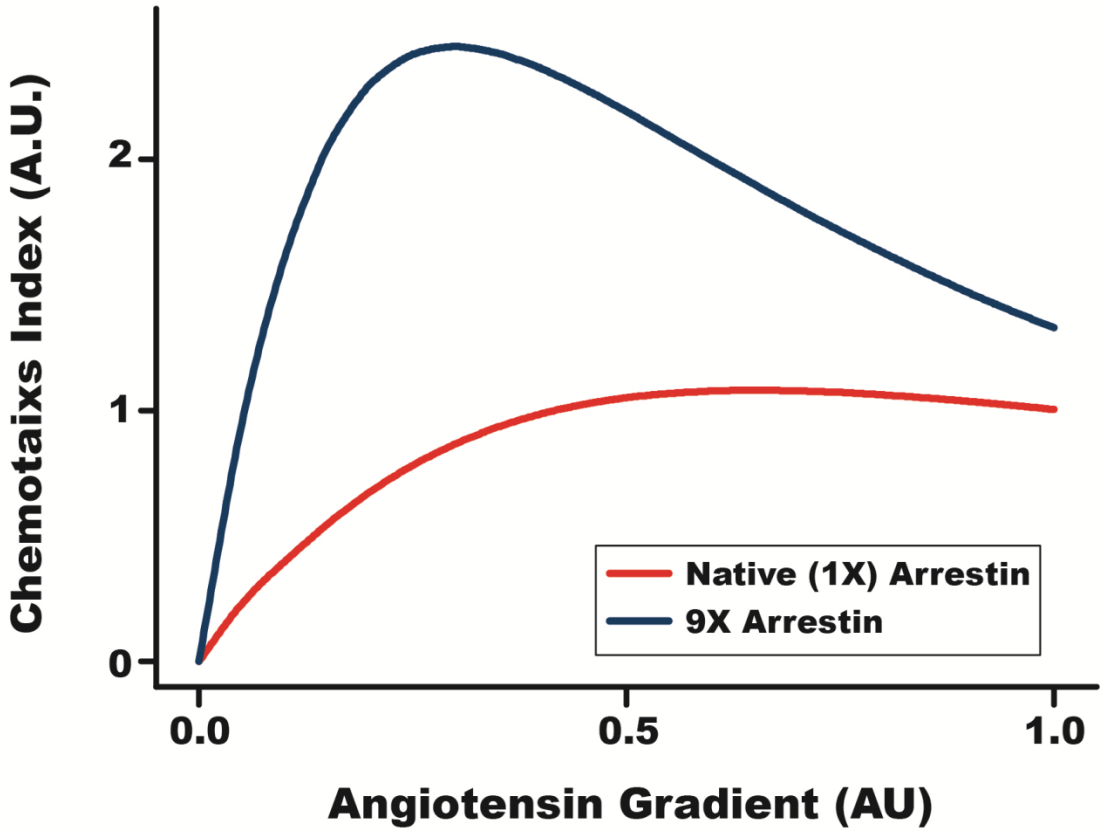


**Figure 4. 30 Model predicts that the cells with different scaffold expression level have different gradient sensitivity.**

At last, again, we happened to find that the actin polymerization and beta-arrestin2 vesicle happen to be colocalized during the cell chemotaxis (Figure 4.31). This means the beta-arrestin2 can regulate the actin polymerization locally. We explored some

mechanisms and found that the beta-arrestin2 locally scaffold the activation of pERK, pERK locally activated the p90RSK (Figure 4.32), and p90RSK can up-regulate the actin polymerization [76].

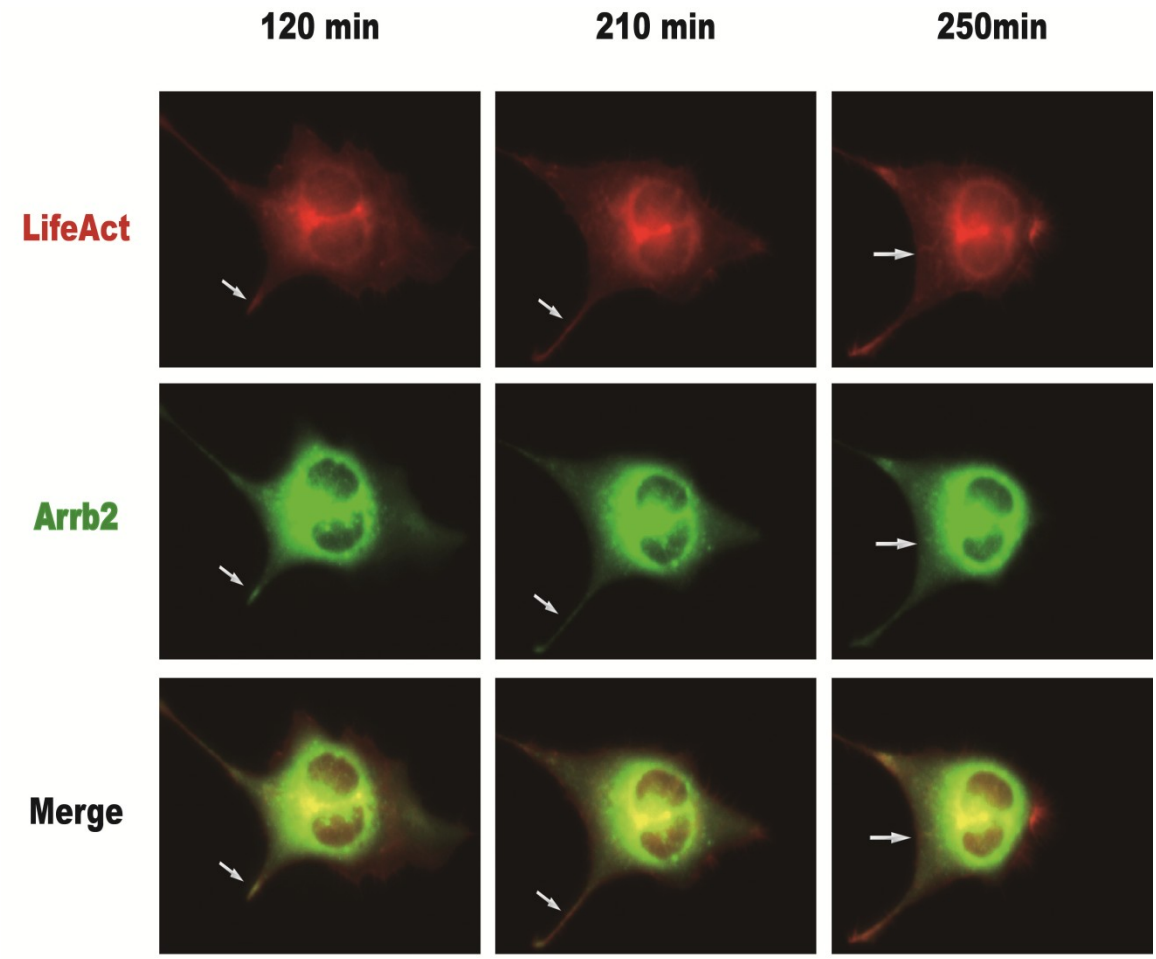


**Figure 4. 31 LifeAct is a probe to detect the actin polymerization *in situ*. The arrows indicate the colocalization of beta-arrestin2 and LifeAct probe.**

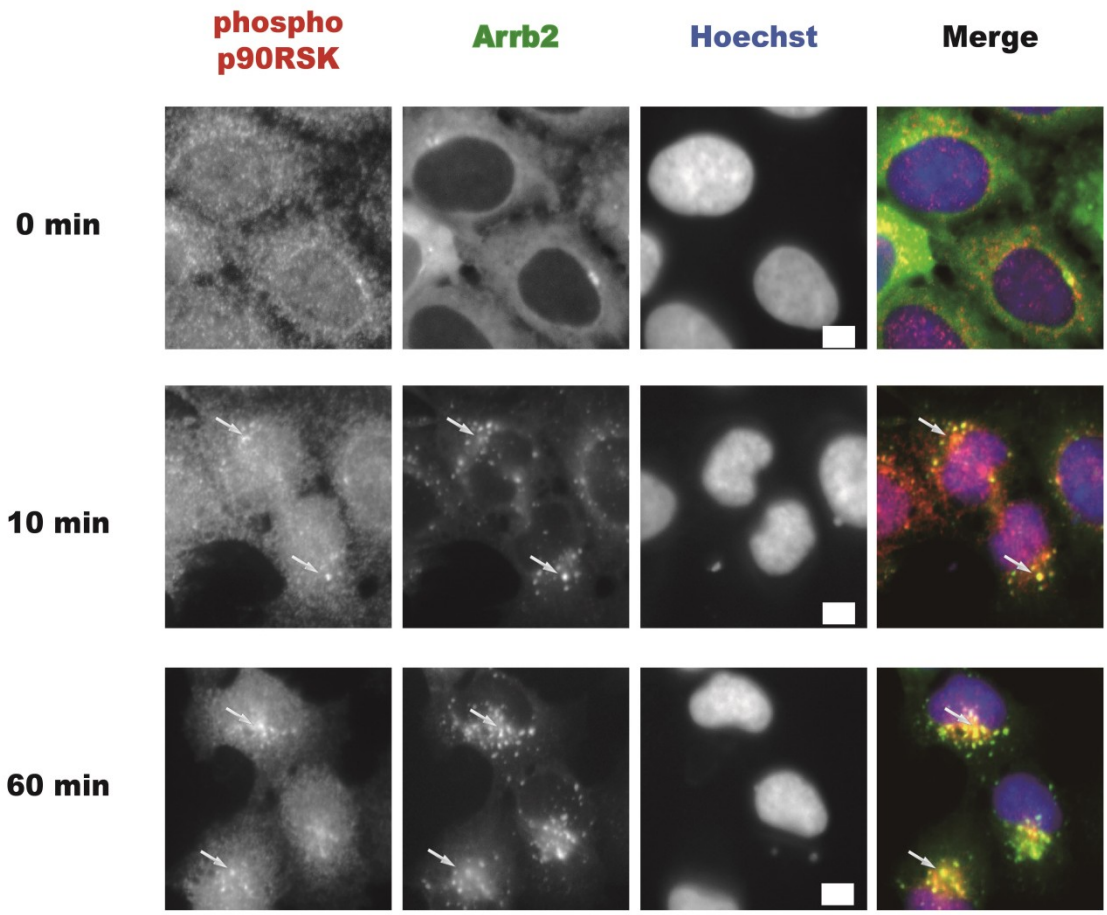


**Figure 4. 32 The p90RSK phosphorylation is colocalized with beta-arrestin2 vesicle when cells are stimulated by AngII**

# Chapter 5

# Conclusions and Perspectives

## *5.1 Conclusions*

My dissertation has been focusing on the mechanistic studies of chemotaxis, with both experimental and computational approaches at the level of cell signaling pathways. In chapter 3, we systematically compared the two popular cell chemotaxis models in parallel: negative feedback (NFB) and incoherent feed-forward loop (iFFL). Our *in silico* experiments pointed out that none of the oscillatory, stepped, or fold-changed input can distinguish the two network topologies. The only input signal that can clearly partition between them is ramped-input, at which condition the NFB showed no adaptation while iFFL still robustly exhibited perfect adaptation.

The two different chemotaxis frameworks are utilized by distinct organisms: bacteria use the NFB while eukaryotes prefer iFFL. More importantly, our simulations indicated that the different choices were resulted from evolution fitness rather than occasional development.

When trying to determine which category the beta-arrestin2-mediated chemotaxis belongs to, we had a few challenges and difficulties. The most significant discrepancy is

that our results suggested that beta-arrestin2-mediated activation of ERK can trigger chemo-attractive and chemo-repulsive responses to the gradients of AngII. This is in contradictory to many popular models of gradient sensing, including the so-called Local Excitation-Global Inhibition (LEGI) model (an extension of iFFL), proposed for chemotaxis of social amoebae cells or neutrophils, the models that cannot account for repulsive responses.

In Chapter 4, we investigated the unconventional mechanism of beta-arrestin2-mediated chemotaxis. The experimental results evidenced that the operation behind this chemotaxis is closely related to the scaffold property of beta-arrestin2. Scaffolding and trafficking of the components in signaling networks can exert important modifying effects on the activity and the ultimate functional outcome of the signaling event. In particular, local enrichment of the signaling complexes within the cell body can lead to a strong spatial polarization of the related intracellular processes. The local control of signaling is achieved by the dual functionality of beta-arrestin2: both as an agent promoting vesicle internalization and as a classical scaffold nucleating the signaling activity. As a result, the polarized signaling activity can amplify the gradient of the extracellular cue, particularly if balanced by reverse polarization of vesicle recycling. These results suggested that vesicle trafficking can have an effect on cell migration that adds to the commonly observed recycling of integrin receptors [77, 78], revealing a potentially critical functional role in detection and response to the extracellular guidance cues.

## *5.2 Perspectives*

The biphasic dependence of the scaffold-mediated signaling response on the concentration of the scaffold proteins provides a convenient mechanism for the possibility of both guiding attractive and repulsive responses in chemotactic migration by the same cue. Since the presence of scaffolds is commonplace, particularly within the MAPK signaling cascades [44], various means of polarizing spatial scaffold distribution within a cell can provide a general means for polarized cell behavior in response to a variety of extracellular cues, including gradients of growth factors or cytokines.

The mechanism of beta-arrestin2-mediated gradients sensing and chemotaxis suggested by our study also may shed additional light on an increasing number of cases strongly implicating Rab11 in directed single and collective cell migration [79]. Coupling of beta-arrestin, as a dual function protein affecting both receptor complex internalization and downstream signaling events, to the complementary recycling role of Rab11 can provide a powerful coupled mechanism regulating signaling events essential for orienting cell polarity and migration. Although many details of the relevant Rab11 regulation processes remain to be elucidated, it will be of particular interest to examine whether in other migratory systems, the function of this small GTPase is also coupled to a counterpart protein network controlling receptor internalization and signaling, yielding a powerful cell polarity mechanism.

The results presented here also highlight the diversity of possible mechanisms of gradient sensing in eukaryotic organisms. The involvement of ERK through coupling to

the beta-arrestin2-mediated activation of the MAPK cascade can provide an alternative or a complement to the commonly observed role of PI3K signaling at the plasma membrane, which was thought be a critical component in many established chemotaxis models [80, 81]. More generally, it will be of great interest to investigate if other mechanisms of achieving bi-phasic dose dependence of signaling responses might mediate chemotactic behavior, particularly, when the same molecules can drive both attractive and repulsive responses [82-84]. Such a mechanism, coupling complex dose responsiveness of signaling networks to non-uniform spatial distribution of signaling components, can dramatically increase the functionality of the resultant phenotypes and reveal the full power and flexibility of stimulus induced cell regulation.

# Bibliography


1. Moro, S., G. Spalluto, and K.A. Jacobson, *Techniques: Recent developments in computer-aided engineering of GPCR ligands using the human adenosine A3 receptor as an example.* Trends Pharmacol Sci, 2005. **26**(1): p. 44-51.

2. Cotton, M. and A. Claing, *G protein-coupled receptors stimulation and the control of cell migration.* Cell Signal, 2009. **21**(7): p. 1045-53.

3. Venkatakrishnan, A.J., et al., *Molecular signatures of G-protein-coupled receptors.* Nature, 2013. **494**(7436): p. 185-94.

4. Marion, S., et al., *A beta-arrestin binding determinant common to the second intracellular loops of rhodopsin family G protein-coupled receptors.* J Biol Chem, 2006. **281**(5): p. 2932-8.

5. Garland, S.L., *Are GPCRs still a source of new targets?* J Biomol Screen, 2013. **18**(9): p. 947-66.

6. Gloriam, D.E., et al., *Definition of the G protein-coupled receptor transmembrane bundle binding pocket and calculation of receptor similarities for drug design.* J Med Chem, 2009. **52**(14): p. 4429-42.

7. Johnston, C.A. and D.P. Siderovski, *Receptor-mediated activation of heterotrimeric G-proteins: current structural insights.* Mol Pharmacol, 2007. **72**(2): p. 219-30.

8. Tilley, D.G., *G protein-dependent and G protein-independent signaling pathways and their impact on cardiac function.* Circ Res, 2011. **109**(2): p. 217-30.

9. Hupfeld, C.J. and J.M. Olefsky, *Regulation of receptor tyrosine kinase signaling by GRKs and beta-arrestins.* Annu Rev Physiol, 2007. **69**: p. 561-77.

10. Gurevich, V.V., E.V. Gurevich, and W.M. Cleghorn, *Arrestins as multi-functional signaling adaptors.* Handb Exp Pharmacol, 2008(186): p. 15-37.

11. Lefkowitz, R.J. and S.K. Shenoy, *Transduction of receptor signals by beta-arrestins.* Science, 2005. **308**(5721): p. 512-7.

12. Maudsley, S., S. Siddiqui, and B. Martin, *Systems analysis of arrestin pathway functions.* Prog Mol Biol Transl Sci, 2013. **118**: p. 431-67.

13. Xiao, K., et al., *Functional specialization of beta-arrestin interactions revealed by proteomic analysis.* Proc Natl Acad Sci U S A, 2007. **104**(29): p. 12011-6.

14. Xiao, K., et al., *Global phosphorylation analysis of beta-arrestin-mediated signaling downstream of a seven transmembrane receptor (7TMR).* Proc Natl Acad Sci U S A, 2010. **107**(34): p. 15299-304.

15. Gurevich, E.V. and V.V. Gurevich, *Arrestins: ubiquitous regulators of cellular signaling pathways.* Genome Biol, 2006. **7**(9): p. 236.

16. Noma, T., et al., *Beta-arrestin-mediated beta1-adrenergic receptor transactivation of the EGFR confers cardioprotection.* J Clin Invest, 2007. **117**(9): p. 2445-58.

17. Lin, A. and K.A. DeFea, *beta-Arrestin-kinase scaffolds: turn them on or turn them off?* Wiley Interdiscip Rev Syst Biol Med, 2013. **5**(2): p. 231-41.

18. Beaulieu, J.M., et al., *An Akt/beta-arrestin 2/PP2A signaling complex mediates dopaminergic neurotransmission and behavior.* Cell, 2005. **122**(2): p. 261-73.

19. Good, M.C., J.G. Zalatan, and W.A. Lim, *Scaffold proteins: hubs for controlling the flow of cellular information.* Science, 2011. **332**(6030): p. 680-6.

20. Chen, Q., et al., *Self-association of arrestin family members.* Handb Exp Pharmacol, 2014. **219**: p. 205-23.

21. Violin, J.D., et al., *Biased ligands at G-protein-coupled receptors: promise and progress.* Trends Pharmacol Sci, 2014. **35**(7): p. 308-316.

22. Soergel, D.G., et al., *First clinical experience with TRV130: pharmacokinetics and pharmacodynamics in healthy volunteers.* J Clin Pharmacol, 2014. **54**(3): p. 351-7.

23. Soergel, D.G., et al., *First clinical experience with TRV027: pharmacokinetics and pharmacodynamics in healthy volunteers.* J Clin Pharmacol, 2013. **53**(9): p. 892-9.

24. De Palo, G. and R.G. Endres, *Unraveling adaptation in eukaryotic pathways: lessons from protocells.* PLoS Comput Biol, 2013. **9**(10): p. e1003300.

25. Hunton, D.L., et al., *Beta-arrestin 2-dependent angiotensin II type 1A receptor-mediated pathway of chemotaxis.* Mol Pharmacol, 2005. **67**(4): p. 1229-36.

26. Ge, L., et al., *A beta-arrestin-dependent scaffold is associated with prolonged MAPK activation in pseudopodia during protease-activated receptor-2-induced chemotaxis.* J Biol Chem, 2003. **278**(36): p. 34418-26.

27. Ge, L., et al., *Constitutive protease-activated receptor-2-mediated migration of MDA MB-231 breast cancer cells requires both beta-arrestin-1 and -2.* J Biol Chem, 2004. **279**(53): p. 55419-24.

28. Pujic, Z., et al., *Assays for eukaryotic cell chemotaxis.* Comb Chem High Throughput Screen, 2009. **12**(6): p. 580-8.

29. Sackmann, E.K., A.L. Fulton, and D.J. Beebe, *The present and future role of microfluidics in biomedical research.* Nature, 2014. **507**(7491): p. 181-9.

30. Toetsch, S., et al., *The evolution of chemotaxis assays from static models to physiologically relevant platforms.* Integr Biol (Camb), 2009. **1**(2): p. 170-81.

31. Paliwal, S., et al., *MAPK-mediated bimodal gene expression and adaptive gradient sensing in yeast.* Nature, 2007. **446**(7131): p. 46-51.

32. Tadross, M.R., et al., *Robust approaches to quantitative ratiometric FRET imaging of CFP/YFP fluorophores under confocal microscopy.* J Microsc, 2009. **233**(1): p. 192-204.

33. Berney, C. and G. Danuser, *FRET or no FRET: a quantitative comparison.* Biophys J, 2003. **84**(6): p. 3992-4010.

34. Cheong, R., C.J. Wang, and A. Levchenko, *High content cell screening in a microfluidic device.* Mol Cell Proteomics, 2009. **8**(3): p. 433-42.

35. Iman, R.L., J. Davenport, M., and D.K. Zeigler, *Latin Hypercube Sampling (Program User's Guide).* Albuquerque, NM: Sandia Labs, 1980: p. 77.

36. Berg, H.C. and D.A. Brown, *Chemotaxis in Escherichia coli analysed by three-dimensional tracking.* Nature, 1972. **239**(5374): p. 500-4.

37. Macnab, R.M. and D.E. Koshland, Jr., *The gradient-sensing mechanism in bacterial chemotaxis.* Proc Natl Acad Sci U S A, 1972. **69**(9): p. 2509-12.

38. Dinauer, M.C., T.L. Steck, and P.N. Devreotes, *Cyclic 3',5'-AMP relay in Dictyostelium discoideum V. Adaptation of the cAMP signaling response during cAMP stimulation.* J Cell Biol, 1980. **86**(2): p. 554-61.

39. Barkai, N. and S. Leibler, *Robustness in simple biochemical networks.* Nature, 1997. **387**(6636): p. 913-7.

40. Alon, U., et al., *Robustness in bacterial chemotaxis.* Nature, 1999. **397**(6715): p. 168-71.

41. Yi, T.M., et al., *Robust perfect adaptation in bacterial chemotaxis through integral feedback control.* Proc Natl Acad Sci U S A, 2000. **97**(9): p. 4649-53.

42. Milo, R., et al., *Network motifs: simple building blocks of complex networks.* Science, 2002. **298**(5594): p. 824-7.

43. Parent, C.A. and P.N. Devreotes, *A cell's sense of direction.* Science, 1999. **284**(5415): p. 765-70.

44. Levchenko, A. and P.A. Iglesias, *Models of eukaryotic gradient sensing: application to chemotaxis of amoebae and neutrophils.* Biophys J, 2002. **82**(1 Pt 1): p. 50-63.

45. Iglesias, P.A. and P.N. Devreotes, *Navigating through models of chemotaxis.* Curr Opin Cell Biol, 2008. **20**(1): p. 35-40.

46. Iglesias, P.A. and A. Levchenko, *Modeling the cell's guidance system.* Sci STKE, 2002. **2002**(148): p. re12.

47. Krishnan, J., *Effects of saturation and enzyme limitation in feedforward adaptive signal transduction.* IET Syst Biol, 2011. **5**(3): p. 208-19.

48. Iglesias, P.A., *Chemoattractant signaling in dictyostelium: adaptation and amplification.* Sci Signal, 2012. **5**(213): p. pe8.

49. Wang, C.J., et al., *Diverse sensitivity thresholds in dynamic signaling responses by social amoebae.* Sci Signal, 2012. **5**(213): p. ra17.

50. Takeda, K., et al., *Incoherent feedforward control governs adaptation of activated ras in a eukaryotic chemotaxis pathway.* Sci Signal, 2012. **5**(205): p. ra2.

51. Dolmetsch, R.E., K. Xu, and R.S. Lewis, *Calcium oscillations increase the efficiency and specificity of gene expression.* Nature, 1998. **392**(6679): p. 933-6.

52. Hersen, P., et al., *Signal processing by the HOG MAP kinase pathway.* Proc Natl Acad Sci U S A, 2008. **105**(20): p. 7165-70.

53. Mettetal, J.T., et al., *The frequency dependence of osmo-adaptation in Saccharomyces cerevisiae.* Science, 2008. **319**(5862): p. 482-4.

54. Lipan, O. and W.H. Wong, *The use of oscillatory signals in the study of genetic networks.* Proc Natl Acad Sci U S A, 2005. **102**(20): p. 7063-8.

55. Paliwal, S., C.J. Wang, and A. Levchenko, *Pulsing cells: how fast is too fast?* HFSP J, 2008. **2**(5): p. 251-6.

56. Ashall, L., et al., *Pulsatile stimulation determines timing and specificity of NF-kappaB-dependent transcription.* Science, 2009. **324**(5924): p. 242-6.

57. Gregor, T., et al., *The onset of collective behavior in social amoebae.* Science, 2010. **328**(5981): p. 1021-5.

58. Sontag, E.D., *Remarks on feedforward circuits, adaptation, and pulse memory.* IET Syst Biol, 2010. **4**(1): p. 39-51.

59. Muzzey, D., et al., *A systems-level analysis of perfect adaptation in yeast osmoregulation.* Cell, 2009. **138**(1): p. 160-71.

60. Tu, Y., T.S. Shimizu, and H.C. Berg, *Modeling the chemotactic response of Escherichia coli to time-varying stimuli.* Proc Natl Acad Sci U S A, 2008. **105**(39): p. 14855-60.

61. Segall, J.E., S.M. Block, and H.C. Berg, *Temporal comparisons in bacterial chemotaxis.* Proc Natl Acad Sci U S A, 1986. **83**(23): p. 8987-91.

62. Block, S.M., J.E. Segall, and H.C. Berg, *Adaptation kinetics in bacterial chemotaxis.* J Bacteriol, 1983. **154**(1): p. 312-23.

63. Brennan, M.D., R. Cheong, and A. Levchenko, *Systems biology. How information theory handles cell signaling and uncertainty.* Science, 2012. **338**(6105): p. 334-5.

64. Cheong, R., et al., *Information transduction capacity of noisy biochemical signaling networks.* Science, 2011. **334**(6054): p. 354-8.

65. Levchenko, A., J. Bruck, and P.W. Sternberg, *Scaffold proteins may biphasically affect the levels of mitogen-activated protein kinase signaling and reduce its threshold properties.* Proc Natl Acad Sci U S A, 2000. **97**(11): p. 5818-23.

66. Maeder, C.I., et al., *Spatial regulation of Fus3 MAP kinase activity through a reaction-diffusion mechanism in yeast pheromone signalling.* Nat Cell Biol, 2007. **9**(11): p. 1319-26.

67. Chapman, S.A. and A.R. Asthagiri, *Quantitative effect of scaffold abundance on signal propagation.* Mol Syst Biol, 2009. **5**: p. 313.

68. DeWire, S.M., et al., *β-Arrestins and Cell Signaling.* Annual Review of Physiology, 2007. **69**(1): p. 483-510.

69. Simard, E., et al., *beta-Arrestin regulation of myosin light chain phosphorylation promotes AT1aR-mediated cell contraction and migration.* PLoS One, 2013. **8**(11): p. e80532.

70. Violin, J.D., X.R. Ren, and R.J. Lefkowitz, *G-protein-coupled receptor kinase specificity for beta-arrestin recruitment to the beta2-adrenergic receptor revealed by fluorescence resonance energy transfer.* J Biol Chem, 2006. **281**(29): p. 20577-88.

71. DeFea, K.A., *Stop that cell! Beta-arrestin-dependent chemotaxis: a tale of localized actin assembly and receptor desensitization.* Annu Rev Physiol, 2007. **69**: p. 535-60.

72. Bray, D. and S. Lay, *Computer-based analysis of the binding steps in protein complex formation.* Proc Natl Acad Sci U S A, 1997. **94**(25): p. 13493-8.

73. Takahashi, S., et al., *Rab11 regulates exocytosis of recycling vesicles at the plasma membrane.* J Cell Sci, 2012. **125**(Pt 17): p. 4049-57.

74. Emery, G. and D. Ramel, *Cell coordination of collective migration by Rab11 and Moesin.* Commun Integr Biol, 2013. **6**(4): p. e24587.

75. Ramel, D., et al., *Rab11 regulates cell-cell communication during collective cell movements.* Nat Cell Biol, 2013. **15**(3): p. 317-24.

76. Woo, M.S., et al., *Ribosomal S6 kinase (RSK) regulates phosphorylation of filamin A on an important regulatory site.* Mol Cell Biol, 2004. **24**(7): p. 3025-35.

77. Jones, M.C., P.T. Caswell, and J.C. Norman, *Endocytic recycling pathways: emerging regulators of cell migration.* Curr Opin Cell Biol, 2006. **18**(5): p. 549-57.

78. Caswell, P.T. and J.C. Norman, *Integrin trafficking and the control of cell migration.* Traffic, 2006. **7**(1): p. 14-21.

79. Wan, P., et al., *Guidance receptor promotes the asymmetric distribution of exocyst and recycling endosome during collective cell migration.* Development, 2013. **140**(23): p. 4797-806.

80. Iglesias, P.A., *Spatial regulation of PI3K signaling during chemotaxis.* Wiley Interdiscip Rev Syst Biol Med, 2009. **1**(2): p. 247-53.

81. Gambardella, L. and S. Vermeren, *Molecular players in neutrophil chemotaxis--focus on PI3K and small GTPases.* J Leukoc Biol, 2013. **94**(4): p. 603-12.

82. Amatschek, S., et al., *CXCL9 induces chemotaxis, chemorepulsion and endothelial barrier disruption through CXCR3-mediated activation of melanoma cells.* Br J Cancer, 2011. **104**(3): p. 469-79.

83. Hopker, V.H., et al., *Growth-cone attraction to netrin-1 is converted to repulsion by laminin-1.* Nature, 1999. **401**(6748): p. 69-73.

84. McCaig, C.D., et al., *Controlling cell behavior electrically: current views and future potential.* Physiol Rev, 2005. **85**(3): p. 943-78.

# Curriculum Vita

Hao Chang was born November 4th, 1980 in Lanzhou, China. His undergraduate education was at Tsinghua University, China. His Master's degree is from Tsinghua University, China; and Ph.D. degree is from Johns Hopkins University.